Model Based Design of Electro-Hydraulic Motion Control Systems for Offshore Pipe Handling Equipment

Morten Kollerup Bak

Model Based Design of Electro-Hydraulic Motion Control Systems for Offshore Pipe Handling Equipment

Doctoral dissertation for the degree of Philosophiae Doctor (Ph.D.) at the Faculty of Engineering and Science, Specialisation in Mechatronics

University of Agder
Faculty of Engineering and Science
2014

Doctoral Dissertation by the University of Agder 85
ISBN: 978-82-7117-764-5
ISSN: 1504-9272

Printed in the Printing Office, University of Agder
Kristiansand

Preface

This dissertation contains the essential results of the research I carried out in my Ph.D. project at the Department of Engineering Sciences, Faculty of Engineering and Science, University of Agder. The research was carried out in close cooperation with Aker Solutions in Kristiansand in the period between December 2009 and December 2013. The project was funded by the Norwegian Ministry of Education and Research and co-funded by Aker Solutions.

I owe my deepest gratitude to my supervisor Prof. Michael Rygaard Hansen for his encouragement and guidance throughout the project. He has always been ready to motivate me and guide me on the right path whenever it was needed and I could not imagine having a better advisor for my work. I would like to thank Aker Solutions for giving me the possibility to work on an exciting project with industrial applications - it has been a great learning experience. I would especially like to thank Pål Andre Nordhammer (Aker Solutions) for his invaluable input and ideas which indeed helped shaping the project.

During the past four years I have met and gotten to know a lot of people who have helped and inspired me in one way or another. I don't know how to thank all these people - their names are far too many to mention here and I'm afraid I will forget someone.

Without mentioning any names I would first of all like to thank my former colleagues in the mechatronics group at the University of Agder. They provide a fun, creative and friendly working environment and are always forthcoming when asked for help. I would also like to thank all my colleagues from Aker Solutions who have helped me during the project. Their help has enabled me to achieve unique results and has quite simply been invaluable to me.

Perhaps most importantly, I would like to thank all my fellow Ph.D. students at the University of Agder - both within and outside the mechatronics group. Some of them started before me and finished before I did. Some of them started after me and have yet to finish. A few of them even started after I did and finished before me. They provided a very nice and fun social environment that has left me with unforgettable memories.

I would also like to thank my former fellow students from Aalborg University in Denmark who formed their own network of Ph.D. students and invited me to join. The last five years or so we have met once or twice a year to discuss our research and, not least, to socialize and catch up. These meetings have been a great motivation and inspiration to me and have always brought fun and good times.

The past four years have been exciting and enriching, but also tough and filled with tremendous workloads. At times I have felt I was losing my mind out of sheer stress, too much coffee and too little sleep. But during these four years I have met a lot of nice people from all over the world and travelled to places I never thought I would go - all while working with what I think is the most interesting. If that is not a privilege I don't know what is.

Morten Kollerup Bak

Grimstad, Norway
January 2014

Summary

Despite the fact that hydraulics, in general, is considered a mature technology, design of hydraulic systems still offers a number of challenges for both component suppliers and manufacturers of hydraulically actuated machines such as offshore pipe handling equipment. This type of equipment is characterized by high price, high level of system complexity and low production numbers. It requires a great level of skill and experience to develop the equipment and the focus on production and development costs is constantly increasing. Therefore design engineers continuously have to improve their procedures for decision making regarding choice of principal solutions, components and materials in order to reach the best possible trade-off between a wide range of design criteria as fast as possible.

In this dissertation methods for modeling, parameter identification, design and optimization of a selected piece of offshore pipe handling equipment, a knuckle boom crane, are put forward and treated in details in five appended papers.

Modeling of mechanical multi-body systems with attention to structural flexibility is treated in papers I and IV. Modeling, testing and parameter identification of directional control valves with main focus on dynamic characteristics are treated in paper II and also discussed in papers III and IV. Modeling of counterbalance valves with main focus on steady-state characteristics is treated in papers III and IV. In paper IV also modeling of hydraulic cylinders is discussed and a procedure for parameter identification for models of hydraulic-mechanical systems is presented.

Steady-state design procedures for hydraulic systems are discussed in paper III and a design optimization method for reduction of oscillations is presented. Paper V deals with dynamic considerations in design of electro-hydraulic motion control systems for offshore pipe handling equipment.

All the presented methods are developed to accommodate the needs of the system designer. They take into account the limited access to component data and time available for model development and design optimization, which are the main challenges for the system designer. The methods also address the problem of required knowledge within several disciplines, e.g., by suggesting modeling assumptions and experimental work suitable for system design.

Contents

Publications **xi**

1 Introduction **1**

1.1 Motivation and Background 3

1.2 State of the Art 5

2 Offshore Pipe Handling Equipment **9**

2.1 The Knuckle Boom Crane 11

3 Modeling and Parameter Identification **15**

3.1 Mechanical Systems 17

3.2 Hydraulic Components and Systems 19

4 Design and Optimization **23**

4.1 Hydraulic System Design 24

4.2 Use of Simulation Models 24

5 Conclusions **29**

5.1 Contributions 29

5.2 Outlook 31

References **33**

Appended papers **40**

I A Method for Finite Element Based Modeling of Flexible Components in Time Domain Simulation of Knuckle Boom Crane **41**

II Modeling, Performance Testing and Parameter Identification of Pressure Compensated Proportional Directional Control Valves **57**

III Model Based Design Optimization of Operational Reliability in Offshore Boom Cranes **79**

IV Analysis of Offshore Knuckle Boom Crane — Part One: Modeling and Parameter Identification **111**

V Analysis of Offshore Knuckle Boom Crane — Part Two: Motion Control **147**

Publications

The following five papers are appended and will be referred to by their Roman numerals. The papers are printed in their originally published state except for changes in format and minor errata.

I J. Henriksen, M. K. Bak and M. R. Hansen, “A Method for Finite Element Based Modeling of Flexible Components in Time Domain Simulation of Knuckle Boom Crane”, *The 24th International Congress on Condition Monitoring and Diagnostics Engineering Management*, pp. 1215-1224. Stavanger, Norway, May 30 - June 1, 2011.

II M. K. Bak and M. R. Hansen, “Modeling, Performance Testing and Parameter Identification of Pressure Compensated Proportional Directional Control Valves” *The 7th FPNI PhD Symposium on Fluid Power*, pp. 889-908. Reggio Emilia, Italy, June 27 - 30, 2012.

III M. K. Bak and M. R. Hansen, “Model Based Design Optimization of Operational Reliability in Offshore Boom Cranes”, *International Journal of Fluid Power*. Vol. 14 (2013), No. 3, pp. 53-65.

IV M. K. Bak and M. R. Hansen, “Analysis of Offshore Knuckle Boom Crane — Part One: Modeling and Parameter Identification”, *Modeling, Identification and Control*. Vol. 34 (2013), No. 4, pp. 157-174.

V M. K. Bak and M. R. Hansen, “Analysis of Offshore Knuckle Boom Crane — Part Two: Motion Control”, *Modeling, Identification and Control*. Vol. 34 (2013), No. 4, pp. 175-181.

The following papers are not included in the dissertation but constitute an important part of the background.

VI M. K. Bak, M. R. Hansen and P. A. Nordhammer, “Virtual Prototyping - Model of Offshore Knuckle Boom Crane”, *The 24th International Congress on Condition Monitoring and Diagnostics Engineering Management*, pp. 1242-1252. Stavanger, Norway, May 30 - June 1, 2011.

VII M. K. Bak, M. R. Hansen and Karimi, H. R., “Robust Tool Point Control for Offshore Knuckle Boom Crane”, *The 18th World Congress of the International Federation of Automatic Control (IFAC)*, pp. 4594-4599. Milano, Italy, August 28 - September 2, 2011.

VIII P. A. Nordhammer, M. K. Bak and M. R. Hansen, “A Method for Reliable Motion Control of Pressure Compensated Hydraulic Actuation with Counterbalance Valves”, *The 12th International Conference on Control, Automation and Systems*, pp. 759-763. Jeju Island, Korea, October 17 - 21, 2012.

IX P. A. Nordhammer, M. K. Bak and M. R. Hansen, “Controlling the Slewing Motion of Hydraulically Actuated Cranes Using Sequential Activation of Counterbalance Valves”, *The 12th International Conference on Control, Automation and Systems*, pp. 773-778. Jeju Island, Korea, October 17 - 21, 2012.

Chapter 1

Introduction

Offshore drilling for oil and gas production dates back to the end of the nineteenth century and began with drilling in fresh water lakes as well as shallow salt waters at the coast of California. During the 1960's, 70's and 80's drilling moved into areas of harsh environments, like the North Sea, and so-called deepwater (water depths between 500 and 1500 m) in the Gulf of Mexico. This development still continues today with drilling in arctic areas and ultra deepwater (water depths beyond 1500 m).
Naturally, this has required and led to a major development of both subsea equipment, e.g., for well control, and topside equipment such as top drives (drilling machines), hoisting systems and pipe handling equipment. The fact that drilling is constantly moving towards harsher environments and deeper waters obviously increases the requirements for the equipment being used. This again leads to a number of challenges for the offshore equipment manufacturers.
For applications such as top drives and hoisting systems the most noticeable design challenge is the increase in required lifting capacity. Today the required lifting capacity often reaches as high as 1500 short tons and in some cases even beyond. In addition, motion compensation is required for hoisting systems whenever used on a floating installation.
For offshore equipment in general, due to remote locations and high cost of down time, reliability and productivity are the most important performance criteria. Therefore design is based on well proven solutions and development of the equipment has been a steady process with incremental improvements of functionality and performance. During the last couple of decades machine development has primarily been concentrated around control systems technology which has led to significant development in automation and safety of machine operations. In terms of technology, structural design and design of actuation systems have developed at a much slower rate with only minor developments of materials and components. However, the development of PCs and CAD/CAE systems has had a significant impact on how design engineers work and has enabled

design improvements based on the existing technology.
Besides most types of top drives and hoisting systems, topside equipment such as pipe handling equipment normally rely on hydraulic or electro-hydraulic actuation. The reason for this is that hydraulic actuation is a well-proven, reliable and robust solution with a number of advantages compared to electrical actuation. Among others, these advantages include:

- **Heat transfer**. The hydraulic fluid carries away generated heat to a convenient heat exchanger. This allows for smaller and lighter components.
- **Lubrication**. The hydraulic fluid acts as a lubricant and facilitates long component life.
- **Power density**. Torque/force developed by a hydraulic actuator is proportional to pressure difference and only limited by permissible stress levels. With respect to size and weight, hydraulic actuators deliver high effort compared to electrical actuators.
- **Price**. Today hydraulic components are relatively cheap compared to many electrical components.

Furthermore, there is a vast amount of experience with hydraulic actuation in the offshore industry and far less experience with electrical actuation. Therefore a change of technology is complicated and represents a relatively high risk even though electric drives have developed significantly over the past decades. Naturally, hydraulic actuation is also associated with a number of disadvantages such as:

- **Contamination**. Contaminated oil can clog valves and actuators or cause wear which leads to permanent loss in performance or failure. Contamination is the most common source of failure in hydraulic systems.
- **Efficiency**. Hydraulic systems normally have quite poor efficiencies compared to electrical systems.
- **System complexity**. Hydraulic systems often require more components than electrical systems which increases the system complexity. Furthermore, the need for passive control elements such as counterbalance valves often introduces instability and lowers the overall efficiency.

Some of these disadvantages may be eliminated by introducing more modern technologies such as separate meter-in separate meter-out control (Eriksson and Palmberg, 2011), digital hydraulics (Linjama and Vilenius, 2007) or integrated actuators (Michel and Weber, 2012) which have yet to be adopted by the offshore industry. The reason these

technologies have not yet been applied is that they are less field proven and therefore represent less reliable solutions.
Hydraulics, or fluid power in general, is a widely used technology with application to, e.g., the automotive and the aerospace industries, off-highway vehicles, wind turbines and production and manufacturing machines. Hydraulics is often divided into two categories; *mobile hydraulics* mainly referring to off-highway applications and *industrial hydraulics* mainly referring to production and manufacturing applications. Industrial applications are typically characterized by high requirements for repeatability, dynamic response and accuracy whereas mobile applications often have high requirements for versatility and human-machine interface. Furthermore, industrial application are usually supplied by a constant pressure system whereas mobile applications usually are supplied by a system with variable supply pressure (load sensing systems).
In terms of requirements for repeatability, dynamic response and accuracy as well as versatility and human-machine interface, offshore applications are located somewhere between mobile and industrial applications. They are usually supplied by constant pressure systems, but use components from both mobile and industrial applications.
Although electric drives and modern fluid power technologies certainly will gain more ground in the offshore industry, a sudden change in actuation technology seems unlikely. Therefore maintenance and development of knowledge within design of hydraulic systems is highly relevant and will continue to be for decades to come.

1.1 Motivation and Background

Despite the fact that hydraulics, in general, is considered a mature technology, design of hydraulic systems still offers a number of challenges for both component suppliers and manufacturers of hydraulically actuated machines such as offshore pipe handling equipment. This type of equipment is characterized by high price, high level of system complexity and low production numbers. It requires a great level of skill and experience to develop the equipment and the focus on production and development costs is constantly increasing. Therefore design engineers continuously have to improve their procedures for decision making regarding choice of principal solutions, components and materials in order to reach the best possible trade-off between a wide range of design criteria as fast as possible.
For hydraulic and electro-hydraulic actuation systems, most design challenges are related to the dynamics of the actuation system and the application it is being designed for. While design procedures based on steady-state considerations are well-known and fairly easy to apply, there is still a lack of robust design procedures that take the system dynamics into account. This includes both stability and accuracy, i.e., the systems

tendency to oscillate and ability to follow a reference signal. These criteria are not easily evaluated and are therefore often left unaddressed until the system has been realized and can be tested. Although, in practice, a substantial amount of tuning is usually required, insufficient focus on dynamics during the design phase often leads to costly and time consuming design changes which can be difficult to implement after the system has been realized. This is especially problematic for areas like the offshore industry where there are very limited opportunities to build prototypes for verification of a new design. The problem calls for a model based approach which enables the designer to evaluate the system dynamics and take measures to improve it before the system is build. Non-linear dynamic models may be linearized and used to check for stability in selected operating points and to analyze how system parameters influence the stability margin. However for analysis of complete operating cycles it quickly becomes impractical to work with linearized models. Furthermore, since stability is an absolute measure and many hydraulic systems are likely to become unstable in one or more operating points or oscillate in limit cycles, it is more meaningful to consider the level of oscillations occurring during the operating cycle.
What is needed for more detailed system analysis is dynamic time domain simulation which can be used to analyze both oscillation level and accuracy during the operating cycle in order to evaluate the system design and possibly carry out design optimization. A model based design approach may be illustrated as in Fig. 1.1.

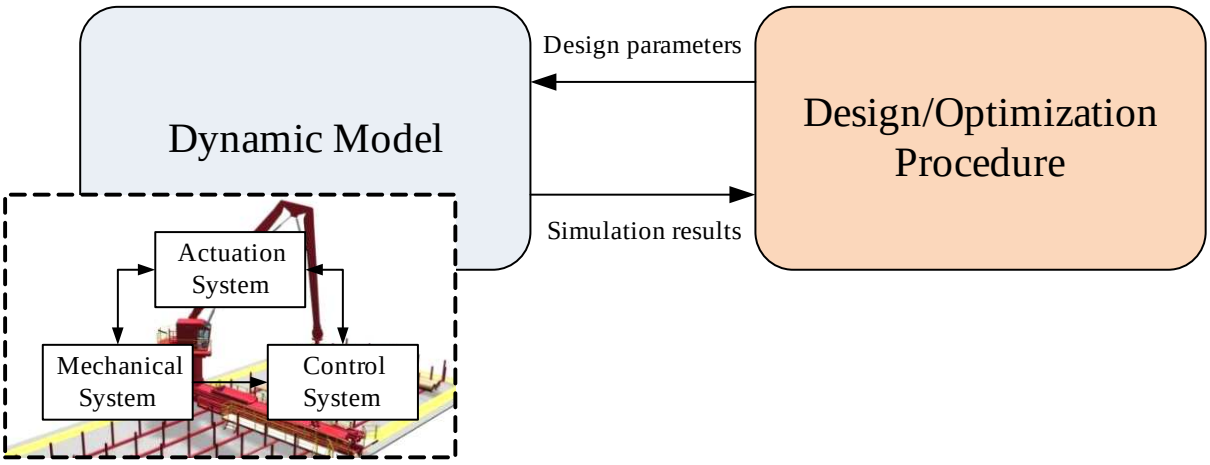

Figure 1.1: Model based design approach.

Depending on the purpose, a more or less extensive model of the considered system is needed. For design of motion control systems for applications like offshore pipe handling equipment, rather detailed models including the mechanical system, the actuation system and the control system are usually required. In addition, environmental effects and even operator behavior may need to be considered.
Simulation models serve as virtual prototypes providing information about machine per-

formance such as overall efficiency, oscillatory behavior and accuracy, enabling engineers to test, redesign and optimize the design before it is manufactured. This may be done by either using the model directly as a design evaluation tool or by coupling it with a numerical optimization routine.
One of the major challenges in model based design is to produce simulation models that, with a reasonable precision, are able to mimic the behavior of a real system. This challenge is especially pronounced for hydraulically actuated machines simply because suppliers of hydraulic components are not used to deliver all the data needed to develop simulation models of their products.
The challenges of model based design may be divided into three categories:

- **Modeling and simulation**. This includes choice of simulation software, modeling techniques and level of modeling detail.
- **Model validation and verification**. This usually involves some sort of experimental work followed up by parameter identification.
- **Use of simulation models**. This includes setting up a suitable frame work for post-processing of simulation results and optimization of critical design parameters.

These topics form the basis for the work presented in this dissertation and are treated in more detail in chapters 3 and 4 and are also subjected to a literature review in the following section.

1.2 State of the Art

Fluid power technology is a relatively small research area, but even so hydraulics has been subject to extensive research during both the past and the current century. An overview of relatively recent research issues is given by Burrows (2000). The technology, as we know it today, has been around for at least a century and has gone through a slow and steady development with research results remaining relevant for a long time. An example of that is the work by Merritt (1967), which is still frequently referred to in both research and education and by practicing engineers.
During the recent decades, with the development of PCs and commercially available software for simulation and technical computing, design and optimization of hydraulic systems has attracted a considerable amount of interest from researchers in the fluid power community. Fundamental design procedures based on steady-state based considerations have been presented by Stecki and Garbacik (2002). System design and component selection using dynamic simulation and numerical optimization has been investigated by Krus et al. (1991), Andersson (2001), Hansen and Andersen (2001), Krim-

bacher et al. (2001), Papadopoulos and Davliakos (2004), Pedersen (2004) and Hansen and Andersen (2005).
Conceptual design and so-called expert systems for automated design have also attracted a considerable amount of attention, (Dunlop and Rayudu, 1993), (Lin and Shen, 1995), (da Silva and Back, 2000), (da Silva, 2000), (Darlington et al., 2001), (Hughes et al., 2001), (Liermann and Murrenhoff, 2005), (Steiner and Scheidl, 2005), (Schlemmer and Murrenhoff, 2008) and (Engler et al., 2010). The impact outside academia, however, remains limited. A reason for this may be that design of hydraulic systems is somewhat application dependent. Design criteria and constraints in combination with design traditions differ from one application area to another, making it difficult to set up and maintain design rules for expert systems. Moreover, skepticism and conservatism may contribute to design engineers being reluctant to make use of such systems.
Hydraulic systems are therefore still designed manually and most often based on existing systems, reducing the design job to a sizing problem where the system architecture is already given. In these cases the design engineer can certainly benefit from tools such as dynamic simulation and optimization. This has already been pointed out by Palmberg (1995) and demonstrated by Hampson et al. (1996).
Computer based time domain simulation and optimization techniques have, by far, proven themselves as excellent tools for the challenged designer and have over the last couple of decades increasingly been employed by drilling equipment manufacturers. However, the use of these techniques still offers a number of challenges both in industry as well as academia. As previously mentioned, the main challenge is to produce reliable simulation models that can be used for design purposes.
Today there are several commercially available software packages for modeling and simulation of multi-domain systems. Many of these software packages include extensive libraries of generic model components making it easy and fast to develop models of control systems and hydraulic-mechanical systems and to combine sub-models of different physical domains. However, efficient modeling still requires a great level of theoretical knowledge and experience within specific disciplines.
For modeling of mechanical systems the use of three-dimensional multi-body modeling techniques, (Nikravesh, 1988), (Eberhard and Schiehlen, 2006), (Schiehlen, 1997), (Schiehlen, 2007) and (Yoo et al., 2007), is especially challenging. This is mainly related to modeling of structural flexibility, although this has been subjected to quite extensive research, (Shabana, 1997), (Pascal, 2001), (Braccesi et al., 2004), (Bouzgarrou et al., 2005), (Gerstmayr and Schöberl, 2006), (Munteanu et al., 2006), (Bauchau et al., 2008) and (Naets et al., 2012). Many of the modern techniques are based on finite element (FE) formulations and are not always possible to apply when using multi-domain simulation software packages. Therefore lumped parameter approaches such as those used by Banerjee and Nagarajan (1997), Hansen et al. (2001) and Raman-Nair and Baddour

(2003) are also highly relevant because they are easy to implement and require relatively little computational effort while offering accuracy that is sufficient for many purposes. Lumped parameters techniques for modeling of structural flexibility and damping are discussed in section 3.1.

For modeling of hydraulic components and systems, challenges are first of all related to the fact that model parameters are difficult to acquire or not available at all. Therefore experimental work is often required and certain model structures have to be assumed which allow for simplifications without ignoring or underestimating important physical phenomena. These challenges are especially pronounced for components such as cylinders, directional control valves and pressure control valves like counterbalance valves.

Modeling of friction is a well-documented topic, (Bo and Pavelescu, 1982), (Armstrong-Hélouvry et al., 1994), (Olsson et al., 1998) and (Maré, 2012). Friction in hydraulic cylinders has been investigated several times and quite accurate models have been developed, (Bonchis et al., 1999), (Yanada and Sekikawa, 2008), (Márton et al., 2011), (Ottestad et al., 2012) and (Tran et al., 2012). However the number of required model parameters represents a problem because they cannot be determined without experimental work. Consequently, simpler model often have to be used which, naturally, neglects certain physical phenomena but nevertheless are sufficient for most design purposes. This is further discussed in section 3.2.

Modeling of spool type directional control valves is also quite well documented and has been investigated, e.g., by Handroos and Vilenius (1991), Käppi and Ellman (1999), Käppi and Ellman (2000), Gordic et al. (2004), Nielsen et al. (2006) and Maré and Attar (2008). Other types of flow control valves and pressure control valves have been investigated by Zhang et al. (2002), Muller and Fales (2008), Opdenbosch et al. (2009), Ruan et al. (2001) and Alirand et al. (2002). Modeling of hydraulic valves is often problematic due to the limited information available from datasheets and due to physical phenomena such as friction and resulting hysteresis, nonlinear discharge area characteristics, varying discharge coefficients and varying flow forces. Computational fluid dynamics (CFD) may be used to provide insight in some of these phenomena, but often experimental work and semi-physical or non-physical modeling approaches are required for time domain simulation. This is addressed in further details in section 3.2.

Today there are no rules for selection of components, design optimization and modeling of hydraulically actuated machines like offshore pipe handling equipment. In this dissertation contributions in these areas are put forward and treated in details in the five appended papers.

Modeling of mechanical multi-body systems with attention to structural flexibility is treated in papers I and IV. Modeling, testing and parameter identification of directional control valves with main focus on dynamic characteristics are treated in paper II and also discussed in papers III and IV. Modeling of counterbalance valves with main focus on

steady-state characteristics is treated in papers III and IV. In paper IV also modeling of hydraulic cylinders is discussed and a procedure for parameter identification for models of hydraulic-mechanical systems is presented.
Steady-state design procedures for hydraulic systems are discussed in paper III and a design optimization method for reduction of oscillations is presented. Paper V deals with dynamic considerations in design of electro-hydraulic motion control systems for offshore pipe handling equipment.
All the presented methods are developed to accommodate the needs of the system designer. They take into account the limited access to component data and time available for model development and design optimization, which are the main challenges for the system designer. The methods also address the problem of required knowledge within several disciplines, e.g., by suggesting modeling assumptions and experimental work suitable for system design.

Chapter 2

Offshore Pipe Handling Equipment

Offshore drilling rigs include a wide range of highly specialized machines, which are used to perform different operations, see Fig. 2.1. Besides the top drive and the hoisting system, topside equipment may be divided into the following categories:

- **Drill floor equipment**. This includes machines such as the roughneck, which is used to connect and disconnect the drill pipes that make up the drill string.
- **Pipe handling equipment**. This includes a number of different handling tools and crane types, which are used to handle and transport drill pipes and risers between different locations on the rig.
- **BOP handling equipment**. This is used to handle the blowout preventer (BOP).
- **Compensaters and tensioners**. Compensators include both passive and active heave compensation equipment and are used to either maintain a constant weight on bit (WOB) while drilling or keeping the top drive in a fixed position while the rig is moving. Tensioners are used to maintain a constant tension in the riser to avoid buckling while the rig is moving.
- **Mud pumps and drilling fluid handling systems**. Mud pumps are used to pump drilling mud into the well while drilling in order to cool and lubricate the drill bit and to carry cuttings from the well to the top side where it is separated from the mud by the drilling fluid handling system.
- **Hydraulic power units**. These are used to supply fluid power to the hydraulically actuated machines onboard the rig.
- **Control and monitoring system**. This is used to control and monitor the equipment and the drilling process.

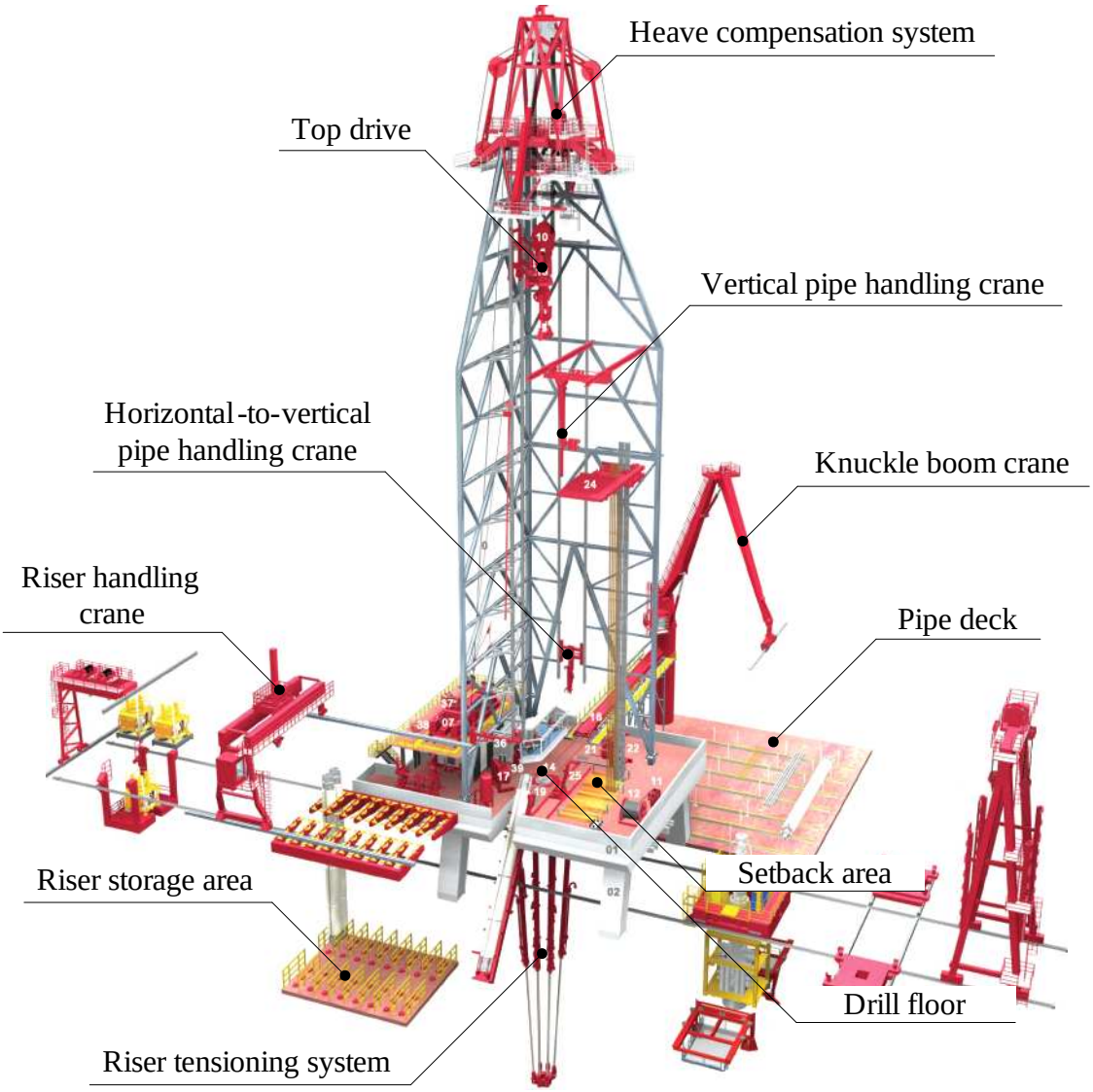

Figure 2.1: Typical drilling rig layout. *Image courtesy of Aker Solutions.*

On a typical drilling rig, the pipe handling equipment consists of a knuckle boom crane and a tubular feeding machine which are used to transport drill pipes between the pipe deck and the drill floor. On the drill floor there is usually a horizontal-to-vertical pipe handling crane, a so-called mousehole and vertical pipe handling system which are all used to build stands (assemblies of either three or four drill pipes) and to transport the stands between the setback area and the well center.
The riser elements are transported between the riser storage area and the drill floor by means of a riser handling crane, a riser chute and a manipulator arm located on the drill floor.

2.1 The Knuckle Boom Crane

For the design engineer, the knuckle boom crane is a challenging application because its dynamic characteristics change significantly with the operating conditions, e.g., size of payload and position and speed of the actuators of the crane.
Knuckle boom cranes are used for a wide range of offshore and marine operations and therefore exist in different variations. The cranes used for pipe handling typically have three booms or jibs as the one shown in Fig. 2.2 and the one considered in paper IV, but may also have of only two jibs as the one considered in paper I.

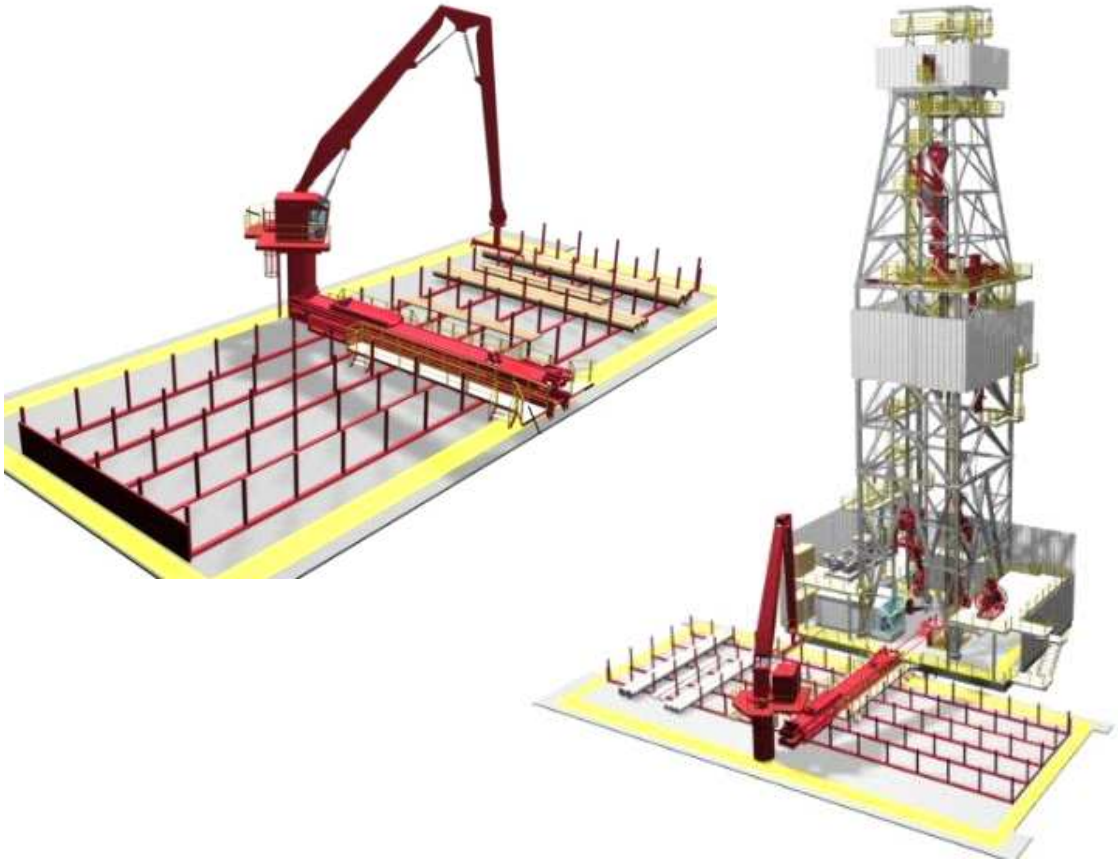

Figure 2.2: Pipe handling knuckle boom crane. *Image courtesy of Aker Solutions*.

The crane may be treated as a large multi-domain system consisting of three interacting systems:

1. A mechanical system.
2. An electro-hydraulic actuation system.
3. An electronic control system.

The mechanical system provides the geometric and structural properties of the crane while the other two systems constitute the motion control system. The main components of the mechanical system are a rotating part mounted on a pedestal with a slewing bearing and either two or three crane jibs and a gripping yoke connected in series by means of hinges. The crane is controlled from the operator's cabin mounted on the rotating part, also called the king.
The actuation system consists of several hydraulic circuits supplied by a hydraulic power unit (HPU) with constant supply and return pressures, p_S and p_R. Together with the control system, the circuits of the actuation system make up a number of motion control sub-systems, each controlling one degree of freedom (DOF). A simplified schematic of a typical motion control sub-system is shown in Fig. 2.3.

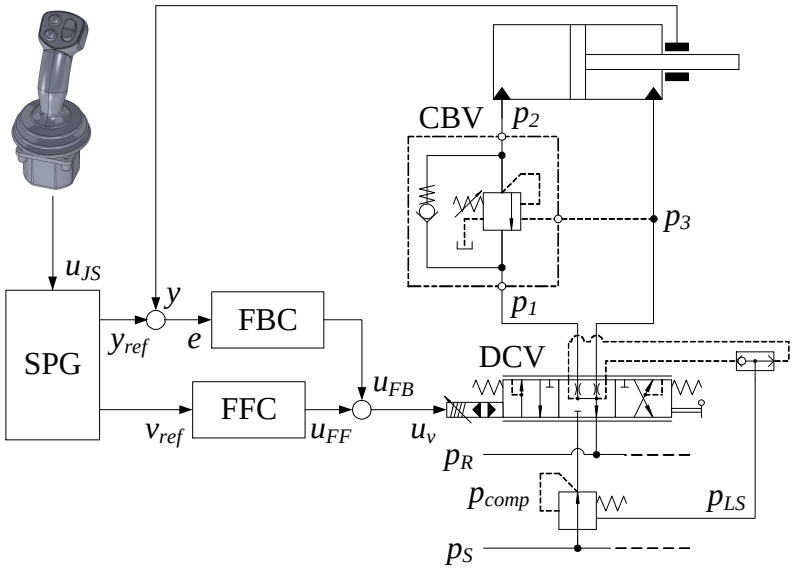

Figure 2.3: Typical motion control sub-system.

The illustrated circuit is used to control the inner jib of the crane and consists of a cylinder with integrated position sensor, a counterbalance valve (CBV) and a directional control valve (DCV) as the main components of the actuation system.
The cylinder motion is controlled with the DCV, which controls the flow into either of the two cylinder chambers. When the cylinder is exposed to negative loads (piston velocity and load force have the same direction), also the outlet pressure of the cylinder needs to be controlled. This is normally handled by the CBV, which provides a relief valve functionality on the outlet side of the cylinder assisted by the pressure on the inlet side. Negative loads occur during load lowering and can occur in both directions of motion for cylinders controlling the intermediate and outer jibs. In these cases CBVs are required on both the piston side and the rod side of the cylinder.

This is also required for motor circuits such as the one controlling the slewing motion of the crane where the inertia load needs to be controlled. CBVs exist in different variations, e.g., externally vented, non-vented and relief compensated, due to the different applications they are used for.
Most often a pressure compensated DCV with electro-hydraulic actuation and closed loop spool position control is used. The reason for this is that it provides load independent flow control which reduces the requirements for the control system and makes it easier to tune the controller gains. Furthermore, load independent flow control is required whenever an operator is to control more than one DOF at the time without assistance from the control system.
Offshore knuckle boom cranes generally feature a high degree of automation compared to other types of cranes. The control strategy relies on position and/or velocity feedback from the individual DOFs. The control system consists of four elements:

- Human-machine interface (HMI)
- Set point generator (SPG).
- Feedforward controller (FFC).
- Feedback controller (FBC).

Besides monitors, push buttons and switches, the HMI contains two joysticks which the operator uses to generate command signals for the control system. Joystick signals are fed to the SPG where they may be treated in different ways depending on the selected control mode. In open loop control mode the joystick signal, u_{JS}, is fed directly to the DCV as a feedforward signal, see Fig. 2.3. In closed loop control mode joystick signals are transformed into velocity and position references for the individual cylinder motions. The latter is used for path control of the crane's gripping yoke where several DOFs are controlled in a coordinated manner.
The FFC is a scaling of the velocity reference, v_{ref} and the FBC is usually a PI controller which compensates for disturbances and accumulated position errors, $e = y_{ref} - y$. The control system usually also contains an element which compensates for deadband of the DCV. The system architecture shown in Fig. 2.3 is a popular structure because of its simple and, consequently, robust design. Furthermore, the controllers are easy to tune because of the load independent flow control.

Chapter 3

Modeling and Parameter Identification

Even though techniques have been around for several decades, modeling for dynamic simulation has become significantly easier during the last decade alone. Today there exists a number of commercially available software packages such as MATLAB/Simulink, SimulationX, AMESim, Dymola, Maple/MapleSim and 20-sim, which can be used for time domain simulation of multi-domain systems such as hydraulic-mechanical systems. All these software packages are based on graphical environments in which models are developed simply by drag-and-drop and connection of generic model components from the integrated model libraries.

Most of the tools also facilitate development of user-defined model components, which is often required for modeling of hydraulic components. Furthermore, with standards like the Modelica language and functional mock-up interface (FMI) models can be exchanged and used with several different simulation tools, making simulation more platform independent.

For the work presented in this dissertation, several different software packages have been used. For the work in paper I, SimulationX is used for modeling and simulation and for the remaining papers Maple/MapleSim is used. In papers II, III, IV and V also MATLAB/Simulink is used for different purposes.

In model based design the actual modeling is closely linked to the design objectives. The main challenge is to minimize the complexity of the models without ignoring or underestimating important physical phenomena. Put in another way, models must be as simple as possible and as detailed as required.

For system designers this challenge involves setting up suitable models of mechanical structures and sub-supplier components for which the required data may be difficult to acquire or not available. This is especially pronounced for hydraulic components and therefore experimental work may be required to identify missing models parameters. As time, resources and practical circumstances seldom allow for full-scale experimental

work for verification of complete system model, testing and experimental work may be carried out with partial systems or separate components for verification of sub-models. Testing and model parameter identification of DCVs and CBVs is treated in papers II and IV, respectively, and in paper IV an approach for experimental model verification of a complete crane model is described. The approach involves three steps where the first is to consider the steady-state forces on the actuators in order to tune the masses and centers of gravity of the bodies of the mechanical model and to identify friction parameters for the actuators. In the second step steady-state pressures are considered in order to tune steady-state characteristics of the valves of the hydraulic model. In the third step the system dynamics, i.e., vibration frequencies and vibration levels, are considered in order to tune mechanical and hydraulic flexibility and damping.
In general the calibration and verification of a model can be illustrated as in Fig. 3.1.

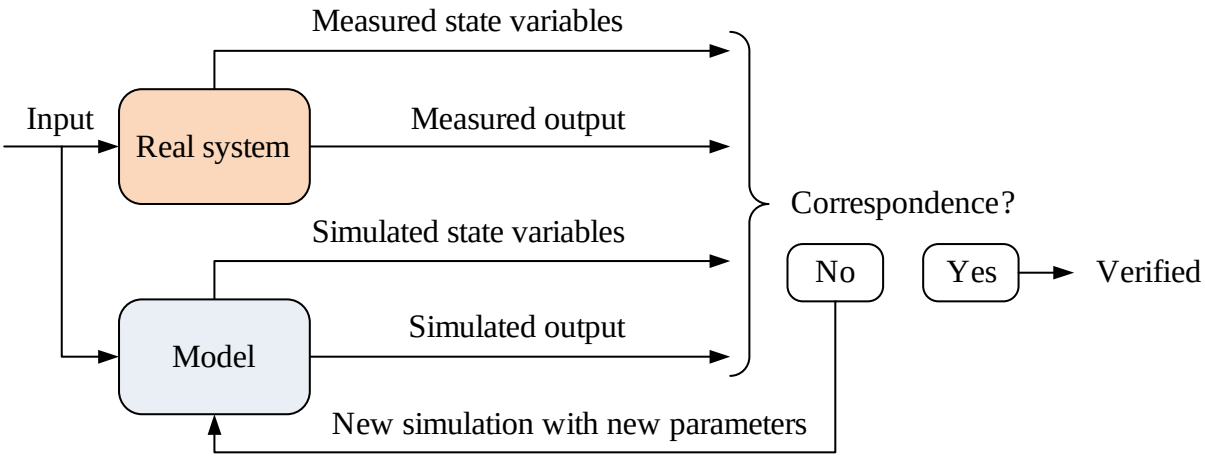

Figure 3.1: Principle of model verification.

In order to calibrate and verify the model, the inputs from the experiments are fed to the model and the uncertain parameters are systematically tuned (identified) until both simulated outputs and state variables correspond to those obtained in the experiments. This is described in further details in paper IV.
Model verification is closely related to model validation, and although the meanings of the two terms are different they are often used interchangeably. Model verification is concerned with implementation of the model and whether the model parameters are correct. Model validation, on the other hand, is concerned with the model structure and whether the model is an accurate representation of the real system being considered. Consequently, if the model verification, i.e., parameters identification, fails then the model validation also fails and the model structure needs to be reconsidered.

3.1 Mechanical Systems

For modeling of complex mechanical systems, like the knuckle boom crane described in section 2.1, it is often an advantage to use a multi-body system (MBS) modeling approach. MBS libraries are available in many of the previously mentioned modeling and simulation tools and even extensive models can be developed relatively fast with generic model components. But even though these tools are intuitive and easy to use, modeling of mechanical systems is still a difficult task.
First of all it may be difficult to identify a suitable kinematic structure for the model. This is often the case when the system contains closed kinematic chains, which is the case for the knuckle boom crane. The topology of the crane is globally an open kinematic chain, formed by the crane jibs, but with locally closed chains formed by the hydraulic cylinders.
To avoid over-constraining the model, it is often helpful to compute the number of DOFs, or *independent coordinates*, which is determined by the number of bodies and the total number of constraints:

$$n_{DOF} = 6 \cdot n_{bodies} - n_{constraints} \tag{3.1}$$

The total number of constraint is determined by the number and types of joints used in the model. For a system like a knuckle boom crane, the most commonly used joints are the prismatic joint (PJ), the revolute joint (RJ), the universal joint (UJ) and the spherical joint (SJ) and the number of DOFs may be determined by:

$$n_{DOF} = 6 \cdot n_{bodies} - 5 \cdot n_{PJ} - 5 \cdot n_{RJ} - 4 \cdot n_{UJ} - 3 \cdot n_{SJ} \tag{3.2}$$

However the main challenge when modeling a system like the knuckle boom crane is to include the structural flexibility in an appropriate way. As mentioned in section 1.2 many modern techniques for flexibility modeling are based on FE formulations, which are not always possible to use together with multi-domain simulation software. Although more and more of these software packages include modules and toolboxes for import of FE results, the use of these formulation are still problematic because they are computational demanding. Furthermore, FE models of the considered structure may not be available and will therefore require additional work if an FE approach is chosen.
Lumped parameter modeling techniques such as the *finite segment method* (FSM), (Huston, 1981), (Huston, 1991), (Huston and Wang, 1993), (Connelly and Huston, 1994a) and (Connelly and Huston, 1994b), are usually less computational demanding, easier to implement and often offer sufficient accuracy. For modeling of bending and torsion, flexible members are divided into a number of rigid segments which are connected with revolute joints and rotation springs corresponding to the considered mode of deflection,

i.e., in-plane bending, out-of-plane bending or torsion. The spring stiffnesses can easily be calculated from geometrical and material properties. Application of the method is described in detail in papers I and IV.

In paper I the effectiveness of the method is investigated by considering the outer jib of a knuckle boom crane. A finite segment (FS) model with nine segments is developed along with an FE model and both static deflections and natural frequencies of in-plane and out-of-plane bending of the two models are compared. Even with a rather rough approximation of the stiffnesses for the FS model a satisfactory correspondence between the FS and FE models is achieved, regarding both dynamic and static behavior. After a simple calibration of the FS model the natural frequencies are equal to those of the FE model, however some deviations for the static deflections remain. Even though FE models may not represent the behavior of real structures, the results in paper I show that FS models are accurate enough for many engineering purposes when compared to FE models.

In paper IV FSM is used to model the structural flexibility of a complete knuckle boom crane. Here the pedestal, the inner jib and the outer jib are assumed to dominate the overall flexibility of the crane and the remaining structural members are modeled as rigid. The three flexible members are divided into a significantly lower number of segments than the one in paper I, but stiffnesses are approximated in the same way.

The damping is also considered and determined using the approach described by Mostofi (1999). With this approach damping parameters are determined by means of predetermined stiffnesses and stiffness multipliers which depend on the natural frequencies and viscous damping ratios of the considered structures.

For this model the stiffness and damping parameters are calibrated along with the stiffness of the hydraulic oil (bulk modulus) in the third step of the verification procedure described in the introduction of this chapter. In order to achieve a satisfactory correspondence between simulations and experimentally obtained results the structural stiffnesses are reduced to almost half of their approximated values and the damping parameters are nearly doubled.

The reason for this significant difference between approximated and calibrated parameters is that a lot of the flexibility and damping of the real system is not included in the model. Only half of the structural members are modeled as flexible, but the remaining members and the foundation of the crane obviously also contribute to the overall flexibility. This also affects the overall damping of the model and besides the structural damping, connections between the members will also offer some damping in terms of friction.

The simple parameter approximations may be reasonable when considering structural members individually, but for multi-body systems with un-modeled dynamics, calibration of flexibility and damping parameters is required. In terms of dynamic behavior

the low number of segments also seems to be acceptable as long as experimental result are available for model calibration. In paper IV the static behavior, i.e., deflections of flexible members, of the mechanical model is not investigated as it is less important for the purpose of the model. However, due to un-modeled flexibility and low number of segments, a relative poor accuracy in terms of static behavior is to be expected.

3.2 Hydraulic Components and Systems

While the model of the mechanical system is based on physical (white-box) modeling, the motion control system model is mostly based on semi-physical (grey-box) modeling. The main reason for this is that manufacturers of hydraulic components do not provide enough and sufficiently detailed information to establish physical models. In addition, physical models of the phenomena related to tribology and fluid mechanics within valves and actuators will quickly become too complex and computational demanding for system simulation. Therefore certain model structures have to be assumed which allow for simplifications without ignoring or underestimating important physical phenomena.
For modeling of hydraulic components, DCVs, CBVs and cylinders have been the main focus as these are the most important components in motion control sub-systems such as the one shown in Fig. 2.3.
Hydraulic valves are generally modeled as variable orifices with linear opening characteristics:

$$Q = \xi \cdot C_V \cdot \sqrt{\Delta p} \tag{3.3}$$

Here ξ is the relative opening of the valve, i.e., a dimensionless number between 0 and 1. It can be a function of system pressures or controlled with an input signal depending on the considered type of valve. Q is the volume flow through the valve and Δp is the pressure drop across it.
The flow coefficient in (3.3) can be expressed as:

$$C_V = C_d \cdot A_d \cdot \sqrt{\frac{2}{\rho_{oil}}} \tag{3.4}$$

The discharge coefficient, C_d, and the discharge area, A_d, are usually not specified for a valve. Instead C_V can be obtained from characteristic flow curves given in the datasheet of the valve. From this, a nominal flow, Q_{nom}, corresponding to a nominal pressure drop, Δp_{nom}, can be identified and used to derive the flow coefficient:

$$C_V = \frac{Q_{nom}}{\sqrt{\Delta p_{nom}}} \tag{3.5}$$

This corresponds to the fully opened state of the valve, so with (3.3) it is assumed that the discharge coefficient, C_d, is constant and only the discharge area, A_d, varies with the relative opening of the valve.
This modeling approach works well for DCVs with closed loop spool position control where dither is used to eliminate static friction and certain design details are used to reduce the disturbances from flow forces.
In some cases the approach may also work for pressure control valves like CBVs. Most often though, attempting to establish physical or semi-physical models of such valves will encounter a number of challenges, e.g., related to friction and resulting hysteresis, non-linear discharge area characteristics, varying discharge coefficients and varying flow forces. Therefore, a better way to model those types of valves may be to use a non-physical (black-box) approach as described in section 3.2.2.
The following sub-sections describe the modeling techniques applied for DCVs, CBVs and hydraulic cylinders.

3.2.1 Directional Control Valves

Modeling of DCVs has been investigated numerous times and many of the mentioned software packages have generic models of 4/3 DCVs included in the model library. But because these models are generic they do not necessarily provide a satisfactory description of all the details of a specific DCV. In papers II, III and IV a tailor-made model of pressure compensated DCVs is presented. In paper II the structure of the model is discussed and in papers II and IV a slightly different model is used.
The main focus of paper II is the dynamics of pressure compensated DCVs and how to investigate this experimentally. An approach for frequency response testing of such valves is presented and as a case study a commonly used DCV, Danfoss PVG32, is considered. The test results reveal a bandwidth of not more than 5 Hz, which is significantly lower than for industrial non-compensated servo valves.
For DCVs it is common to define the bandwidth as the frequency at 90° phase lag in a Bode plot. This differs from the traditional definition used in control theory where the bandwidth is defined as the frequency at - 3 dB magnitude. The main reason for using the frequency at 90° phase lag may be that it is a more reliable point of reference. Secondly, the dynamics of DCVs is classically modeled as a second order system and therefore the bandwidth is equal to the natural frequency used for the model. As seen from the test results in paper II, a second order system is not an accurate representation of the valve dynamics. However, up to and around the frequency at 90° phase lag, a second order model corresponds quite well to the test results.
A more accurate description of the valve dynamics can be achieved by using a third order system, as it has been shown by Tørdal and Klausen (2013). However, this involves

more parameters to be determined. In this work it is generally assumed that a second order system is sufficient.
The model in paper II also uses a second order system to represent the valve dynamics. The main spool is modeled as four variable orifices and four opening functions which represent the relation between a normalized spool position signal (output of the second order system) and the opening of the orifices that represent the spool edges. The pressure compensator is also modeled as a variable orifice with an opening function based on a pressure equilibrium. In papers III and IV the compensator model is replaced by a simple function that only requires one parameter, the pressure setting of the compensator, which is usually known. Although this representation may be conservative, it is considered to be a more reliable modeling approach and, furthermore, it eliminates the need to model the volume between the compensator and the main spool. This is usually a very small volume which may generate stiff models. By excluding this volume, the model therefore becomes less computational demanding.

3.2.2 Counterbalance Valves

Due to their tendency to generate instability and generally oscillatory behavior, modeling and use of CBVs have been subject to quite extensive research, (Miyakawa, 1978), (Overdiek, 1981), (Persson et al., 1989), (Handroos et al., 1993), (Chapple and Tilley, 1994), (Ramli et al., 1995), (Zähe, 1995), (Rahman et al., 1997), (Lisowski and Stecki, 1999) and (Andersen et al., 2005). As previously mentioned, physical modeling of CBVs is often complicated by unpredictable physical behavior and lack of model parameters. In papers III and IV two different CBVs are considered and modeled with two different approaches.
In paper III a simple semi-physical model is used. It consists of a variable orifice for which the opening is determined by a pressure equilibrium. It does not take phenomena like friction and flow forces into account, but it is experimentally verified that the model is accurate enough to describe the steady-state behavior of the considered valve.
In paper IV a novel non-physical (black-box) model is developed and presented. The model uses two different pressure ratios to compute the flow through the valve together with a number of parameters that must be experimentally determined. Ideally, these should be identified through a thorough mapping of the flow through the valve for different pressure combinations at the individual ports. Alternatively, as it is done in the paper, they can be determined with parameter identification techniques and suitable measurements from the system where the valve is installed.
The parameter identification represents the second step the in verification procedure introduced in the beginning of this chapter and is carried out by means of an optimization routine that minimizes the deviation between the measured flow and the simulated flow

through the CBV. For the considered valve it is not possible to use a semi-physical model as in paper III and only with the developed black-box model it is possible to model the real behavior with sufficient accuracy.

3.2.3 Cylinders

Modeling of cylinders and cylinder friction has been investigated numerous times and also for cylinders generic models are available in simulation software packages.
The friction in the cylinder is quite complex, especially around zero velocity. As described in Ottestad et al. (2012), it consists of both static and coulomb friction as well as velocity dependent and pressure dependent friction, which may be described with a model of five parameters. Even though the model is not very complex, the number of parameters represents a problem because they cannot be determined without an extensive experimental study of the considered cylinder. Consequently, an even simpler model must be used as it is done in papers III and IV.
In both papers the friction force is modeled as a static friction and pressure dependent friction. In paper III experimentally determined parameters from Ottestad et al. (2012) are used, as cylinders of equal size are used in both papers. In paper IV the friction model parameters are identified during the first step in verification procedure described in the introduction of the chapter and is carried out by means of an optimization routine that minimizes the deviation between the measured pressure forces and simulated pressure forces for the considered cylinder.
In terms of steady-state behavior the simple friction model seems to be sufficient for hydraulic system design. The simple model is acceptable because the system behavior around zero-velocity of the cylinder is less important.

Chapter 4

Design and Optimization

The usability of dynamic simulation has increased rapidly during the last decade and is becoming a popular design evaluation tool in many industries including the offshore industry. Naturally, the reason for this is the development of simulation software packages, as the ones mentioned in the previous chapter, combined with the computational power and availability of modern PCs.
In other industries, like the automotive and aerospace industries, simulation has been used for several decades and today it is an integrated part of the design process. In that perspective, the offshore industry has yet to develop. The main reason for this is probably that the offshore industry historically has relied mostly on experience and less on academic skills. Another reason is that products are much less standardized. New products are often delivered, practically as prototypes, and existing products are often delivered with modifications. This requires time consuming work and a lot of experience and at the same time the required time-to-market is constantly being reduced.
This only promotes the need for model based design approaches where virtual prototypes can be used to evaluate a design in order to avoid mistakes, making better and faster decisions and optimize solutions. Design of offshore equipment like a knuckle boom crane is obviously an iterative process involving design of the mechanical system, the hydraulic system and the control system. In reality, however, detailed design of these systems is carried out separately as concurrent activities and with constraints imposed by a conceptual design. The conceptual design is then revisited if it later proves to be unsuitable.
This approach leaves a potential for several design changes during the individual design activities which affect other design activities because design of the individual systems depend on each other. Having parameterized simulation models and procedures for post-processing of simulation results for the different design activities will certainly be both helpful and time saving.

4.1 Hydraulic System Design

The task of designing hydraulic systems involves two main activities; choice of system architecture and sizing/selection of system components. The first one is often based on design rules and experience with suitable architectures for the considered application. Selection and sizing of the system component is an iterative process because the choices of the individual component affect each other. Changes regarding types and sizes of components may need to be made after the first design iteration and even a change of system architecture may need to be included in the following iterations before arriving at a satisfying design. To reduce the number of iterations the design process can be set up as a systematic and stepwise procedure based on simple steady-state considerations and empirical design rules. An example of a general procedure is described by Stecki and Garbacik (2002).
For a piece of offshore equipment like the knuckle boom crane a steady-state procedure for design of the hydraulic system typically consists of the following steps:

1. Selection/sizing of actuators.
2. Selection of directional control valves.
3. Selection of pressure control valves, e.g., counterbalance valves.

This is described in further details in paper III. Furthermore, pipelines and any protective components such as shock and anti-cavitation valves also need to be sized. HPU design including selection and sizing of pump(s), sizing of reservoir, design of cooling system and selection of filtering system could represent additional steps in the procedure. However, since the HPU is used to supply several machines, this is designed through a separate procedure based on the requirements and operating cycles of all the machines it is used to supply.
With steady-state design procedures, components can relatively easy be sized to ensure sufficient force/torque and speed for control of the considered function. However, dynamic characteristics such as stability and accuracy cannot be addressed through such procedures.

4.2 Use of Simulation Models

The only way to investigate the dynamic characteristics of a system before it is build, is to develop a model with the techniques described in the previous chapter and to simulate the relevant operating cycles and conditions. For motion control systems, like the one

shown in Fig. 2.3, the components that influence the dynamic behavior of the system are the CBV and the DCV.
Among other parameters, the one that affects the stability the most, is the pilot area ratio of the CBV. Usually it is set high for energy efficiency purposes and only lowered if the system becomes too oscillatory. The accuracy of an electro-hydraulic closed loop control system is affected by the DCV bandwidth, but also less controllable parameters like actuator friction, hose/pipe volumes and the effective stiffness of the system.
In paper III stability issues are addressed by considering a nominal design of an electro-hydraulically actuated crane boom which is inherently unstable. A concept for reducing the oscillations in the system during load lowering is presented and subjected to a design optimization. The concept is based on increasing the pilot area ratio of the CBV, as opposed to the classical approach of reducing it, and narrowing the return edge of the DCV in order to increase system pressures and force the CBV to open fully. By forcing it to open fully, it works as a fixed orifice and the basic oscillatory behavior related to the CBV is removed.
The concept is also compared to a concept of throttling both with the CBV and the return edge of the DCV. For both designs optimal design parameters are identified using the Complex method, (Box, 1965), and their feasible load ranges are identified. The results show that throttling with both the CBV and DCV will reduce oscillations in any case and that this concept is the best if large load ranges are to be handled. However, if smaller load ranges are to be handled, the concept of forcing the CBV to open fully is the best solution because the unreliable behavior of the CBV is removed.
The applied optimization method, the Complex method, has been used several times for design and optimization of hydraulic systems, e.g., by Krus et al. (1991), Andersson (2001) and Hansen and Andersen (2001) and has the advantage of being fast and easy to implement. The method is based on repetitive substitution of the worst design in a design population, typically twice the size as the number of design variables, by reflecting the point representing the worst design through the centroid of the remaining points in the design space. This process is repeated until a convergence criterion is met; i.e., the points in the design space are gathered around the same point, the optimum, within some tolerance.
For optimization of hydraulic systems, non-gradient based methods such as the Complex method and genetic algorithms are often used, probably because it is relatively easy to evaluate the design with a simple performance index, which can be obtained on the basis of a dynamic simulation. The main requirement, when using simulation for design optimization, is to have a procedure for design evaluation, i.e., post-processing of the simulation results. For hydraulic systems, a good nominal design can usually be obtained based on systematic steady-state design procedures, leaving only a few parameters to be optimized. The final tuning may then simply be carried out by means of brute

force optimization, where the designer is changing the design parameters manually.
In paper V the influence of the DCV bandwidth and ramp signals are investigated. An often referred design rule states that the bandwidth, ω_v, of the DCV should be at least three times higher than the natural frequency, ω_{hm}, of the hydraulic-mechanical system it is used to control, (MOOG, 2012):

$$\omega_v \geq 3 \cdot \omega_{hm} \tag{4.1}$$

This applies if the valve bandwidth should not affect the overall bandwidth of the total system consisting of the valve and the hydraulic-mechanical system it is used to control. Furthermore, it applies for servo applications where fast response and high precision is required and where non-compensated DCVs are used. By considering a simplified representation of a DCV and a hydraulic-mechanical system (two second order systems in series), it is shown that when applying (4.1) then the overall bandwidth of the system will not be less than 90 % of that of the hydraulic-mechanical system.
In the paper it is also investigated how the natural frequency, ω_n, affects the system's ability to follow a reference motion. By considered the ramping of a simple mass-spring-damper system a rule of thumb is derived which sets a lower limit of the ramp time, t_r, of the reference signal for the system:

$$t_r \geq \frac{6}{\omega_n} \tag{4.2}$$

To investigate how well this rule of thumb applies to a real system, like a knuckle boom crane, the experimentally verified model from paper IV is considered. First a map of how the natural frequency of the crane varies with the cylinder lengths is generated. The map is used to identify a relevant natural frequency to be considered for design purposes. Next the model is used to simulate the position error for various ramp times and DCV bandwidths.
The simulations show a similar effect as seen for the mass-spring-damper system. The relative error increases significantly for $t_r \cdot \omega_{hm} < 6$ at least for $\omega_v > \omega_{hm}$. Furthermore, the relative error is doubled by choosing $\omega_v = 2 \cdot \omega_{hm}$ and tripled for $\omega_v = \omega_{hm}$ compared to the ideal situation of $\omega_v = \infty$. Only minor improvements are achieved for $\omega_v > 3 \cdot \omega_{hm}$. The results seem to support the design rules in (4.1) and (4.2).
The simulations also show that the maximum position error is almost independent of the ramp time and only depend on the DCV bandwidth. This indicates that if the relative error is irrelevant, then the ramp time does not need to be taken into account. However too short ramp times may cause instability while too long ramp times increase the maximum reference velocity and consequently the required flow.

The simulation results confirm the validity of (4.1) and (4.2) and usefulness as general design rules. However, the selection of these design parameters always depend on the acceptable error level for the application to be controlled and for offshore knuckle boom crane the investigated design rules may be too conservative. A prerequisite to evaluate this is to have a simulation model, like the one described in paper IV.

Chapter 5

Conclusions

In this dissertation methods for modeling, parameter identification, design and optimization of a selected piece of offshore pipe handling equipment, a knuckle boom crane, have been put forward. Most of the modeling methods are general and can be used for other types of hydraulically actuated cranes. Some of the design methods are also general and can be used for many types of electro-hydraulic motion control systems. A part of the design methods, though, are specifically targeting offshore knuckle boom cranes and are not suited for other cranes like onshore cranes, simply because design requirements are different.
The presented methods are developed to accommodate the needs of the system designer. They take into account the challenges encountered by the system designer such as limited access to component data and time available for model development by applying a level of modeling detail that is suited for system design.

5.1 Contributions

The main challenge of modeling mechanical systems like a knuckle boom crane is to include the structural flexibility in an appropriate way. In paper I the finite segment method (FSM) is used to model a single crane boom. The finite segment (FS) model is compared to a finite element (FE) model and very good conformity for both static and dynamic behavior is achieved. Even though FSM does not represent state of the art of flexibility modeling, this paper shows that FSM is both efficient and sufficient for modeling for system design.
This is confirmed in paper IV where FSM is used to model structural flexibility and damping of a complete knuckle boom crane and experimentally obtained results are used to calibrate and verify the model. In the paper, approaches for approximation of flexibility and damping parameters are also presented. However, these parameters usually have

to be experimentally verified and, as it is shown in the paper, it is not uncommon that the flexibility parameters must be reduced by a factor of two and vice versa for the damping parameters. Naturally, the reason for this is the un-modeled flexibility and damping that is inconvenient or too difficult to introduce separately.

For modeling of directional control valves (DCVs) the main challenge is to include a sufficiently accurate representation of the valve dynamics. This is often modeled as second order system, as it is in paper II. However, for many valves, like pressure compensated DCVs, information about dynamic performance is not available and have to be experimentally determined. In paper II an approach for frequency response testing is presented and it is shown that a second order system is only able to describe the valve dynamics up to and around the bandwidth of the valve. However, this is sufficient for system design purposes.

For pressure compensated DCVs another challenge is the modeling of the pressure compensator. In paper II one suggestion is given and in papers III and IV an alternative model is used. The alternative model include less parameters and is less computational demanding. This is an example of always looking for a best practice within modeling for system design.

With respect to modeling, as well as system design, counterbalance valves (CBVs) are some of the most difficult components to handle. In some cases they can be modeled with rather simple semi-physical approaches, but often this leads to a number of challenges, e.g., related to friction and resulting hysteresis, nonlinear discharge area characteristics, varying discharge coefficients and varying flow forces. In those cases the only option may be to use a non-physical (black-box) approach as the one presented in paper IV.

Using this black-box model the steady-state behavior of the considered CBV is simulated with an accuracy that is not possible to achieve with a semi-physical model. The disadvantage of the black-box model is that it relies on several parameters that have to be experimentally determined. However, sufficiently accurate modeling of CBVs will probably always require some sort of experimental work. This is also shown in paper III, where a semi-physical model is used.

In general, modeling for system design of a knuckle boom crane, will require experimental work for model verification. In paper IV a stepwise approach for calibration and verification of a complete crane model is presented. In each step separate sub-models are considered and both optimization techniques and manual tuning is used identify uncertain parameters. This approach may be generalized and used for verification of other types of systems as well.

In paper III design and optimization of hydraulic systems is discussed. It is shown how to arrive at a nominal design with relatively simple steady-state considerations and how simulation can be used to analyze dynamic system behavior. One of the major challenges

with hydraulic systems containing CBVs, is to avoid instability and ensure an acceptable level of oscillations during load lowering. A new method for reduction of oscillations is discussed and subjected to a design optimization using the Complex method. The new method is compared to a more classic method and it is concluded that the new method is the most suitable for offshore knuckle boom cranes.
A central challenge in hydraulic system design is selection of DCVs and to specify the required bandwidth of the valve. In paper V simple design rules for required DCV bandwidth and minimum ramp times for input signals are presented and discussed. An experimentally verified simulation model is used to investigate how these parameters influence both relative and absolute position errors for an electro-hydraulic motion control system.
The investigations confirm the validity of these simple design rules. It is also clear that required DCV bandwidth and minimum ramp times always depend on the acceptable error level for the specific application. For offshore knuckle boom cranes these design rules may be too conservative, however, a prerequisite for investigating this is to have a reliable simulation model.

5.2 Outlook

The main challenge for any model based design approach lies within the ability to produce simulation models that, with a reasonable precision, are able to mimic the behavior of the real system to be designed. Throughout this dissertation and the appended papers a number of modeling challenges have been addressed. While most of them involve existing modeling techniques and mainly aim to identify the required level of modeling detail, also novel modeling techniques have been presented like the black-box model for counterbalance valves presented in paper IV.
The model yield encouraging results in terms of steady-state behavior and it may very well be used for other types of pressure control valves as well. However, there are still issues to be investigated in relation to the applied modeling approach. They include phenomena such as dynamic behavior and the influence of hysteresis. This will require more experimental work and, in general, an approach for mapping of valve characteristics is needed.
A major challenge in the offshore industry is that there are very limited opportunities to build prototypes for design verification. This of course promotes the use of model based design approaches, although it is difficult to verify models before any real systems have been realized. Even then, it may be difficult to carry out experimental studies required for model verification due to cost and time constraints. Therefore there is a need for procedures for both model validation and verification which do not require full scale

experimental work. Such procedures may be based on scale model tests or testing of individual components and mapping of their characteristics as it is suggested in paper II for directional control valves.

Design of hydraulic systems should always be based on sound steady-state considerations before attempting to carry out design optimization. Since system design is often based on existing system architectures the remaining part of the job, the component sizing/selection, could be automated or standardized by setting up systematic procedures and using parameterized steady-state models. The use of dynamic simulation models for design optimization could also be automated. However, after the initial design procedure there are often only a few parameters left to be optimized and the potential gain for automating this procedure is relatively low. The most important value is to have a dynamic simulation model that can be used as a design evaluation tool.

Introducing new actuation technologies such as separate meter-in separate meter-out control and digital hydraulics represent a higher potential than automated design, because they have the potential to improve or even eliminate problems related to stability and efficiency. However, they also represent a higher risk and, once again, the best way to reduce those risks is to utilize dynamic simulation for design evaluation together with an appropriate amount of testing and model verification.

References

Alirand, M., Favennec, F., and Lebrun, M. (2002). Pressure components stability analysis: A revisited approach. *International Journal of Fluid Power*, 3(1):33–46.

Andersen, T. O., Hansen, M. R., Pedersen, P., and Conrad, F. (2005). The influence of flow forces on the performance of over center valve systems. In *Proceedings of the Ninth Scandinavian International Conference on Fluid Power*. Linköping, Sweden.

Andersson, J. (2001). *Multiobjective optimization in engineering design. Applications to fluid power systems*. PhD thesis, Linköping University, Linköping, Sweden.

Armstrong-Hélouvry, B., Dupont, P., and de Wit, C. C. (1994). A survey of models, analysis tools and compensation methods for the control of machines with friction. *Automatica*, 30(7):1083–1138.

Banerjee, A. K. and Nagarajan, S. (1997). Efficient simulation of large overall motion of beams undegoing large deflections. *Multibody System Dynamics*, 1(1):113–126.

Bauchau, O. A., Epple, A., and Heo, S. (2008). Interpolation if finite rotations in flexible multi-body dynamics simulations. *Proceedings of the Institution of Mechanical Engineers, Part K: Journal of Multi-body Dynamics*, 222(4):353–366.

Bo, L. C. and Pavelescu, D. (1982). The friction-speed relation and its influence on the critical velocity of stick-slip motion. *Wear*, 82(3):277–289.

Bonchis, A., Corke, P. I., and Rye, D. C. (1999). A pressure-based, velocity independent, friction model for asymmetrical hydraulic cylinders. In *Proceedings of the 1999 International Conference on Robotics and Automation*, pages 1746–1751. Detroit, Michigan, USA.

Bouzgarrou, B. C., Ray, P., and Gogu, G. (2005). New approach for dynamic modelling of flexible manipulators. *Proceedings of the Institution of Mechanical Engineers, Part K: Journal of Multi-body Dynamics*, 219(3):285–298.

Box, M. J. (1965). A new method for constrained optimization and a comparison with other methods. *The Computer Journal*, 8(1):42–52.

Braccesi, C., Landi, L., and Scaletta, R. (2004). New dual meshless flexible body methodology for multi-body dynamics: simulation of generalized moving loads. *Proceedings of the Institution of Mechanical Engineers, Part K: Journal of Multi-body Dynamics*, 218(1):51–62.

Burrows, C. R. (2000). Fluid power systems - some research issues. *Proceedings of the Institution of Mechanical Engineers, Part C: Journal of Mechanical Engineering Science*, 214(1):203–220.

Chapple, P. J. and Tilley, D. G. (1994). Evaluation techniques for the selection of counterbalance valves. In *Proceedings of the Expo and Technical Conference for Electrohydraulic and Electropneumatic Motion Control Technology*, pages 351–359. Anaheim, USA.

Connelly, J. and Huston, R. L. (1994a). The dynamics of flexible multibody systems: A finite segment approach — I. Theoretical aspects. *Computers and Structures*, 50(2):255–258.

Connelly, J. and Huston, R. L. (1994b). The dynamics of flexible multibody systems: A finite segment approach — II. Example problems. *Computers and Structures*, 50(2):259–262.

da Silva, J. C. (2000). Artificial intelligence enhancing fluid power system design. In *Proceeding of the 48th National Conference on Fluid Power*, pages 157–168. Chicago, Illinois, USA.

da Silva, J. C. and Back, N. (2000). Shaping the process of fluid power system design applying an expert system. *Research in Enginnering Design*, 12(21):8–17.

Darlington, M., Culley, S., and Potter, S. (2001). Knowledge and reasoning issues raised in automating the conceptual design of fluid power systems. *International Journal of Fluid Power*, 2(2):75–85.

Dunlop, G. R. and Rayudu, R. K. (1993). An expert assistant for hydraulic systems. In *Proceedings of the First New Zealand International Two-Stream Conference on Artificial Neural Networks and Expert Systems*, pages 314–316. Dunedin, New Zealand.

Eberhard, P. and Schiehlen, W. (2006). Computational dynamics of multibody systems: History, formalisms, and applications. *Journal of Computational and Nonlinear Dynamics*, 1(1):3–12.

Engler, F., Baum, H., and von Dombrowski, R. (2010). Development environment for fluid-power-mechatronic systems. In *Proceedings of the 7th International Fluid Power Conference*. Aachen, Germany.

Eriksson, B. and Palmberg, J.-O. (2011). Individual metering fluid power systems: challenges and opportunities. *Proceedings of the Institution of Mechanical Engineers, Part I: Journal of Systems and Control Engineering*, 225(2):196–211.

Gerstmayr, J. and Schöberl, J. (2006). A 3d finite element method for flexible multibody systems. *Multibody System Dynamics*, 15(4):309–324.

Gordic, D., Barbic, M., and Jovicic, N. (2004). Modelling of spool position feedback servovalves. *International Journal of Fluid Power*, 5(1):37–50.

Hampson, S. P., Brain, C., Tomlinson, S. P., Chawdhry, P. K., Medland, A. J., and Burrows, C. R. (1996). System design - improved efficiency through software integration. In *Proceedings of the 9th Bath International Fluid Power Workshop*. Bath, UK.

Handroos, H., Halme, J., and Vilenius, M. (1993). Steady-state and dynamic properties of counter balance valves. In *Proceedings of the 3rd Scandinavian International Conference on Fluid Power*, pages 215–235. Linköping, Sweden.

Handroos, H. M. and Vilenius, M. J. (1991). Flexible semi-empirical models for hydraulic flow control valves. volume 113, pages 232–238.

Hansen, M. R. and Andersen, T. (2005). System topology optimization. volume 2, pages 133–141.

Hansen, M. R., Andersen, T., and Conrad, F. (2001). Experimentally based analysis and synthesis of hydraulically actuated loader crane. In *Bath Workshop on Power Transmission and Motion Control*, pages 259–274. Bath, UK.

Hansen, M. R. and Andersen, T. O. (2001). A design procedure for actuator control system using design optimization. In *Proceedings of the 7th Scandinavian International Conference on Fluid Power*. Linköping, Sweden.

Hughes, E. J., Richards, T. G., and Tilley, D. G. (2001). Development of a design support tool for fluid power system design. *Journal of Engineering Design*, 12(2):75–92.

Huston, R. L. (1981). Multi-body dynamics including the effects of flexibility and compliance. *Computers and Structures*, 14(5-6):443–451.

Huston, R. L. (1991). Computer methods in flexible multibody dynamics. *International Journal for Numerical Methods in Engineering*, 32(8):1657–1668.

Huston, R. L. and Wang, Y. (1993). Flexibility effects in multibody systems. In *Computer Aided Analysis of Rigid and Flexible Mechanical Systems: Proceedings of the NATO Advanced Study Institute*, pages 351–376. Troia, Portugal.

Käppi, T. and Ellman, A. (1999). Modelling and simulation of proportional mobile valves. In *Proceedings of the 4th JHPS International Symposium on Fluid Power*, pages 531–536. Tokyo, Japan.

Käppi, T. and Ellman, A. (2000). Analytical methods for defining pressure compensator dynamics. *Fluid Power Systems and Technology*, 7:121–125.

Krimbacher, N., Garstenauer, M., and Scheidl, R. (2001). Optimization of hydraulic systems by means of numerical simulation. In *Proceedings of the 2nd International Workshop on Computer Software for Design*, pages 76–83. Ostrava-Malenovice, Czech Republic.

Krus, P., Jansson, A., and Palmberg, J.-O. (1991). Optimization for component selection in hydraulic systems. In *Proceedings of the 4th Bath International Fluid Power Workshop*, pages 219–231. Bath, UK.

Liermann, M. and Murrenhoff, H. (2005). Knowledge based tools for the design of servo-hydraulic closed loop control. *Power Transmission and Control*, pages 17–28.

Lin, Z.-C. and Shen, C.-C. (1995). An investigation of an expert system for hydraulic circuit design with learning. *Artificial Intelligence in Engineering*, 9(3):153–165.

Linjama, M. and Vilenius, M. (2007). Digital hydraulics - towards the perfect valve technology. In *Proceedings of the Tenth Scandinavian International Conference on Fluid Power*. Tampere, Finland.

Lisowski, E. and Stecki, J. S. (1999). Stability of a hydraulic counterbalancing system of hydraulic winch. In *Proceedings of the Sixth Scandinavian International Conference on Fluid Power*, pages 921–933. Tampere, Finland.

Maré, J.-C. (2012). Friction modelling and simulation at system level: a practical view for the designer. *Proceedings of the Institution of Mechanical Engineers, Part I: Journal of Systems and Control Engineering*, 226(6):728–741.

Maré, J.-C. and Attar, B. (2008). Enhanced model of four way valves characteristics and its validation at low temperature. *International Journal of Fluid Power*, 9(3):35–43.

Merritt, H. E. (1967). *Hydraulic control systems*. Wiley.

Michel, S. and Weber, J. (2012). Electrohydraulic compact-drives for low power applications considering energy-efficiency anf high inertial loads. In *Proceedings of the 7th FPNI PhD Symposium on Fluid Power*, pages 869–888. Reggio Emilia, Italy.

Miyakawa, S. (1978). Stability of a hydraulic circuit with a counterbalance valve. *Bulletin of the JSME*, 21(162):1750–1756.

MOOG (2012). Electrohydraulic valves... a technical look. Technical report, Moog Inc. http://www.moog.com/literature/ICD/Valves-Introduction.pdf.

Mostofi, A. (1999). The incorporation of damping in lumped-parameter modelling techniques. *Proceedings of the Institution of Mechanical Engineers, Part K: Journal of Multi-body Dynamics*, 213(1):11–17.

Márton, L., Fodor, S., and Sepehri, N. (2011). A practical method for friction identification in hydraulic actuators. *Mechatronics*, 21(1):350–356.

Muller, M. T. and Fales, R. C. (2008). Design and analysis of a two-stage poppet valve for flow control. *International Journal of Fluid Power*, 9(1):17–26.

Munteanu, M. G., Gogu, R., and Ray, P. (2006). Fast and simple dynamic analysis of flexible multi-body systems. *Proceedings of the Institution of Mechanical Engineers, Part K: Journal of Multi-body Dynamics*, 220(4):219–237.

Naets, F., Tamarozzi, T., Heirman, G. H. K., and Desmet, W. (2012). Real-time flexible multibody simulation with global model parameterization. *Multibody System Dynamics*, 27(3):267–284.

Nielsen, B., Entwistle, R. T., Tandrup, L. B., and Andersen, T. O. (2006). Parameterised dynamic model of a 4-way spool valve - an experimental study.

Nikravesh, P. E. (1988). *Computer-aided analysis of mechanical systems*. Prentice Hall.

Olsson, H., Åström, K. J., Canudas de Wit, C., Gäfvert, M., and Lischinsky, P. (1998). Friction models and friction compensation. *Europena Journal of Control*, 4(3):176–195.

Opdenbosch, P., Sadegh, N., Book, W., Murray, T., and Yang, R. (2009). Modelling an electro-hydraulic poppet valve. *International Journal of Fluid Power*, 10(1):7–15.

Ottestad, M., Nilsen, N., and Hansen, M. R. (2012). Reducing the static friction in hydraulic cylinders by maintaining relative velocity between piston and cylinder. In *Proceedings of the 12th International Conference on Control, Automation and Systems*, pages 764–769. Jeju Island, Korea.

Overdiek, G. (1981). Design and characteristics of hydraulic winch controls by counterbalance valves. In *Proceedings of the European Conference on Hydrostatic Transmission for Vehicle Applications*. Achen, Germany.

Palmberg, J.-O. (1995). Design of fluid-mechanical systems - methods and tools to meet future needs. In *Proceedings of Hydraulikdagar i Linköping*. Linköping, Sweden.

Papadopoulos, E. and Davliakos, I. (2004). A systematic methodology for optimal component selection of electrohydralic servosystems. *International Journal of Fluid Power*, 5(3):15–24.

Pascal, M. (2001). Some open problems in dynamic analysis of flexible multibody systems. *Multibody System Dynamics*, 5(4):315–334.

Pedersen, H. C. (2004). Power management in mobile hydraulic applications - an approach for designing hydraulic power supply systems. In *Proceedings of the 3rd FPNI PhD Symposium on Fluid Power*, pages 125–139. Terrassa, Spain.

Persson, T., Krus, P., and Palmberg, J.-O. (1989). The dynamic properties of over-center valves in mobile systems. In *Proceedings of the 2nd International Conference on Fluid Power Transmission and Control*. Hangzhou, China.

Rahman, M. M., Porteiro, J. L. F., and Weber, S. T. (1997). Numerical solution and animation of oscillating turbulent flow in a counterbalance valves. In *Proceedings of the Thirty-Second Intersociety Energy Conversion Engineering Conference*. Honolulu, Hawaii, USA.

Raman-Nair, W. and Baddour, R. E. (2003). Three-dimensional dynamics of a flexible marine riser undergoing large elastic deformations. *Multibody System Dynamics*, 10(4):393–423.

Ramli, Y., Chapple, P. J., and Tilley, D. G. (1995). Application of computer aided design (cad) in hydraulic systems using counterbalance valves. In *Proceedings of the 4th International Conference on Computer-Aided Design and Computer Graphics*. Wuhan, China.

Ruan, J., Burton, R., Ukrainetz, P., and Xu, Y. M. (2001). Two-dimensional pressure control valve. *Proceedings of the Institution of Mechanical Engineers, Part C: Journal of Mechanical Engineering Science*, 215(9):1031–1039.

Schiehlen, W. (1997). Multibody system dynamics: Roots and perspectives. *Multibody System Dynamics*, 1(2):149–188.

Schiehlen, W. (2007). Research trends in multibody systems dynamics. *Multibody System Dynamics*, 18(1):3–13.

Schlemmer, K. and Murrenhoff, H. (2008). Development of an expert system for electrohydraulic motion control design. In *The 20th International Conference on Hydraulics and Pneumatics*, pages 259–268. Prague, Czech Republic.

Shabana, A. A. (1997). Flexible multibody dynamics: Review of past and recent developments. *Multibody System Dynamics*, 1(2):189–222.

Stecki, J. S. and Garbacik, A. (2002). Fluid Power Net Publications.

Steiner, B. and Scheidl, R. (2005). A computer aided conceptual design method for hydraulic components. *Power Transmission and Control*, pages 209–221.

Tran, X. B., Hafizah, N., and Yanada, H. (2012). modeling of dynamic friction behaviors of hydraulic cylinders. *Mechatronics*, 22(1):65–75.

Tørdal, S. S. and Klausen, A. (2013). Dynamiske karakteristikker av Brevini HPV41 med åpen og lukket sløyferegulering. Bachelor's thesis, University of Agder, Grimstad, Norway. *In Norwegian*.

Yanada, H. and Sekikawa, Y. (2008). Modeling of dynamic behaviors of friction. *Mechatronics*, 18(7):330–339.

Yoo, W.-S., Kim, K.-N., Kim, H.-W., and Sohn, J.-H. (2007). Developments of multibody systems dynamics: Computer simulations and experiments. *Multibody System Dynamics*, 18(1):35–58.

Zähe, B. (1995). Stability of load holding circuits with counterbalance valves. In *Proceedings of the 8th Bath International Fluid Power Workshop*, pages 60–75. Bath, UK.

Zhang, R., Alleyne, A. G., and Prasetiawan, E. A. (2002). Performance limitations of a class of two-stage electro-hydraulic flow valves. *International Journal of Fluid Power*, 3(1):47–53.

Paper I

A Method for Finite Element Based Modeling of Flexible Components in Time Domain Simulation of Knuckle Boom Crane

Jan Henriksen, **Morten Kollerup Bak** and Michael Rygaard Hansen

This paper has been published as:

J. Henriksen, M. K. Bak and M. R. Hansen, “A Method for Finite Element Based Modeling of Flexible Components in Time Domain Simulation of Knuckle Boom Crane”, *The 24th International Congress on Condition Monitoring and Diagnostics Engineering Management*, pp. 1215-1224. Stavanger, Norway, May 30 - June 1, 2011.

A Method for Finite Element Based Modeling of Flexible Components in Time Domain Simulation of Knuckle Boom Crane

Jan Henriksen, Morten Kollerup Bak and Michael Rygaard Hansen
Department of Engineering Sciences
Faculty of Engineering and Science, University of Agder
Jon Lilletunsvei 9, 4879 Grimstad, Norway

Abstract — In this paper emphasis is on modeling of the flexibility of the different main structural components of an offshore knuckle boom crane. The modeling approach uses results from finite element analysis of the structural components to calibrate a multi-body dynamic model of the crane. The calibration is a parameter identification that minimizes the deviation between the static and dynamic behavior of the finite element model of the beam-like jibs of the crane with that of lumped beam models. The latter approach allows for an efficient simulation of tool point control schemes that takes into account all important structural deflections and vibrations.

Keywords — Hydraulic crane, multi-body system mechanics, lumped beam model.

1 Introduction

The ongoing competition between manufacturers of hydraulically actuated offshore equipment continuously sets new references for main performance parameters such as price, payload and reach, controllability, weight, efficiency and reliability. Since development time and costs must be kept at a minimum this leaves the design engineer in a challenged position typically facing a complex task of a strongly dynamic and multidisciplinary nature. As already pointed out in Palmberg (1995) computer based time domain simulation and optimization techniques are potentially excellent tools for the challenged designer in the iterative design phase. Another important parameter concerning said equipment is model based condition based maintenance (CBM). The aim of this work is to investigate the possibilities of using time domain simulation on the hydraulic-mechanical system of hydraulically actuated cranes with a view to obtain computational efficient models that are sufficiently precise to be used both online but also as a diagnostics tool in CBM.
There are many factors that influence the performance of hydraulic cranes. The mechanical structure of a boom causes gravitational and inertia loads. Friction forces may also be significant, especially in a telescopic manipulator. A hydraulic crane uses full stroke control and is subjected to hard non-linearities, time varying parameters, external disturbances, a number of saturation phenomena and coupling effects and even though the hydraulic system in principle is quite simple, dynamic problems may appear in practice. To avoid cavitation and for safety reasons, often the most practical way is to use counterbalance valves. The influence of load pressure variations on the velocity of the actuators may be eliminated in several ways, Andersen and Hansen (2001), but the simplest method is to apply a pressure compensated proportional valve. However, the combination of these two hydraulic valves will often decrease the stability margin significantly. Hence, a certain pressure feedback/load dependancy or other design manipulations of the individual hydraulic circuits are often introduced/accepted in one or more of the main cylinder functions. In terms of kinematic structure, the hydraulic cranes can be treated as mechanisms made of several stiff and flexible links connected with revolute joints. From the point of view of topology, the manipulator is globally an open kinematic chain, with locally closed kinematic chains from the steering and control systems in the shape of cylinders and dyad links. Closed loop control of pipe handler cranes is rapidly developing. Position and pressure transducers are generally accepted and fully integrated in tool point control.
An important question is whether models with an acceptable and useful accuracy may be established without excessive testing and tuning of simulation parameters. Previous work, Mikkola and Handroos (1996) and Ellman et al. (1996), has shown very encouraging accuracy of models on hydraulic driven boom mechanisms. There are several parameters associated with the modeling of an entire hydraulic crane that are difficult to

estimate and measure, see for example Ebbesen and Hansen (2010) and Pedersen et al. (2010). They include damping, friction, flexibility and backlash in both the hydraulic and mechanical components. In this paper the importance of including the flexibility of the structural parts are investigated and an approach to the flexibility modeling of the beam-like arms that are present in any hydraulic crane is put forward. A so-called knuckle boom crane used for pipe handling is used to exemplify the approach. For such a crane there might be different failure mechanisms both related to the hydraulics and the mechanics. The dynamic response of the crane booms during operation can be a significant indicator of a number of wear and fatigue phenomena.

2 Considered System

Knuckle boom cranes are used for a wide range of offshore and marine operations and therefore exist in different variations. The considered crane is used on a drilling rig for handling of the drill pipes.
Considering the crane as a general mechatronic system, three different sub-systems can be identified:

1. A mechanical system providing the geometric and load carrying properties.
2. A primarily hydraulic actuation system driving the mechanical system.
3. An electronic control system for control of the crane through the actuation system.

The main components of the mechanical system are a rotating part mounted on a pedestal with a slewing bearing in between, an inner jib, an outer jib and a gripping yoke for the pipe handling. See Fig. 1.

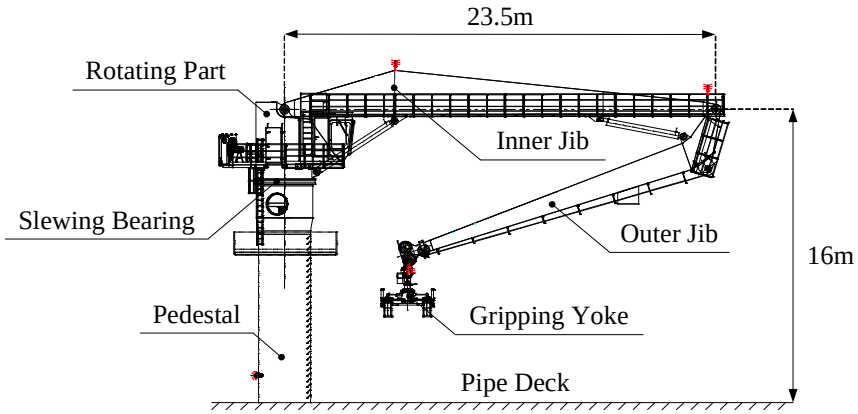

Figure 1: Main components of the cranes mechanical system.

The hydraulic system consists of three primary circuits for:

1. Tilting of the inner jib.
2. Tilting of the outer jib.
3. Slewing of the crane.

Furthermore it contains some secondary circuits for opening and closing etc. of the gripping yoke, which are not considered here. A total model of the crane is described in detail in Bak et al. (2011). In the following the modeling of the outer jib is given special attention since it qualifies as a structural component where the flexibility should be taken into account.

3 Modeling of the Outer Jib Flexibility

The outer jib is a beam-like structure, see Fig. 2, that is kinematically connected to the inner jib via a revolute joint, point A. The rotation around the axis of the revolute joint is controlled by means of two double acting hydraulic cylinders in parallel that connect to the outer jib in a spherical joint, point B. The axis of the revolute joint corresponds to the y-axis of the local coordinate system attached to the outer jib, see Figure 2. The gripping yoke is connected to the outer jib via a hydraulically damped universal joint at the tip of the outer jib, point C.
The shape of the jib roughly reflects the bending moment in the structure and increases in cross section dimensions from the revolute joint to the cross section at the cylinder connection. Thereafter, the cross section gradually decreases in size until the end of the jib where the gripping yoke connection is attached. Seen from a solid mechanics point of view the outer jib may be thought of as a beam that is hinged in point A and simply supported in point B when considered in the xz-plane, and as a cantilever beam fixed in point A when considered in the xy-plane.

3.1 Finite Element Model

Finite element analysis is a widely accepted method for linear deflections, stress, strains and vibrational analysis of structural parts. This method has been used to generate a precise picture of the flexibility of the outer jib and to act as foundation for the calibration of a more simple lumped multi-body model.
The finite element analysis comprises different linear analyses of the outer jib. The outer jib is modeled as a plate structure with cross sectional reinforcements at different intervals. The physical model is built up by plates with different thickness, however,

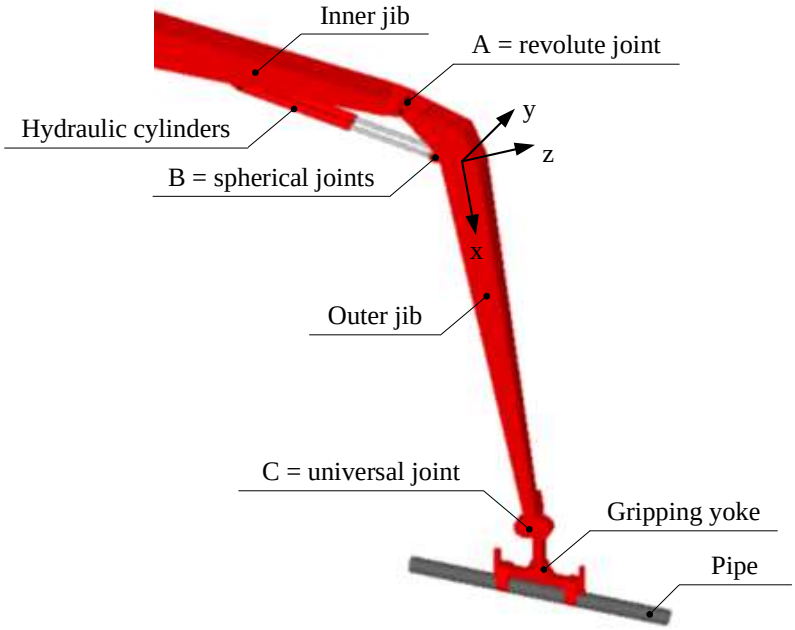

Figure 2: Outer jib of crane and its surrounding components.

for this study the element model applies equal plate thickness of 10 mm for the whole structure as the purpose of the analysis is to calibrate a lumped model rather than do an experimental based verification. This simplification is simply transferred to the lumped model.
The element type used is isotropic triangular plate elements including both membrane and bending capacity. The material properties used in the analysis are listed in Table 1. Displacement restraints are applied to the model at the bolt holes of the revolute joint

Table 1: Finite element model parameters.

Young's modulus = 210 GPa	Shear modulus = 82 GPa	Poisson's ratio = 0.28

where the outer jib is connected to the inner jib as presented in Fig. 3. These nodal points are restricted to translate in radial and axial directions according to cylindrical coordinate system with center for each bolt hole.
A number of different load cases were applied to the finite element model including:

- A static load of 10 kN in the y- and z-directions, respectively, applied at point C.
- A static torque of 6.6 kNm around the x-axis, applied at point C.
- Eigenfrequency analysis.

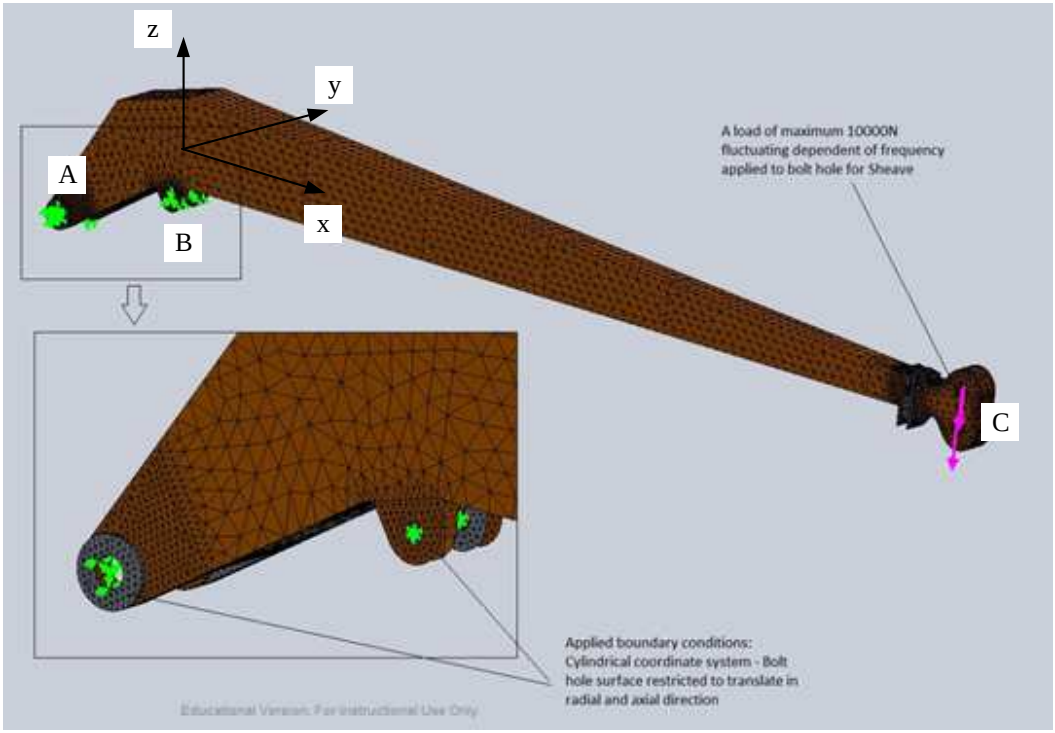

Figure 3: Boundary conditions applied to outer jib.

3.2 Lumped Model

In a lumped model the mechanical system is modeled as a chain of 3D-rigid segments kinematically attached to each other by means of kinematic joints. The main advantages of lumping a beam in a multibody simulation model are:

- Simple model development from cross sectional data.
- Possible to use standard joints and rigid bodies available in libraries.
- Possible to apply external loading anywhere on the beam like component via the rigid bodies.
- Possible to discard unwanted degrees of freedom.

The individual segments are modeled as rigid bodies with rotational springs that may be attached to the two neighboring bodies. The original work within this area was carried out by Kane et al. (1987) and Huston and Wang (1993).
For bending the segment stiffness is:

$$k_S = \frac{2 \cdot E \cdot I}{L} \tag{1}$$

Where E is the Young's modulus, I is the area moment of inertia and L is the length of the segment.
For torsion the segment stiffness is:

$$k_S = \frac{2 \cdot G \cdot I_p}{L} \tag{2}$$

Where G is the shear modulus, Ip is the polar moment of inertia and L is the length of the segment.
If two segments are connected, then the resulting connecting stiffness is:

$$k_C = \frac{1}{\frac{1}{k_{S,1}} + \frac{1}{k_{S,2}}} \tag{3}$$

Where kS,1 is the stiffness of the first segment and kS,2 is the stiffness of the second segment of the connection.
If the segment is the first or last segment of the beam then, depending on the physical connection between the beam and its surroundings, the rotational springs may either be connected to a fixed interface or to nothing yielding the following possible connection stiffnesses at the beam ends:

$$\begin{aligned} k_C &= k_S \quad fixed \\ k_C &= 0 \quad free \end{aligned} \tag{4}$$

In the current work the kinematical connections between the segments discard the positional degrees of freedom thereby avoiding a stiff model. Also, the force from the hydraulic cylinder (point B) is easily applied to the third segment as an exterior force. The segmentation is shown in Fig. 4.
The outer jib has been divided into nine segments but this number can be reduced for most practical problems. The topology of the segmentation is listed and in Table 2. The segments have tapered rectangular hollow cross sections. For simplicity an average

Table 2: Topology of segmentation of outer jib.

OJ segment	Previous body	Next body	Previous joint	Next joint
S1	Last IJ segment	S2	Revolute joint	Spherical joint
Si, $i = 1...8$	S$i-1$	S$i+1$	Spherical joint	Spherical joint
S9	S8	Gripping yoke	Spherical joint	Revolute joint

value of the stiffnesses of the segments was used, so that each segment had a single value for each of its three stiffnesses. In Table 3 the different segment and connection stiffnesses are listed.

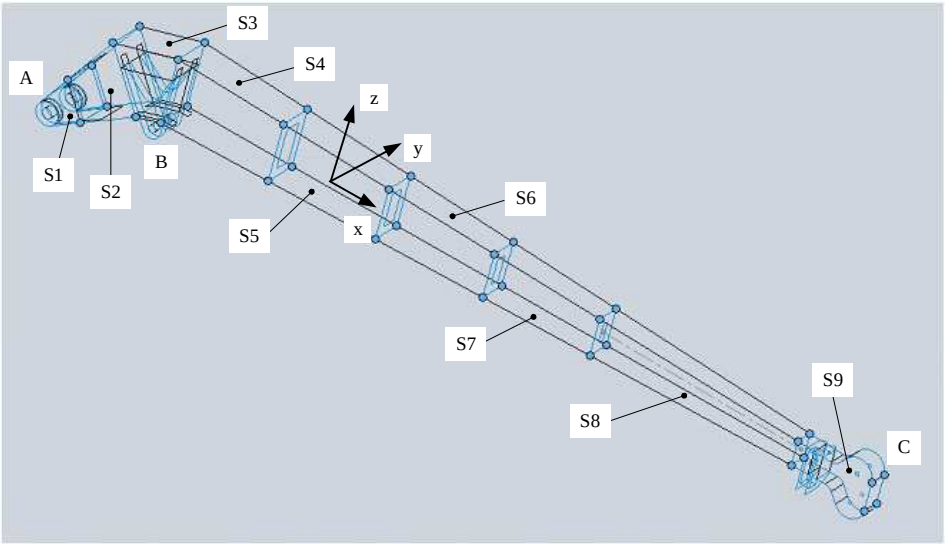

Figure 4: Segmentation of outer jib. The local coordinate system of segment 5 (S5) is shown.

Table 3: Stiffnesses [MNn/rad] of outer jib segmentation for nominal lumped model.

No.	$l[m]$	k_{Sx}	k_{Sy}	k_{Sz}	$k_{C,x}^{prev}$	k_{Cx}^{next}	k_{Cy}^{prev}	k_{Cy}^{next}	k_{Cz}^{prev}	k_{Cz}^{next}
S1	0.7	2300	3100	2940	2300	834	0	1280	2940	879
S2	2.05	1310	2180	1250	975		1670		877	
S3	1.045	3830	7140	2910		984		1820		765
S4	2.5	1330	2440	1040	551		886		530	
S5	2.5	943	1390	1080		363		613		318
S6	2.5	590	1100	450	229		442		177	
S7	2.5	374	687	292		80		139		71
S8	4.653	102	174	93	65		109		61	
S9	1.4	179	294	177		179		0		0

3.3 Comparison and Calibration

In the following the main results from the finite element model and the lumped model are compared. Two different lumped models are displayed, the nominal that is derived directly from cross sectional data, see Table 3, and a calibrated model that is tuned so that the two fundamental eigenfrequencies correspond to that of the finite element model. The calibration has been performed by simply scaling the segment rotational stiffnesses

with the same scaling factor. Hence, only two calibration parameters were introduced:

$$\begin{aligned} k^*_{Sx,i} &= k_{Sx,i} \\ k^*_{Sy,i} &= 1.05 \cdot k_{Sy,i} \\ k^*_{Sz,i} &= 0.96 \cdot k_{Sz,i} \end{aligned} \tag{5}$$

Where $i = 1...9$ and * indicates the calibrated model.
In Fig. 5 the deflections of what approximates the neutral axis of the beam are shown for the 10 kN static load cases.
Further, in Table 4 the two lowest eigenfrequencies of the model are listed. The corresponding eigenmodes are the fundamental bending mode in the xy-plane and the xz-plane, respectively.
The non-calibrated model has some deviations from the finite element model, however, they would be acceptable for most engineering purposes. With a relatively simple calibration it is possible to adjust the fundamental eigenfrequencies quite close to that of the finite element model. The deflection curves show a more pronounced deviation, especially in the out-of-plane direction, i.e., in the xy-plane. Since the effect of adding the flexibility of beams in simulation of hydraulic cranes is expected to have most significant impact on dynamic results the main target of the calibration has been to fit the eigenfrequencies and the static deflections have been considered secondary because they fit quite well. If the static deflections had shown a larger deviation from the finite element model, the calibration might need to be carried out as a multi-criteria optimization where both deviations from eigenfrequencies as well as static deflections are minimized simultaneously.

Table 4: Eigenfrequencies of the different models.

Model	f_{xy} [Hz]	f_{xz} [Hz]
Finite element	3.21	5.40
Lumped (nom.)	3.26	5.29
Lumped (cal.)	3.21	5.40

4 Simulation Results

In this section the importance of adding flexibility of crane jibs are shown by using the calibrated lumped model in a time domain simulation model that includes the hydraulic circuit that control the motion of the outer jib relative to that of the inner jib and compare the results with those obtained using a rigid body model.

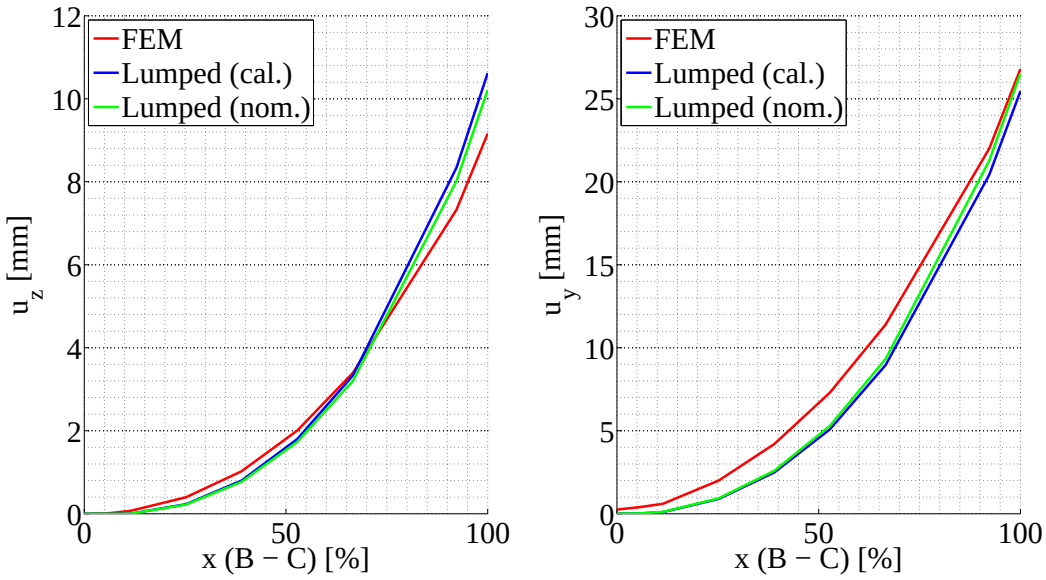

Figure 5: Deflections of outer jib neutral axis versus percentage distance from B to C for 10 kN loads in y- and z-directions.

4.1 Hydraulic Circuit

The hydraulic circuit, Fig. 6, consists of a pressure compensated proportional directional valve, counterbalance valves for controlled load lowering and two cylinders.
The control valve consist of a 4/3 proportional directional valve and a pressure reducing valve representing the pressure compensator. A small volume is added between the two valves to avoid algebraic loops. The circuit which directs the load sensing pressure to the spring side of pressure compensator is modeled as a pressure source and a function block which sets the value of the pressure source equal to the highest value of the 4/3 valve's A- and B-port pressures. This does not represent the actual functionality of the load sensing circuit, but since the load sensing pressure always is the highest of the A- and B-port pressures the result is the same and it simplifies the model.
The control signal for the valve is modeled as a normalized signal which can be varied continuously between 1- and 1 and thereby controlling both flow rate and direction of the hydraulic fluid through the control valve. It is represented by a signal block which allows specifying the control signal as a function of the simulation time.
Each counterbalances valve consists of a check valve for free flow into the actuator and a pilot operated check valve which opens at a certain cracking pressure, in this case 220 bar, for flow out of the actuator. The cracking pressure indicates the value at which the valve's A-port pressure is able to open the valve itself. The valve therefore also serves as both shock- and relief valves with setting of 220 bar. For the main function the opening of the valve is assisted by the pilot pressure, i.e., the pressure of the opposite side of the

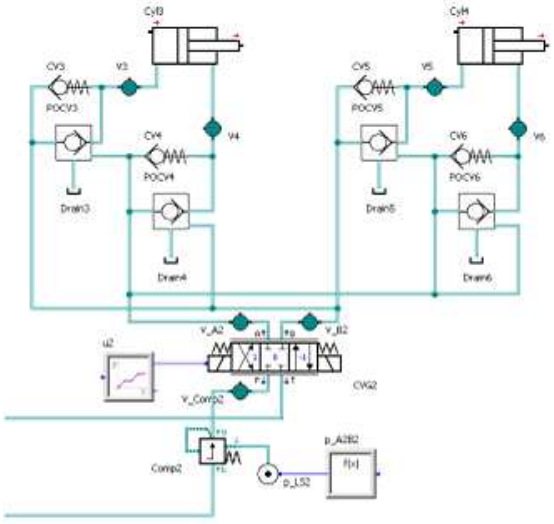

Figure 6: Model structure of hydraulic circuit for tilting of outer jib.

actuator to which the counterbalance valve is connected. The pilot pressure lowers the effective setting of the valve by a factor determined by the pilot ratio, which is 3:1 for both counterbalance valves.

4.2 Simulation Sequence

To demonstrate the importance of including the flexibility in models of multi-body systems, a simulation is carried out for both a rigid body model and a flexible model. The sequence of the simulation is illustrated in Fig. 7 and is modeled by prescribing the normalized input signal to the directional control valve as a time series. The hydraulic cylinder is retracted for the first 11 seconds, then held fixed for 5 seconds before it is extended to its initial position in 19 seconds. The extra time used for extending is because of the differential area of the cylinder yielding two different gearings between valve flow and cylinder speed. The simulation model is developed and executed using the commercial simulation software SimulationX®.

The behavior of the system changed significantly when replacing the lumped model with a single rigid body representing the entire outer jib. In Fig. 8 the cylinder force is shown for both cases.

Obviously, the rigid body model predicts instability in the system during cylinder extraction. The steady state values are the same for the two simulation models but the dynamic results and derived values such as vibration level, fatigue etc. are totally different.

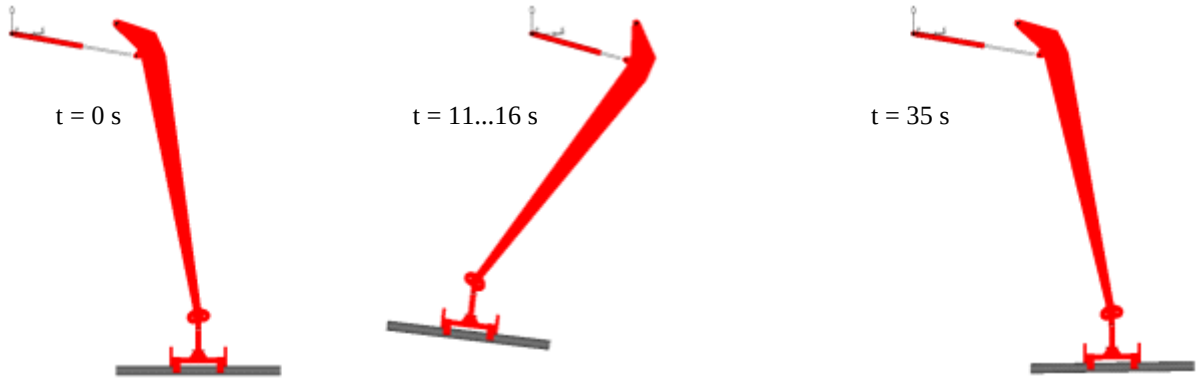

Figure 7: Model structure of hydraulic circuit for tilting of outer jib.

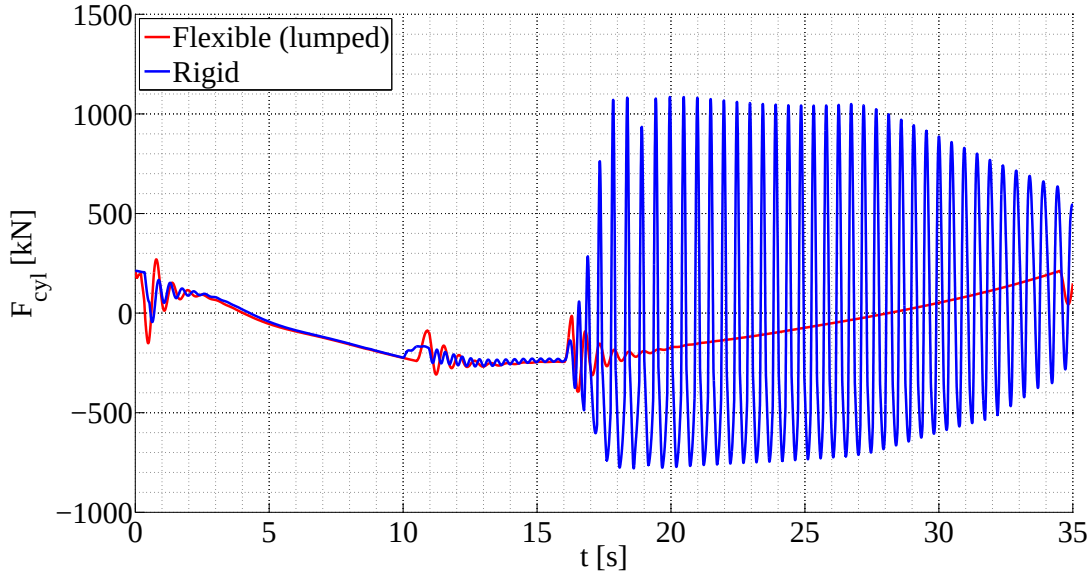

Figure 8: Variation in cylinder force.

5 Conclusions

In this paper the modeling of flexible hydraulically actuated cranes has been investigated. Emphasis has been on the modeling of the structural flexibility of the outer jib of a knuckle boom crane used for pipe handling in offshore applications. An approach using segments to a 3D lumped model is put forward. A finite element model has been developed and used to evaluate and calibrate the lumped model. Comparison between the finite element model and the lumped model show that a rather rough approximation of the bending stiffness of the segments of the lumped model yields quite satisfactory results both regarding dynamic and static behavior. Also, two simple one-dimensional calibrations within a few percentages of the nominal model yields a behavior of the lumped model that for most engineering applications corresponds to that of the finite element

model. From a CBM point of view the lumped model seems to be well suited for both diagnostics capable of analyzing large time series with a relatively low computational effort. Further, the importance of including flexibility in the modeling of hydraulically actuated cranes is clearly demonstrated on the investigated knuckle boom crane. A simulation model that take into account the hydraulic circuit and the cylinders that control the outer jib produce totally different dynamic behavior depending on whether the outer jib is modeled as a single rigid body or as the calibrated lumped model.

Acknowledgment

The work presented in this paper is funded by the Norwegian Ministry of Education and Research and Aker Solutions.

References

Andersen, T. O. and Hansen, M. R. (2001). Evaluation of velocity control concepts involving counter balance valves in mobile cranes. In *Proceedings of the 5th International Conference on Fluid Power Transmission and Control*. Hangzhou, China.

Bak, M. K., Hansen, M. R., and Nordhammer, P. A. (2011). Virtual prototyping - model of offshore knuckle boom crane. In *Proceedings of the 24th International Congress on Condition Monitoring and Diagnostics Engineering Management*, pages 1242–1252. Stavanger, Norway.

Ebbesen, M. K. and Hansen, M. R. (2010). Correction scheme for tool point velocity control of a flexible hydraulically actuated manipulator. In *Proceedings of the IASTED 29th International Conference on Modeling, Identification and Control*. Innsbruck, Austria.

Ellman, A., Käppi, T., and Vilenius, M. J. (1996). Simulation and analysis of hydraulically driven boom mechanisms. In *Proceedings of the 9th Bath International Fluid Power Workshop*, pages 413–429. Bath, UK.

Huston, R. L. and Wang, Y. (1993). Flexibility effects in multibody systems. In *Computer Aided Analysis of Rigid and Flexible Mechanical Systems: Proceedings of the NATO Advanced Study Institute*, pages 351–376. Troia, Portugal.

Kane, T. R., Ryan, R. R., and Banerjee, A. K. (1987). Dynamics of a cantilever beam attached to a moving base. *Journal of Guidance, Control and Dynamics*, 10(2):139–151.

Mikkola, A. and Handroos, H. (1996). Modeling and simulation of a flexible hydraulic-driven log crane. In *Proceedings of the 9th Bath International Fluid Power Workshop*. Bath, UK.

Palmberg, J.-O. (1995). Design of fluid-mechanical systems - methods and tools to meet future needs. In *Proceedings of Hydraulikdagar i Linköping*. Linköping, Sweden.

Pedersen, M. M., Hansen, M. R., and Ballebye, M. (2010). Developing a tool point control scheme for a hydraulic crane using interactive real-time dynamic simulation. *Modeling, Identification and Control*, 31(4):133–143.

Paper II

Modeling, Performance Testing and Parameter Identification of Pressure Compensated Proportional Directional Control Valves

Morten Kollerup Bak and Michael Rygaard Hansen

This paper has been published as:

M. K. Bak and M. R. Hansen, “Modeling, Performance Testing and Parameter Identification of Pressure Compensated Proportional Directional Control Valves” *The 7th FPNI PhD Symposium on Fluid Power*, pp. 889-908. Reggio Emilia, Italy, June 27 - 30, 2012.

Modeling, Performance Testing and Parameter Identification of Pressure Compensated Proportional Directional Control Valves

Morten Kollerup Bak and Michael Rygaard Hansen
Department of Engineering Sciences
Faculty of Engineering and Science, University of Agder
Jon Lilletunsvei 9, 4879 Grimstad, Norway

Abstract — This paper presents a practical approach for dynamic performance testing of pressure compensated proportional directional control valves and parameter identification for a proposed model of such types of valves. The performance test is based on the methods described in BS ISO 10770-1:2009, Institution (2009). The proposed valve model is intended for time domain simulation of hydraulic-mechanical systems and uses a second order model to describe the dynamics of the valve. As a case study a Sauer-Danfoss PVG32 is considered.

Keywords — Directional control valve, dynamics, modeling, performance testing.

1 Introduction

Pressure compensated proportional directional control valves (PCPDCVs) were originally developed for mobile applications with large variations in load pressure and with the need for load independent flow control. Initially the valves were mechanically or hydraulically actuated, i.e., either directly controlled by a handle connected to the main spool or remotely controlled from a manually operated pilot stage regulating a pilot pressure to move the main spool. While these actuation types are still used, a more common solution is electro-hydraulic actuation (EHA), i.e., hydraulic control of the main spool by means of an electrically actuated pilot stage.
The two most important features of EHA are:

1. Closed loop position control of the main spool by means of a linear variable differential transformer (LVDT) connected to the main spool and integrated electronics with a microprocessor for control of the pilot stage.

2. Dither for elimination of static friction (stiction) between the main spool and the valve housing.

With these features PCPDCVs take upon some of the characteristics of servo valves in terms of precision and repeatability (low hysteresis), however with a significantly lower bandwidth.
Usually the valves are used in an operator controlled open loop configuration, i.e., the operator closes the control loop, without significant bandwidth requirements. However, for both mobile and especially offshore applications, the valves are increasingly being used in closed loop configurations with more emphasis on the bandwidth requirements.
In design of hydraulic closed loop control systems, an important design parameter is the bandwidth of the control valve. The bandwidth of the selected valve, in combination with the one of the hydraulic-mechanical system to be controlled, must match the required bandwidth and dynamic characteristics of the closed loop control system in order to avoid instability and insufficient accuracy. As a rule of thumb the bandwidth of the control valve is recommended to be at least three times larger than the one of the hydraulic-mechanical system to avoid reducing the overall bandwidth, MOOG (2012).
For servo valves, which traditionally have been used for closed loop applications, the bandwidth can usually be identified by the valve's datasheet. This information is generally not available for PCPDCVs, probably because manufacturers have focused less on this kind of data. Therefore a practical test approach is needed to quickly identify the bandwidth with a reasonable precision. Furthermore a valve model with a detail level appropriate for simulation of hydraulic-mechanical systems is needed, which includes the bandwidth of the valve.

Related work with spool type valves has mainly been devoted to servo valves and since its birth it has been subject to extensive research, recent work include Gordic et al. (2004) and Liu et al. (2009), however mostly dealing with rather detailed modeling and analysis, which is outside the scope of this paper. Similar research on poppet type valves has been presented in Zhang et al. (2002) and Opdenbosch et al. (2009), also including reduced-order models which is more in line with the work of this paper.
Previous research on PCPDCVs, focused on semi-empirical modeling, have been presented in Käppi and Ellman (1999) and Käppi and Ellman (2000). This paper focus on retrieving information to be used for modeling and simulation of hydraulically actuated systems using PCPDCVs for closed loop control. More explicitly the objectives are:

1. To establish a practical approach for performance testing and analysis of PCPDCVs based on the standardized test methods described in BS ISO 10770-1:2009 Institution (2009).

2. Based on the test results, to perform parameter identification for a proposed valve model for time domain simulation of hydraulic-mechanical systems.

The paper is organized in the following way: First, a considered valve is described and the proposed model is presented. Next, the approach for carrying out the tests and processing the test data is explained. This is followed by a presentation of the test results together with parameter identification for the proposed model. The paper ends with conclusions on the results.

2 Considered Valve

Within the class of PCPDCVs a wide range of valves are available from manufacturers such as Sauer-Danfoss, Brevini Hydraulics, HAWE Hydraulics, Parker, Bosch Rexroth, HUSCO and others. As a case study a Sauer-Danfoss PVG32 is considered. The particular valve is schematically illustrated by Fig. 1 and consists of:

1. Supply module for constant supply pressure, containing a pressure reducing valve and a pressure relief valve.

2. Service module for actuator control, containing a load sensing (LS) circuit, a pressure compensator and a main spool with centering spring.

3. EHA module, PVES-SP series 4, and handle for manual actuation.

4. End module.

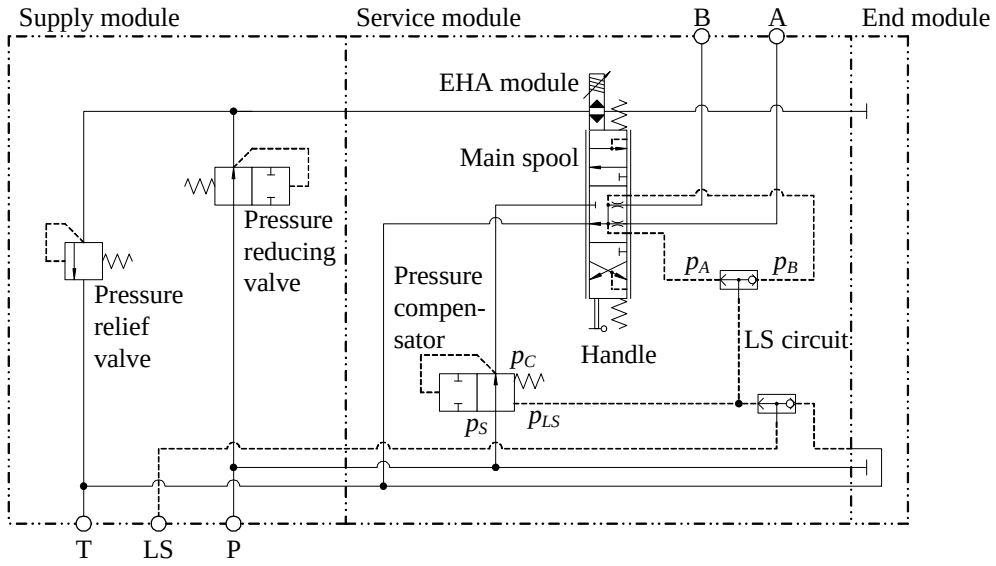

Figure 1: Simplified hydraulic diagram of considered PVG32.

The pressure reducing valve in the supply module reduces the supply pressure to a level needed for the pilot stage, which is integrated in the EHA module. The pressure relief valve protects the pilot stage from pressure peaks.

Via the main spool the pressure, p_A or p_B, on the controlled valve port is transmitted through the LS circuit to the pressure compensator. The compensator thereby works as a pressure reducing valve with a variable pressure setting. The pre-compression of the compensator spring corresponds to a pressure of 7 bar; hence the pressure between the compensator and the main spool, p_C, is always reduced to a level approximately 7 bar higher than the LS pressure, p_{LS}. With a constant pressure drop across the metering edge, the controlled flow is independent of the load pressure and proportional to the position of the main spool. For this reason PCPDCVs are also referred to as *load independent*.

A more detailed schematic of the main spool and the EHA module is given by Fig. 2.

The four edges, P-B, A-T, P-A and B-T, of the main spool are identical although the two return edges, A-T and B-T, are open in the centered spool position. The opening characteristics of the metering edges, P-B and P-A, are linear, i.e., the cross sectional opening areas of the edges are linearly dependent of the spool position.

Based on the deviation between the spool position, measured with the LVDT, and the control signal, a spool position reference, the pilot stage is controlled to create an axial pressure difference on the main spool, causing it to move. The pilot stage consist of four on/off valves, two normally open and two normally closed, controlled by means of pulse width modulated (PWM) signals. The details of the control scheme for the valve are however out of the scope of this paper. Further information about the PVG32 and the EHA module (the PVE) is given by Sauer-Danfoss (2013).

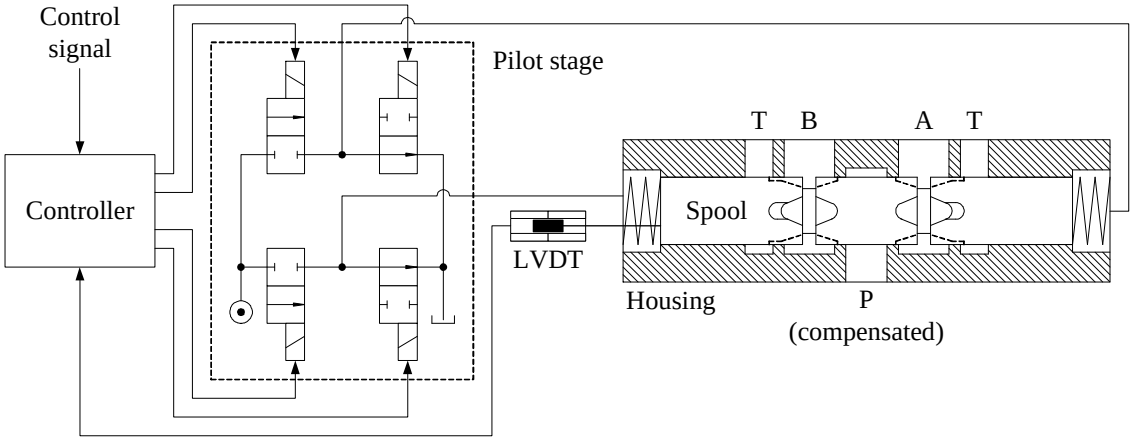

Figure 2: Simplified schematic of main spool and EHA module.

3 Valve Model

The proposed valve model is not intended for detailed analysis of the valve itself, but for use in models of hydraulic-mechanical systems for which the influence of valve's dynamic performance must be included. Therefore the model does not include the functionality of the controller and the pilot stage, but instead a simplified representation of the dynamics between the control signal and the main spool position, modeled as a second order system. The position of the main spool is represented by a normalized signal which can be varied continuously between -1 and 1, with 0 being the center position of the spool. The four spool edges are modeled as variable orifices of which the openings depend on the normalized spool position signal.
The model is developed in MapleSim^{TM} and consists of both predefined library components and custom made components. This, as opposed to encapsulating the model in a single custom made component, offers flexibility and facilitates both re-use of components and changes in the model later on. The model structure, as it appears in the MapleSim^{TM} environment, is shown in Fig. 3. The blue lines are signal lines transferring only a single state variable. The red lines transfer the two hydraulic state variable, pressure and flow, between the hydraulic components. The control signal (spool position reference), u_{ref}, is fed to a second order system, 1, representing the dynamics of the valve:

$$\frac{u_{spool}}{u_{ref}} = \frac{1}{\frac{s^2}{\omega_n^2} + 2 \cdot \zeta \cdot \frac{s}{\omega_n} + 1} \tag{1}$$

The output, u_{spool}, is the normalized spool position signal which is limited to $u_{spool,min} = -1$ and $u_{spool,max} = 1$ by the limiter function, 2.
The openings of the four main spool edges are represented by dimensionless numbers, u_{PB}, u_{AT}, u_{PA} and u_{BT}, which are functions of u_{spool} and with the range $u_{edge} = [0,1]$ as

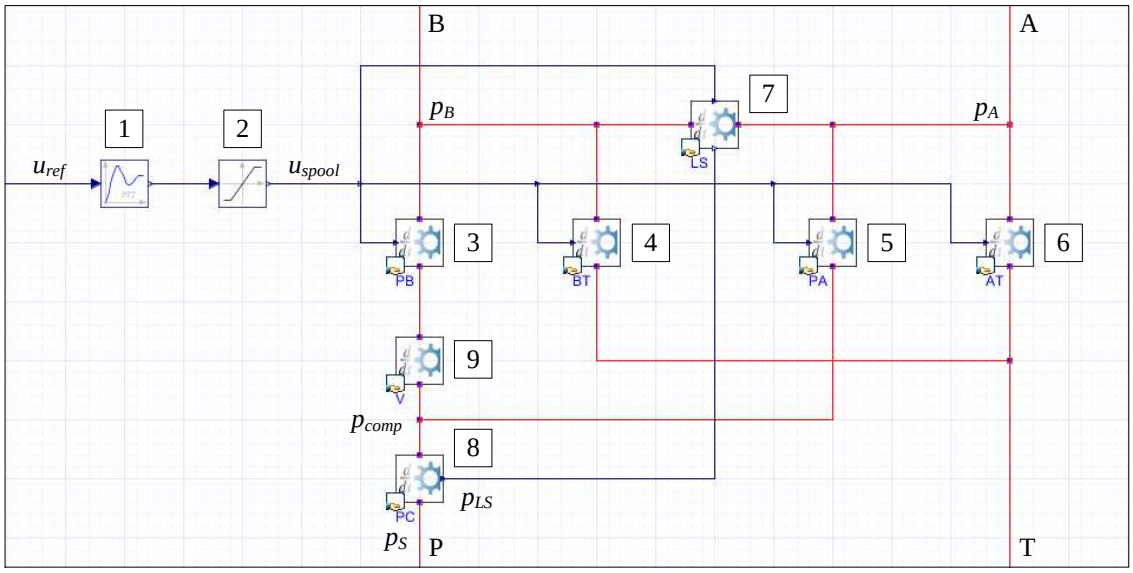

Figure 3: Structure of proposed valve model.

shown in Fig. 4.
The metering edge P-B opens for positive values of the spool position signal, starting from the overlap, OL_{PB}:

$$u_{PB} = \begin{cases} 0 & \text{for} \quad u_{spool} \leq OL_{PB} \\ \frac{u_{spool} - OL_{PB}}{1 - OL_{PB}} & \text{for} \quad OL_{PB} < u_{spool} \end{cases} \tag{2}$$

The return edge A-T opens together with the P-B edge, however starting at the underlap, UL_{AT}, modeling the open A-T connection in the centered spool position. The edge then opens gradually to the point of $u_{spool} = 2 \cdot OL_{PB}$, from where it opens along with P-B:

$$u_{AT} = \begin{cases} 0 & \text{for} \quad u_{spool} \leq UL_{AT} \\ \frac{(u_{spool} - UL_{AT}) \cdot OL_{PB}}{(1 - OL_{PB}) \cdot (-UL_{AT} + 2 \cdot UL_{AT})} & \text{for} \quad UL_{AT} < u_{spool} < 2 \cdot OL_{PB} \\ \frac{u_{spool} - OL_{PB}}{1 - OL_{PB}} & \text{for} \quad 2 \cdot OL_{PB} \leq u_{spool} \end{cases} \tag{3}$$

The metering edge P-A opens for negative values of the spool position signal, starting from the overlap, OL_{PA}:

$$u_{PA} = \begin{cases} 0 & \text{for} \quad OL_{PA} \leq u_{spool} \\ \frac{-(u_{spool} - OL_{PA})}{1 + OL_{PA}} & \text{for} \quad u_{spool} < OL_{PA} \end{cases} \tag{4}$$

The return edge B-T opens together with the P-A edge, however, starting at the underlap, UL_{BT}, modeling the open B-T connection in the centered spool position. The edge then

opens gradually to the point of $u_{spool} = 2 \cdot OL_{PA}$, from where it opens along with P-A:

$$u_{BT} = \begin{cases} 0 & \text{for} \quad UL_{BT} \leq u_{spool} \\ \frac{(u_{spool} - UL_{BT}) \cdot OL_{PA}}{(1+OL_{PA}) \cdot (UL_{BT} - 2 \cdot OL_{PA})} & \text{for} \quad 2 \cdot OL_{PA} < u_{spool} < UL_{BT} \\ \frac{-(u_{spool} - OL_{PA})}{1+OL_{PA}} & \text{for} \quad u_{spool} \leq 2 \cdot OL_{PA} \end{cases} \tag{5}$$

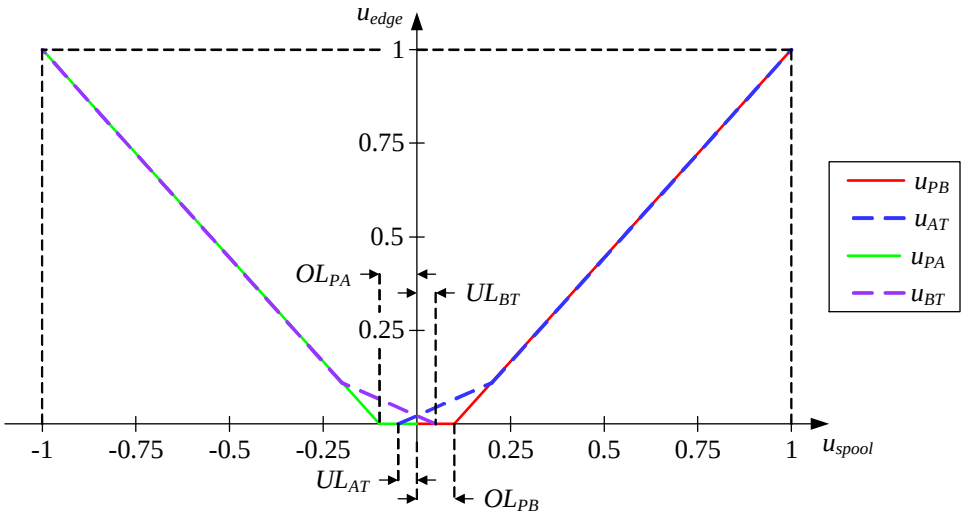

Figure 4: Edge openings as function of the spool position.

The over- and underlap values for the model, related to the normalized spool position signal, are given in Table 1. Assuming turbulent flow across the spool edges they can be

Table 1: Model values for over- and underlaps of main spool edges.

OL_{PB}	UL_{AT}	OL_{PA}	UL_{BT}
0.1	-0.05	-0.1	0.05

modeled as:

$$Q_{edge} = u_{edge} \cdot C_{edge} \cdot \sqrt{\Delta p_{edge}} \tag{6}$$

Q_{edge} is the flow for the considered edge, δp_{pedge} is the pressure drop across it and u_{edge} is opening. Hence, model components 3, 4, 5 and 6 contain (2), (3), (4) and (5), respectively, to determine the opening of the edge, and (6) to compute the flow.
In (6) C_{edge} is the flow coefficient of the fully opened edge which can be expressed as:

$$C_{edge} = C_d \cdot A_{edge} \cdot \sqrt{\frac{2}{\rho}} \tag{7}$$

C_d is the discharge coefficient, typically in the range of 0.5 to 0.75 for spool valves with notch-type edges, Borghi et al. (2005). A_{edge} is the cross sectional area of the fully opened edge and ρ is the density of the hydraulic fluid. Values of C_d and A_{edge} are usually not available as catalogue data, however, the flow coefficient may be derived from characteristic curves as the one in Fig. 5.

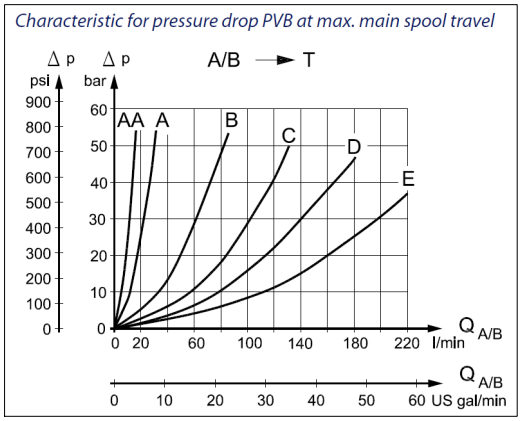

Figure 5: Flow characteristic for different spools available for the PVG32. Source: Sauer-Danfoss.

The characteristics of the considered spool is represented by the curve marked with E, which corresponds to $C_{edge} \approx 36\,\mathrm{l/min \cdot bar^{0.5}} \approx 1.9 \cdot 10^{-6}\,\mathrm{m^3/s \cdot Pa^{0.5}}$.
The LS circuit, which directs the load pressure the compensator, is included in component 7 and modeled as a piecewise function:

$$p_{LS} = \begin{cases} p_A & \text{for} \quad u_{spool} < 0 \\ p_B & \text{for} \quad 0 < u_{spool} \\ 0 & \text{otherwise} \end{cases} \tag{8}$$

The model of the pressure compensator is included in component 8. Like the main spool edges, the compensator is modeled as a variable orifice with a dimensionless opening $u_C = [0,1]$, i.e., a normalized position of the compensator spool. Based on a simple steady-state equilibrium for the compensator spool, see Figure 1, formulated as a pressure balance:

$$p_C = p_{LS} + p_0 + (1 - u_C) \cdot K_C \tag{9}$$

The opening can be determined:

$$u_C = \frac{p_{LS} + p_0 + K_C - p_C}{K_C} \tag{10}$$

p_0 is the pre-compression of the compensator spring, which is $7 \cdot 10^5$ Pa, and K_C is the normalized spring stiffness with the unit [Pa/−].
The compensator is initially fully open, but will immediately start to close and, in turn, move to a position where the compensated pressure, p_C, reaches a level of:

$$p_C = p_{LS} + p_0 + (1 - u_C) \cdot K_C \approx p_{LS} + p_0 \tag{11}$$

Assuming that the compensator spring has a relatively flat characteristic.
The flow through the compensator, i.e., the throttling from the supply pressure, p_S, to the compensated pressure:

$$Q_C = u_C \cdot C_C \cdot \sqrt{p_S - p_C} \tag{12}$$

Since the characteristics of the pressure compensator is usually not available as catalogue data, the normalized spring stiffness, K_C, and the flow coefficient, C_C, simply have to be fitted to yield the correct functionality, i.e., reducing the supply pressure according to the load pressure to maintain an approximately constant pressure drop across the metering edge. For this valve model, this is a reasonable modeling approach since the pressure compensator has been carefully designed to achieve this functionality. For this valve model the spring stiffness has been set to $K_C = 1 \cdot 10^5$ Pa/− and the flow coefficient has been set to $C_C = 1.9 \cdot 10^{-6}$ m^3/s$\cdot$Pa$^{0.5}$, i.e., identical to the spool edge values.
The pressure gradient in the volume, component 9 in the model, between the compensator and the main spool:

$$\dot{p}_C = \frac{\beta}{V_C} \cdot (Q_C - Q_{PB/PA}) \tag{13}$$

β is the stiffness of the hydraulic fluid. V_C is the size of volume between the compensator and the main spool. $Q_{PB/PA}$ is the flow through either the P-B or P-A edge, expressed by (6).

4 Testing and Data Processing

The test is based on the methods described in BS ISO 10770-1:2009, Institution (2009), which include both steady-state and dynamic performance testing. Sufficient information about steady-state characteristics is usually given by the datasheet of the considered type of valve, whereas information about dynamic performance is more deficient. This is typically given as reaction times to step inputs and specified as a range of typical values. As is customary for high-end proportional valves and servo valves, the preferred presentation of the valve dynamics would be a Bode plot, which can be used to identify the bandwidth of the valve.

In order to produce such data, a series of frequency response tests are carried out, where three signals are recorded as time series data:

1. Control signal (input).
2. Position of main spool (first output).
3. Flow on controlled port (second output).

The test setup is illustrated schematically in Fig. 6. It consists of:

1. Hydraulic constant-pressure supply unit set to $p_S = 100$ bar.
2. PVG32 with PVES-SP.
3. Parker SCQ-150 flow meter.
4. NI USB-6211 DAQ board.
5. PC with NI LabVIEW and Virtual Instrument programmed for the purpose.
6. DC power supply (not illustrated) for PCPDCV and flow meter.

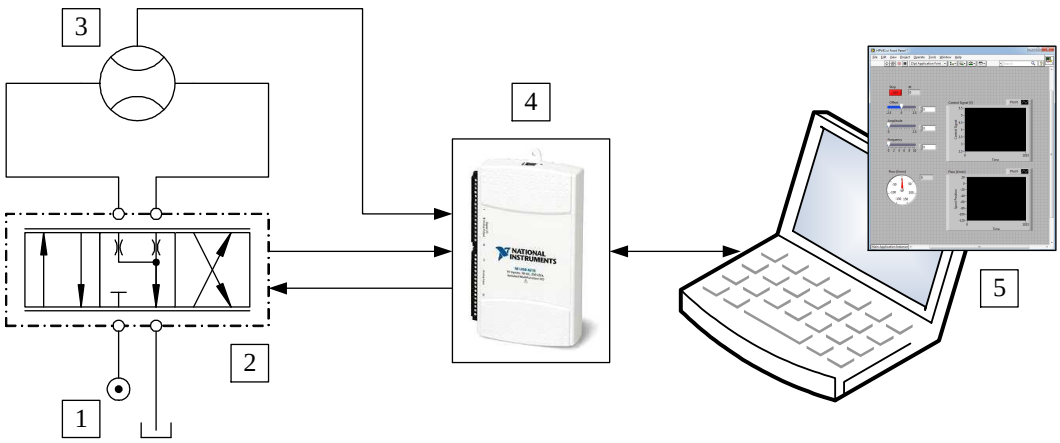

Figure 6: Test setup.

The frequency response is obtained by stimulating the valve with a sinusoidal input signal and comparing it to the output signals. To investigate the dependency of signal offset and amplitude the tests are carried out in six different cases; at 50 % negative and 50 % positive offset, respectively, and with 5 %, 10 % and 25 % amplitudes for each offset. In each case the frequency of the sinusoidal input signal is varied from 0.1 Hz and up to the frequency that results in approximately 180° phase lag of the output signals. The variation is a discrete sweep with a step size of 0.1 Hz and with a recording for each step in frequency.

As the input signal is sinusoidal and the valve has an approximately linear flow characteristic, both output signals, spool position and flow, are also sinusoidal. To produce a Bode plot for the entire frequency sweep, the magnitude and the phase lag must be computed for each step in frequency.
Since the measured outputs are rather noisy they cannot be used directly for computation. Instead of filtering the signals, they are simply approximated with a sine curve:

$$y_A = O_A + A_A \cdot \sin(2 \cdot \pi \cdot f \cdot \mathbf{t} + \phi_A) \tag{14}$$

y_A is the approximated output signal, either spool position or flow. f is the test frequency in Hz] and $\mathbf{t}$ is the time vector of the measured output signal.
To achieve the best possible approximation, the offset, O_A, amplitude, A_A, and phase lag, ϕ_A, are tuned by means of a gradient based optimization algorithm which minimizes the deviation between the measured and the approximated output signal. An example of an optimized output signal approximation is shown in Fig. 7.

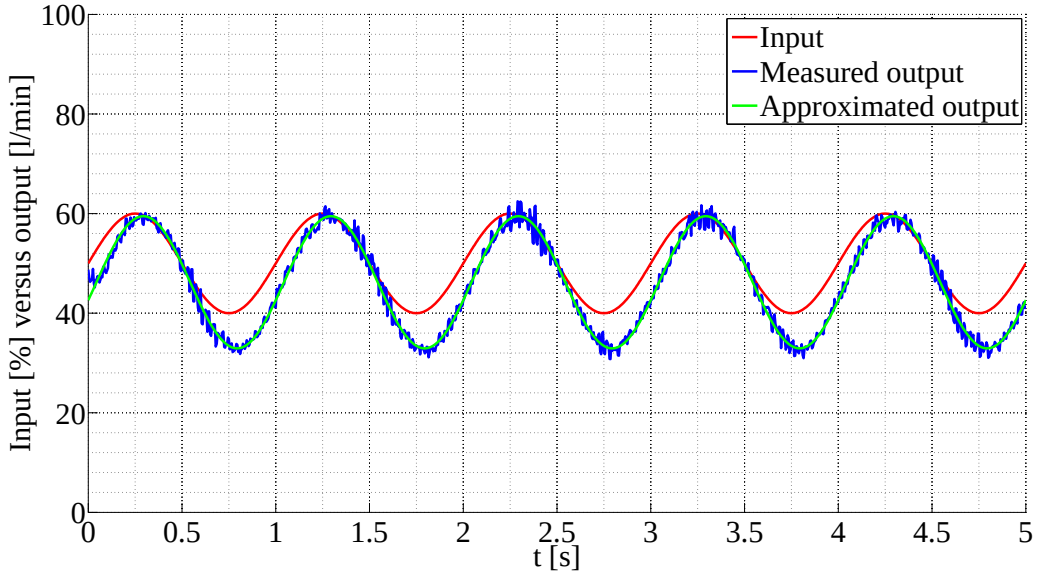

Figure 7: Example of output approximated by means of optimization.

With this approach the phase lag is identified automatically by optimization. The magnitude is computed as:

$$M = 20 \cdot \frac{A_A}{A_0} \tag{15}$$

A_A is the approximated amplitude at the considered frequency and A_0 is the approximated output amplitude at the lowest frequency (0.1 Hz). Since the input and output signals have different units and different scale, the low-frequency output amplitude is

used instead of the input amplitude to obtain a magnitude of 0 dB at the start frequency. With the magnitude and phase lag computed for each frequency step, a Bode plot can be produced as shown in Fig. 8.

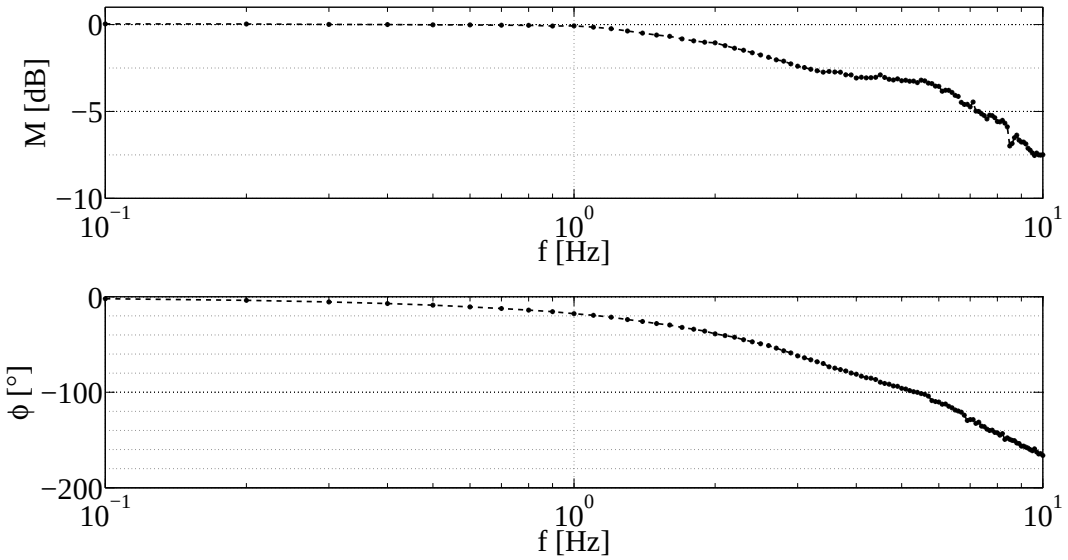

Figure 8: Example of Bode plot produced from test data.

5 Test Results and Parameter Identification

Based on the Bode plots for the six test cases the bandwidth of the valve can now be identified. As for servo valves, the frequency of $-90°$ phase lag is used as the upper limit of the bandwidth, (MOOG, 2012).

The bandwidth frequency is therefore identical with the natural frequency of a second order system, which is needed for the valve model described in section 3. The Bode plots for the six test cases are given in Fig. 9 - 14. Both flow and spool position responses are given together with second order models fitted to the measured response.

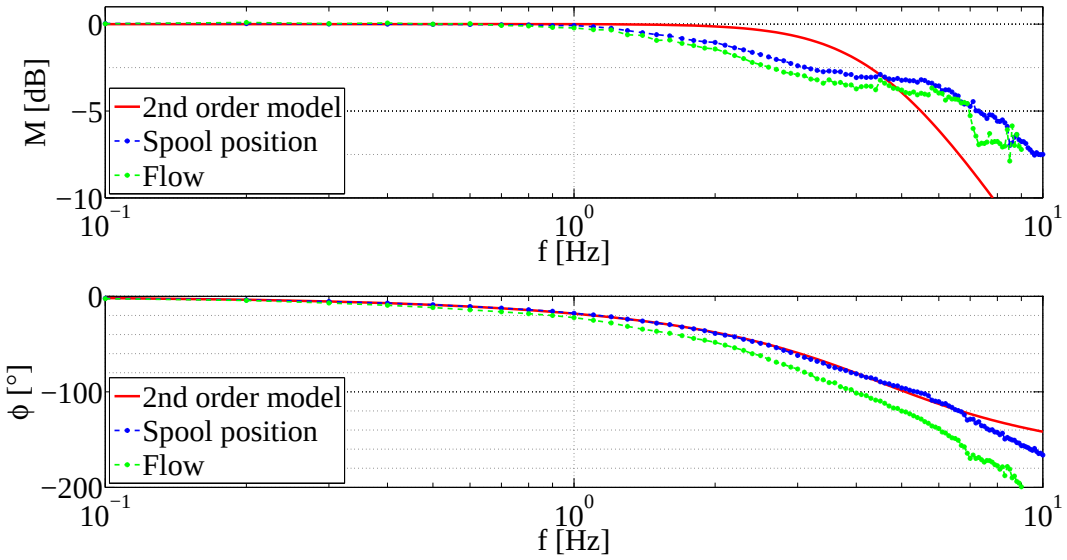

Figure 9: 5 % amplitude @ 50 % negative offset.

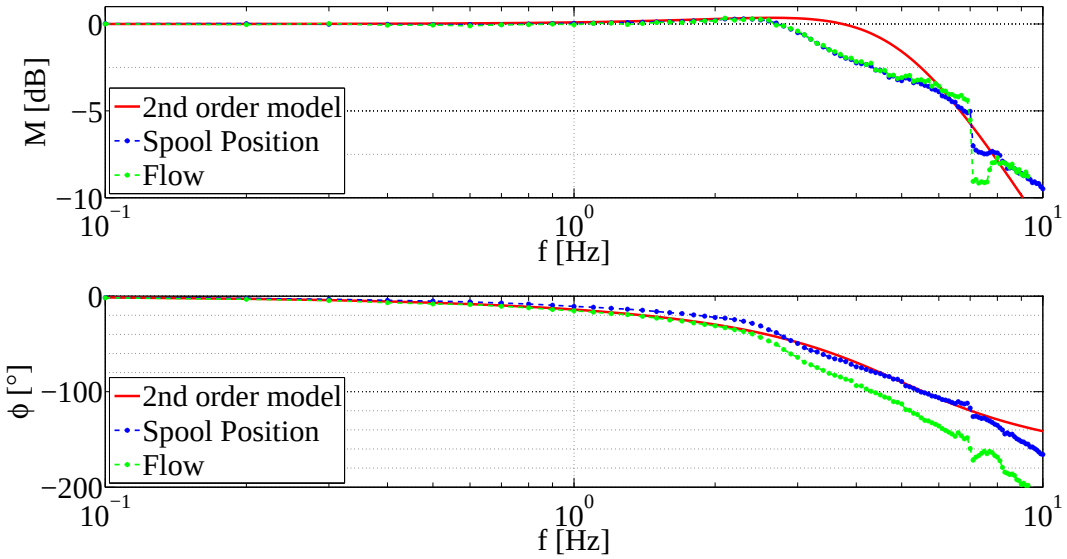

Figure 10: 5 % amplitude @ 50 % positive offset.

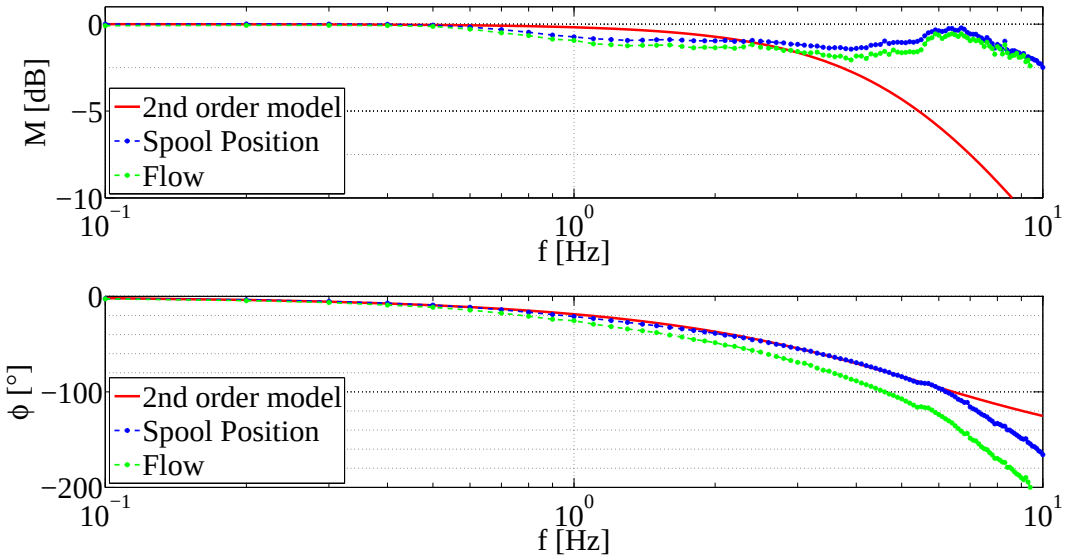

Figure 11: 10 % amplitude @ 50 % negative offset.

The spool position response is used to identify the two model parameters, ω_n and ζ. Since the natural frequency can be identified directly from the Bode plots, only the damping ratio needs to be adjusted to match the measured response.
As seen from all six Bode plots, the second order model is not an accurate description of the valve dynamics. The phase lag of the model fits the measured response quite well up to around $-90°$, but the magnitude does not fit very well.
While the dynamics of the valves main stage alone may be modeled as a second order system, the pilot stage and the controller obviously also influence the overall dynamic behavior of the valve. However, since the proposed valve model is not intended for detailed analysis of the valve itself, but for simulation of hydraulic-mechanical systems, the second order model will, for many applications, be sufficient to capture the valve's influence on the overall system dynamics.
The bandwidths and model parameters identified from the tests are listed in Table 2.

For practical reasons the valve has only been tested up to 5 Hz in the two cases of 25 % amplitude, see Fig. 13 - 14. In these two cases the bandwidth cannot be directly identified and the data in the last two rows of Table 2 therefore represent the best fit of the second order model.
Considering the remaining data, a reasonable estimate of the bandwidth is 5 Hz, corresponding to roughly $\omega_n = 30$ rad/s as the natural frequency of the second order model with a damping ratio of $\zeta = 0.8$.

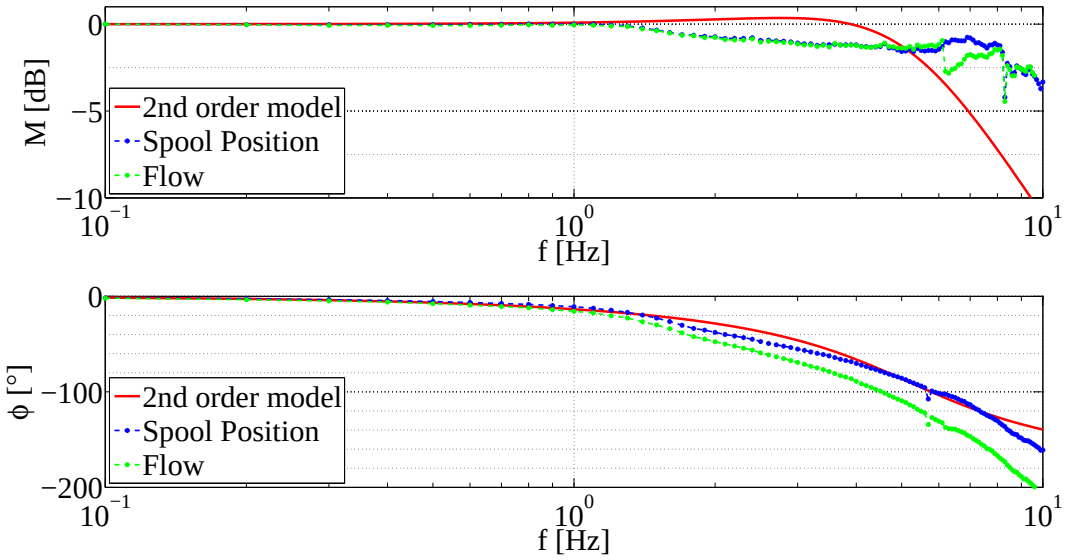

Figure 12: 10 % amplitude @ 50 % positive offset.

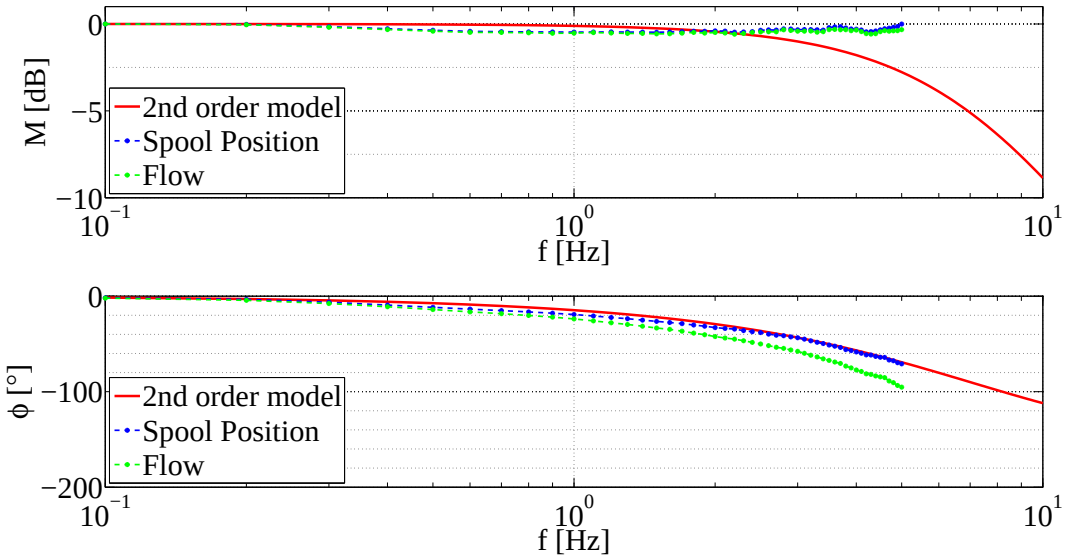

Figure 13: 25 % amplitude @ 50 % negative offset.

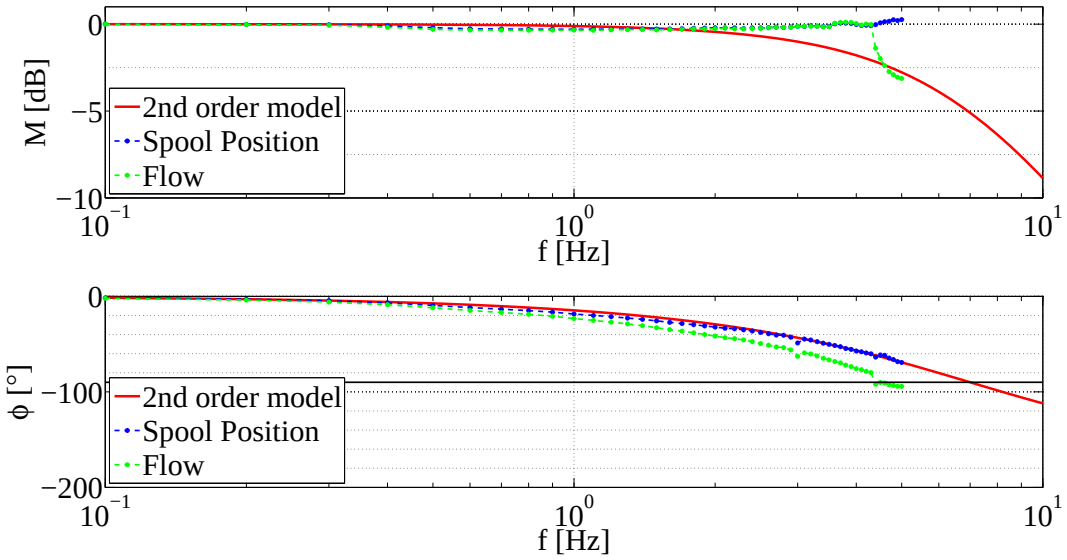

Figure 14: 25 % amplitude @ 50 % positive offset.

Table 2: Identified bandwidths and models parameters.

Offset [%]	Amplitude [%]	f_{BW} [Hz]	ω_n [rad/s]	ζ
− 50	5	4.5	28.3	0.7
+ 50	5	5	31.4	0.6
− 50	10	5.5	34.6	0.9
+ 50	10	5.2	32.7	0.6
− 50	25	7	44	0.9
+ 50	25	7	44	0.9

6 Conclusions

In this paper, an approach for dynamic performance testing of pressure compensated proportional directional control valves (PCPDCVs) has been presented along with identification of parameters for a proposed model of the considered type of valve.
In the model, the dynamics of the valves is represented by a second order system and therefore only requires two parameters. This limits the level of model complexity while still capturing the overall dynamic system behavior for simulation of hydraulic-mechanical systems.
For detailed component analysis, e.g., for design of valves, a second order model is not an adequate representation of the valve dynamics. For that a more detailed model is required.
As a case study a Sauer-Danfoss PVG32 has been considered. With the presented test

approach, the bandwidth has been determined to 5 Hz, corresponding to a natural frequency of $\omega_n = 30$ rad/s and a damping ratio of $\zeta = 0.8$.

Acknowledgements

The work presented in this paper is funded by the Norwegian Ministry of Education and Research and Aker Solutions.
The authors would like to thank Aker Solutions and Sauer-Danfoss for sponsoring components used for the experimental work.

Nomenclature

u_{ref}	Spool postion reference (control signal)	-
u_{spool}	Spool postion (normalized)	-
u_{edge}	Opening, P-B, A-T, P-A, or B-T edge	-
u_C	Opening, compensator	-
OL_{edge}	Overlap, P-B or P-A edge	-
UL_{edge}	Underlap, A-T or B-T edge	-
Q_{edge}	Flow, P-B, A-T, P-A, or B-T edge	[m^3/s]
Q_C	Flow, compensator	[m^3/s]
C_{edge}	Flow coefficient, P-B, A-T, P-A, or B-T edge	[$m^3/s \cdot Pa^{0.5}$]
C_{edge}	Flow coefficient, compensator	[$m^3/s \cdot Pa^{0.5}$]
C_d	Discharge coeffiecient	-
A_{edge}	Cross sectional area, fully opened edge	[m^2]
Δp_{edge}	Pressure drop, P-B, A-T, P-A, or B-T edge	[Pa]
p_A	Pressure, A-port	[Pa]
p_B	Pressure, B-port	[Pa]
p_{LS}	Load sensing pressure	[Pa]
p_C	Compensated pressure	[Pa]
p_0	Pre-compression, compensator spring	[Pa]
p_S	Supply pressure	[Pa]
K_C	Stiffness, compensator spring	[$Pa/-$]
V_C	Volume	[m^3]
ρ	Density, hydraulic fluid	[kg/m^3]
β	Stiffness (bulk modulus), hydraulic fluid	[Pa]
y_A	Approximated output	[%]
O_A	Approximated offset	[%]

A_A	Approximated output amplitude	[%]
A_0	Low-frequency output amplitude	[%]
ϕ_A	Approximated phase lag	[°]
t	Time vector	[s]
M	Magnitude	[dB]
f	Test frequency	[Hz]
f_{BW}	Bandwidth frequency	[Hz]
ω_n	Natural frequency	[rad/s]
ζ	Damping ratio	-

References

Borghi, M., Milani, M., and Paoluzzi, R. (2005). Influence of notch shape and number of notches on the metering characteristics of hydraulic valves. *International Journal of Fluid Power*, 6(4):5–18.

Gordic, D., Barbic, M., and Jovicic, N. (2004). Modelling of spool position feedback servovalves. *International Journal of Fluid Power*, 5(1):37–50.

Institution, B. S. (2009). Bs iso 10770-1:2009. hydraulic fluid power - electrically modulated hydraulic control valves. part 1: Test methods for four port directional flow control valves. Technical report, British Standards Institution.

Käppi, T. and Ellman, A. (1999). Modelling and simulation of proportional mobile valves. In *Proceedings of the 4th JHPS International Symposium on Fluid Power*, pages 531–536. Tokyo, Japan.

Käppi, T. and Ellman, A. (2000). Analytical methods for defining pressure compensator dynamics. *Fluid Power Systems and Technology*, 7:121–125.

Liu, X., Huang, Q., Dacheng, C., Han, J., and Lin, X. (2009). Analysis of performance effect factors of three-stage electro-hydraulic servo valve. *Journal of Computer*, 4(12):1216–1222.

MOOG (2012). Electrohydraulic valves... a technical look. Technical report, Moog Inc. http://www.moog.com/literature/ICD/Valves-Introduction.pdf.

Opdenbosch, P., Sadegh, N., Book, W., Murray, T., and Yang, R. (2009). Modelling an electro-hydraulic poppet valve. *International Journal of Fluid Power*, 10(1):7–15.

Sauer-Danfoss (2013). Pvg proportional valves. http://www.sauer-danfoss.com/Products/PVGProportionalValves/index.htm.

Zhang, R., Alleyne, A. G., and Prasetiawan, E. A. (2002). Performance limitations of a class of two-stage electro-hydraulic flow valves. *International Journal of Fluid Power*, 3(1):47–53.

Paper III

Model Based Design Optimization of Operational Reliability in Offshore Boom Cranes

Morten Kollerup Bak and Michael Rygaard Hansen

This paper has been published as:

M. K. Bak and M. R. Hansen, “Model Based Design Optimization of Operational Reliability in Offshore Boom Cranes”, *International Journal of Fluid Power*. Vol. 14 (2013), No. 3, pp. 53-65.

Model Based Design Optimization of Operational Reliability in Offshore Boom Cranes

Morten Kollerup Bak and Michael Rygaard Hansen
Department of Engineering Sciences
Faculty of Engineering and Science, University of Agder
Jon Lilletunsvei 9, 4879 Grimstad, Norway

Abstract — This paper presents a model based approach for design of reliable electro-hydraulic motion control systems for offshore material handling cranes. The approach targets the system engineer and is based on steady-state computations, dynamic time domain simulation and numerical optimization.
In general, the modeling takes into account the limited access to component data normally encountered by engineers working with system design. A system model is presented which includes the most important characteristics of both mechanical system and hydraulic components such as the directional control valve and the counterbalance valve. The model is used to optimize the performance of an initial design by minimizing oscillations, maximizing the load range and maintaining operational reliability.

Keywords — System modeling, system design, counterbalance valve, directional control valve.

1 Introduction

Despite the fact that hydraulics, in general, is considered a mature technology, design of hydraulic motion control systems still offers a number of challenges for both component suppliers and manufacturers of hydraulically actuated machines. For the system designer, the main challenge is to meet the functional requirements for the system, a set of design constraints, while satisfying a number of performance criteria such as cost, weight, overall efficiency and response time, which are often conflicting and also subject to constraints.

Design of hydraulic systems has been subjected to extensive research including steady-state based design, (Stecki and Garbacik, 2002), as well as component selection using dynamic simulation and numerical optimization, (Krus et al., 1991), (Hansen and Andersen, 2001), (Andersson, 2001) and (Papadopoulos and Davliakos, 2004). Automated design through so-called expert systems with the ability to handle both conceptual and detailed design have attracted a considerable amount of interest from researchers, (da Silva and Back, 2000), (Hughes et al., 2001), (Liermann and Murrenhoff, 2005) and (Schlemmer and Murrenhoff, 2008). The impact outside academia, however, remains limited. A reason for this may be that design of hydraulic systems is somewhat application dependent. Design criteria and constraints in combination with design traditions differ from one application area to another, making it difficult to set up and maintain design rules for expert systems. Moreover, scepticism and conservatism may contribute to design engineers being reluctant to make use of such systems.

Hydraulic systems are therefore still designed manually and in many cases based on existing systems, reducing the design job to a sizing problem where the system architecture is already given. In these cases the design engineer can certainly make benefit from previously mentioned tools such as dynamic simulation and optimization. However, using these tools still requires a great level of application specific knowledge.

For offshore applications, which are the focus of this paper, reliability and productivity are the most important performance criteria. They are especially important for offshore applications because of remote locations and high cost of down time. Therefore price and efficiency are less important criteria than for other applications like agriculture or construction machines.

In the offshore industry, the problem of designing reliable systems is further complicated by limited opportunities to build prototypes to verify new designs. This only promotes the need for model based design approaches where *virtual prototypes* can be used to evaluate and optimize a design.

In this paper an offshore material handling application is considered which uses a pressure compensated directional control valve (DCV) and a counterbalance valve (CBV) - classically prone to instability and therefore unreliable. A dynamic model and a typical

steady-state sizing procedure are presented as seen from a system designer's point of view. Next, an optimization procedure, based on the Complex method, is applied in order to investigate two different design concepts; one that represents a traditional way of choosing design parameters for the considered system and one that represents a new and reliable way of handling the problem of using a pressure compensated DCV together with a CBV. The two methods are compared and their limitations are discussed.

2 Considered System

The considered system is part of a smaller crane used for material handling on an offshore drilling rig. It is put forward as a representative problem within offshore crane design where the mechanical system and operating cycles are determined a priori.
The mechanical system is a crane boom actuated by a hydraulic cylinder, configured as shown in Fig. 1.

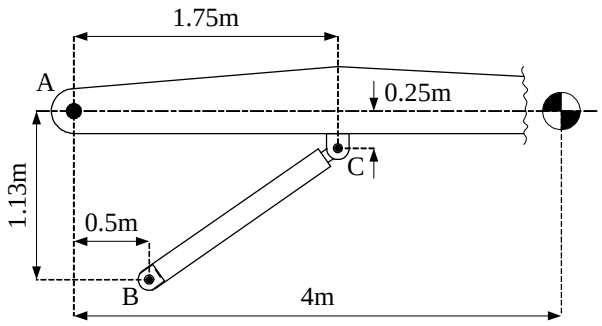

Figure 1: Mechanical system.

The total mass of the boom and the load attached to it is 5000 kg with COG located at a distance of 4 m from the pivoting point of the boom.
The cylinder is controlled with an electro-hydraulically actuated DCV with integrated load sensing (LS) circuit and pressure compensator which maintains an approximately constant pressure drop of $p_{comp} - p_{LS} = 7 \cdot 10^5$ Pa across the metering edge of the DCV, see Fig. 2. This makes the controlled flow independent of the load pressure and proportional to the position of the DCV main spool.
An externally vented (drained) CBV is used to control the piston pressure, p_2, during load lowering, i.e., when the cylinder is exposed to negative loads. The system is supplied by a hydraulic power unit (HPU) with constant supply pressure, $p_S = 210 \cdot 10^5$ Pa, and return pressure, $p_R = 0$.
The control system consists of a feedforward controller (FFC) which is a scaling of the velocity reference, vref, and a feedback controller (FBC), which is a PI controller that regulates the actuator position, s, according to the position reference, s_{ref}.

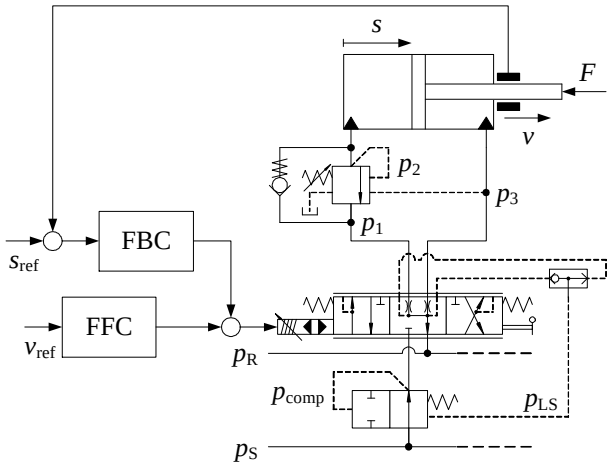

Figure 2: Electro-hydraulic motion control system.

This type of electro-hydraulic motion control system is widely used for offshore material handling equipment where closed loop control of the individual actuators is used to achieve control of a manipulator end point and where several machines are supplied by a common HPU with a ring line system connected to the individual machines.
Design of such a system is an iterative process involving design of both the mechanical system and the motion control system. In practice, detailed design of both systems is carried out separately with constraints imposed by a conceptual design. The conceptual design is then revisited if it later proves to be unsuitable.
As an example placement and size of the cylinder may be determined during the conceptual design phase. To ensure the lifting capacity, the required cylinder piston diameter can be obtained by:

$$D_p \geq \sqrt{\frac{4}{\pi} \cdot \frac{F_{max}}{\eta_{hmc} \cdot (p_2 - p_3 \cdot \phi)}} \tag{1}$$

The force F_{max} includes the steady-state load force and, for offshore equipment, a certain contribution from environmental loads, e.g., wind and waves.
The return pressure, p_3, can often be neglected or alternatively set to, e.g., $5...10 \cdot 10^5$ Pa to account for the pressure drop through the return path. The inlet pressure, p_2, is typically set to $20...30 \cdot 10^5$ Pa below the supply pressure, e.g., $180 \cdot 10^5$ Pa if the supply is $210 \cdot 10^5$ Pa. The hydro-mechanical efficiency, η_{hmc}, depends on the cylinder design and type of sealings. In practice it is typically set to 0.9 for the considered type of cylinder, (Rasmussen et al., 1996).
Simultaneously, the minimum required rod diameter must be determined in order to avoid buckling of the cylinder. A simple and common approach is to use the rod diameter as an effective diameter throughout the length of the whole cylinder and apply the

formula for *Euler buckling* of an ideal column:

$$D_r \geq \sqrt[4]{\frac{64 \cdot f_s \cdot (l^2 \cdot F)_{max}}{\pi^3 \cdot E}} \tag{2}$$

Since the load on the cylinder varies with the position of the piston the maximum product of the squared cylinder length, l, and the force, F, is used and an appropriate safety factor, f_s, is introduced.
The system may have several operating cycles which need to be considered when designing it. For a crane with coordinated control of multiple actuators, inverse kinematics may be applied to obtain the operating cycles for the individual actuators. However, independent operating cycles are usually defined for each actuator and used as design references. The most common is to use a trapezoidal velocity profile to determine the maximum velocity:

$$v_{max} = \frac{\Delta s}{\Delta t - t_{ramp}} \tag{3}$$

Cylinders are usually required to use the full stroke, h, i.e., $\Delta s = h$. Δt is the time of the operating cycle, i.e., time for lifting or lowering, and t_{ramp} is the ramping time.
Parameters for the cylinder and the operating cycle, for which the motion control system is to be designed, are given in Table 1.

Table 1: Parameters for cylinder and operating cycle.

Cylinder		
$F_{max} = 195$ N	$\eta_{hmc} = 0.9$	$f_s = 4$
$l_{min} = 1.536$ m	$h = 1$ m	$E = 2.1 \cdot 10^9$ Pa
$D_p = 0.125$ m	$D_p = 0.08$ m	$\phi = 0.59$
Operating cycle		
$\Delta t = 10$ s	$t_{ramp} = 1.5$ s	$v_{max} = 0.118$ m/s

3 System Modeling

In model based design the actual modeling is closely linked to the design objectives. The main challenge is to minimize the complexity of the system model without ignoring or underestimating important physical phenomena. For systems manufacturers this challenge involves setting up suitable models of a number of sub-supplier components for which the required data may be difficult to acquire or not available. For the considered

system this includes, among other parameters, the bandwidth of the DCV, steady-state characteristics of the CBV and cylinder friction.
The model of the hydraulic-mechanical system is developed with MapleSim™ and consists of both predefined library components and custom made components developed via Maple™. This combination facilitates both efficient model development and modeling at a detail level that is not supported by library components.
The design analysis and optimization (section 5) is carried out with MATLAB® and Simulink®. For this purpose an S-function (compiled C-code) is generated from the MapleSim™ model and used to carry out simulations in Simulink®.
The advantage of this use of the two software packages is the speed and efficiency with which models can be developed in MapleSim™ combined with fast simulation of the S-function in Simulink® and predefined functions in MATLAB® for post processing and design optimization.

3.1 Mechanical System

The mechanical system is modelled as a three-dimensional multi-body system with three rigid bodies; boom, cylinder barrel and cylinder piston.
The hinges in points A, B and C (see Fig. 1) are modelled as a revolute joint, a spherical joint and a universal joint, respectively. The translational degree of freedom (DOF) between the cylinder barrel and piston is modelled as a prismatic joint. This gives a system with a single DOF which is actuated by the hydraulic cylinder. Fig. 3 shows the chosen model structure as it appears in MapleSim™.

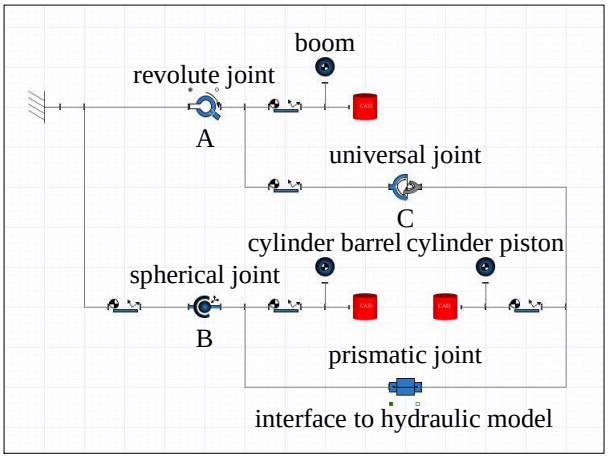

Figure 3: Structure of mechanical model.

The flexibility of the boom may have some influence on the system dynamics but is not included here.

3.2 Hydraulic System

For the considered system all hydraulic valves are modelled as variable orifices with linear opening characteristics:

$$Q = \xi \cdot C_v \cdot \sqrt{\Delta p} \tag{4}$$

Here ξ is the relative opening of the valve, i.e., a dimensionless number limited to the interval [0,1]. It can be a function of system pressures or controlled directly via an input signal depending on the considered type of valve.
The flow coefficient in (4) can be expressed as:

$$C_v = C_d \cdot A_d \cdot \sqrt{\frac{2}{\rho}} \tag{5}$$

The discharge coefficient, C_d, and the discharge area, A_d, are usually not specified for a valve. Instead C_v can be obtained from characteristic flow curves given in the datasheet of the valve. From this, a nominal flow, Q_{nom}, corresponding to a nominal pressure drop, Δp_{nom}, can be identified and used to derive the flow coefficient:

$$C_v = \frac{Q_{nom}}{\sqrt{\Delta p_{nom}}} \tag{6}$$

This corresponds to the fully opened state of the valve, so with (4) it is assumed that the discharge coefficient, C_d, is constant and only the discharge area, A_d, varies with the relative opening of the valve.
The pipelines between the DCV and the CBV/cylinder are assumed to be short enough to neglect the pressure drop and only the capacitance is modelled:

$$\dot{p} = \frac{\beta}{V} \cdot (Q_{in} - Q_{out}) \tag{7}$$

In the following the models of the cylinder, the CBV and the DCV are described.

3.2.1 Hydraulic Cylinder

The model of the hydraulic cylinder includes the capacitance of the chambers as well as the friction between the piston and the barrel. The cylinder force is:

$$F = \begin{cases} F_h - F_{friction} & \text{for} \quad v_0 < v \\ F_h - F_{friction} \cdot \frac{v}{v_0} & \text{for} \quad -v_0 \leq v \leq v_0 \\ F_h + F_{friction} & \text{for} \quad v < -v_0 \end{cases} \tag{8}$$

The hydraulic force is $F_h = p_2 \cdot A_p - p_3 \cdot \phi \cdot A_p$. The actual friction in the cylinder is quite complex, especially around zero velocity. As described in Ottestad (2012) it consists of both static and coulomb friction as well as velocity dependent and pressure dependent friction, which may be described with a model of five parameters. Even though the model is not very complex, the number of parameters represents a problem for a system designer because they need to be experimentally determined.
Consequently, an even simpler model must be used:

$$F_{friction} = F_S + C_p \cdot |F_h| \tag{9}$$

The first term is the static friction which may be set to $F_S \approx A_p \cdot 1 \cdot 10^5$ m^2 $\cdot$ Pa. In Ottestad et al. (2012) it was experimentally determined to $F_S = 580$ N for a cylinder of the same size as the one used here. The second term is the pressure dependent friction which may constitute 2...3 % of the hydraulic force, e.g., $C_p = 0.02$. v_0 in Eq. (8) is used to handle the transition around zero velocity in order to avoid computation difficulties and can be set to a small value of, e.g., $v_0 = 0.005$ m/s.
Even though the friction model described by Eq. (9) is quite simple, it is sufficient for the considered system because the operating cycle does not contain any position control around zero velocity.
The pressure gradients in the two chambers are:

$$\dot{p}_2 = \frac{\beta}{V_1} \cdot (Q_1 - v \cdot A_p) \tag{10}$$

$$\dot{p}_3 = \frac{\beta}{V_2} \cdot (v \cdot \phi \cdot A_p - Q_2) \tag{11}$$

The chamber volumes, V_1 and V_2, are functions of the piston position, s. Q_1 and Q_2 are the flows on the piston-side and the rod-side of the cylinder, respectively.

3.2.2 Counterbalance Valve

The model of the CBV consists of two components; check valve and pilot assisted relief valve (the CBV itself), both modelled according to Eq. (4).
The relative opening of the check valve is:

$$\xi_{cv} = \frac{p_1 - p_2 - p_{cr,cv}}{k_{s,cv}} \tag{12}$$

The cracking pressure, $p_{cr,cv}$, of the check valve is usually specified for a CBV and the normalized spring stiffness can be set to a value of, e.g., $k_{s,cv} = 1 \cdot 10^5$ Pa.

The relative opening for the CBV is:

$$\xi_{cbv} = \frac{p_3 \cdot \psi + p_2 - p_{cr,cbv}}{k_{s,cbv}} \tag{13}$$

The normalized spring stiffness, $k_{s,cbv}$, is usually not specified for a CBV but may be provided by the supplier on request. With Eq. (13) any non-linearity of the discharge area as function of the spool position is neglected. Also variations in the discharge coefficient and the influence of flow forces are neglected.
To determine the usefulness of the proposed model, experimental work has been carried out with a double CBV often used in offshore cranes. The pilot area ratio of the CBV is $\psi = 5$ and the nominal pressure drop is $\Delta p_{nom} = 16 \cdot 10^5$ Pa at a nominal flow $Q_{nom} = 120$ l/min in the fully opened state. This corresponds to a flow coefficient of $C_{v,cbv} = 1.58 \cdot 10^{-6}$ m^3/s $\cdot$ Pa$^{0.5}$. The cracking pressure is $p_{cr,cbv} = 180 \cdot 10^5$ Pa.
In the experiment the flow through the valve is increased linearly from 0 to 100 l/min. The flow is recorded along with three pressures, see Fig. 4. This is used to estimate the opening of the CBV using both Eq. (4) and (13) in order to identify the spring stiffness.

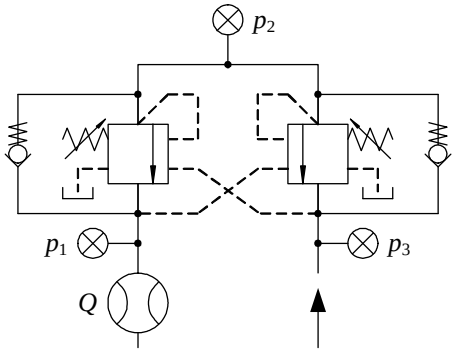

Figure 4: Experimental setup for test of CBV.

With the measured flow and pressures, p_1 and p_2, (measured values are indicated by $\sim$) the relative opening can be estimated using Eq. (4):

$$\xi_{est}^{(1)} = \frac{\widetilde{Q}}{C_v \cdot \sqrt{\widetilde{p}_2 - \widetilde{p}_1}} \tag{14}$$

To investigate the validity of Eq. (13) this is used to estimate the opening with p_2 and p_3 as inputs:

$$\xi_{est}^{(2)} = \frac{\widetilde{p}_2 + \widetilde{p}_3 \cdot \psi - p_{cr,cbv}}{k_{s,cbv}} \tag{15}$$

The spring stiffness is tuned until the best match between $\xi_{est}^{(1)}$ and $\xi_{est}^{(2)}$ is obtained. The result is shown in Fig. 5 together with the input flow. The relative openings are given in percentage.

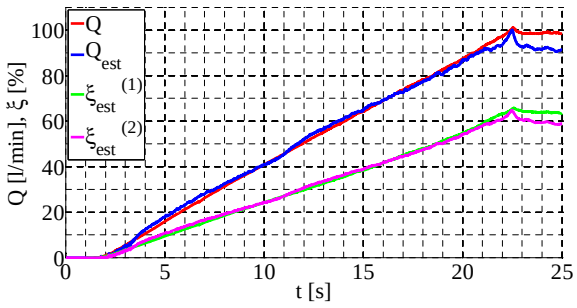

Figure 5: Estimated and openings and flow and measured flow.

The best match between the two estimated openings is obtained with $k_{s,cbv} = 295 \cdot 10^5$ Pa. Also shown in Fig. 5 is the estimated flow obtained by means of $\xi_{est}^{(2)}$ and p_1 and p_2:

$$Q_{est} = \xi_{est}^{(2)} \cdot C_v \cdot \sqrt{\widetilde{p}_2 - \widetilde{p}_1} \tag{16}$$

From the correspondence shown in Fig. 5 there seems to be limited influence from flow forces and, although the suggested model is relatively simple, the results show that it is adequate to describe the steady-state characteristics of the considered type of CBV.

3.2.3 Directional Control Valve

The DCV model consists of several smaller models representing the main components of the valve; main spool, LS circuit and pressure compensator. The model does not include the functionality of the electro-hydraulic actuation, but instead a simplified model of the dynamics between the input signal and the main spool position, represented by a second order system:

$$\frac{u_{spool}}{u_{ref}} = \frac{1}{\frac{s^2}{\omega_v^2} + 2 \cdot \zeta \cdot \frac{s}{\omega_v} + 1} \tag{17}$$

The control signal, u_{ref}, is the sum of the feedforward control signal, u_{FF}, and the feedback control signal, u_{FB}. The spool position, u_{spool}, is a normalized signal which can vary continuously between -1 and 1, with 0 being the center position of the spool.
For servo valves and high-performance proportional valves the bandwidth, ω_v, can usually be identified from the valves datasheet. For pressure compensated DCVs there is usually no information available about the bandwidth and the only way to identify it may be to carry out a frequency response test of the considered valve. An approach for such

a test is described in Bak and Hansen (2012) along with some test results for a Sauer-Danfoss PVG32. The identified bandwidth, $\omega_v = 30$ rad/s, and damping ratio, $\zeta = 0.8$, are also used here. This represents the overall dynamics between the input signal and the controlled flow, i.e., it includes the dynamics of the electro-hydraulic actuation, the main spool, the pressure compensator and the LS circuit of the DCV.
The four spool edges are modelled as variable orifices, Eq. (4), of which the relative opening, ξ_{edge}, for each spool edge is a function of the normalized spool position signal as shown in Fig. 6.

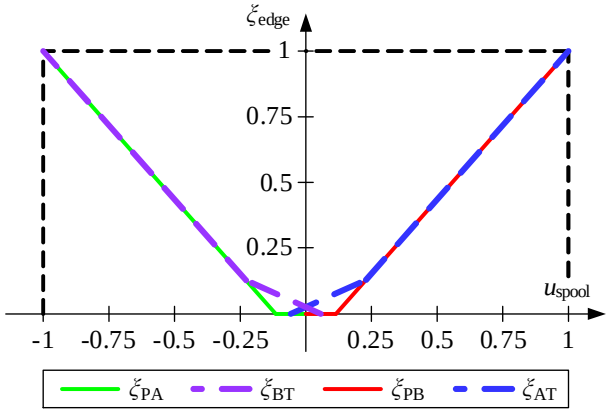

Figure 6: Opening functions for spool edges.

The spool edge openings are modelled as piecewise functions to include the overlaps of the metering edges, PB and PA, and the underlaps of the return edges, AT and BT. A more detailed description of the opening functions is given in Bak and Hansen (2012).
Usually very little or no information about the pressure compensator is available from valve datasheets making it difficult to estimate when the pressure saturation will occur. However, if the nominal pressure drop, p_0, is known the compensated pressure, p_{comp}, can be described as:

$$p_{comp} = \begin{cases} p_{LS} + p_0 & p_0 \leq p_S - p_{LS} \\ p_S - p_{LS} & 0 < p_S - p_{LS} < p_0 \\ p_{LS} & p_S - p_{LS} \leq 0 \end{cases} \tag{18}$$

The first case describes the normal operating condition of the compensator, maintaining the nominal pressure drop. The second case describes the condition where the load pressure is too close to the supply pressure to maintain the nominal pressure drop. The third case describes the build-in check valve function of the compensator that prevents negative flow if the load pressure exceeds the supply pressure.
The LS circuit directing the load pressure to the pressure compensator is modelled as a

piecewise function:

$$p_{LS} = \begin{cases} p_3 & u_{spool} < 0 \\ 0 & u_{spool} = 0 \\ p_2 & 0 < u_{spool} \end{cases} \tag{19}$$

3.2.4 Model Structure

Fig. 7 shows the model structure of the hydraulic system as it appears in the graphical environment of MapleSim™. The red lines represent transfer of the two hydraulic power variables, pressure and flow, between the hydraulic components. The blue lines are signal lines.

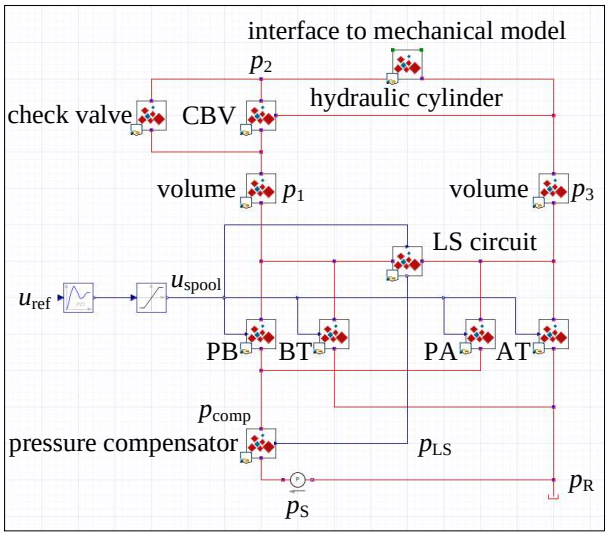

Figure 7: Structure of hydraulic model.

3.3 Control System

In the control system model the velocity reference, v_{ref}, is split into two signals, for lifting and lowering, which are scaled by the two feedforward gains, $K_{v,1}$ and $K_{v,2}$ respectively, to make up the feedforward controller (FFC). The velocity reference is integrated to obtain the position reference, sref, for the feedback controller (FBC).
The structure of the Simulink® model, with the control system and the S-function containing the hydraulic-mechanical model, is shown in Fig. 8.
The input to the hydraulic-mechanical model is the control signal to the DCV, uref in Eq. (17). The outputs are the three system pressures, p_1, p_2 and p_3 and the position of the cylinder piston, s. The latter is used to compute the position error, $e_s = s_{ref} - s$, which is the input to the feedback controller (FBC).

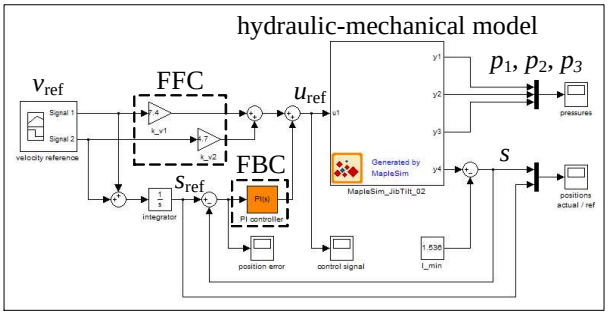

Figure 8: Structure of Simulink® model.

4 Steady-State Design

The task of designing a hydraulic system involves two main activities; choice of system architecture and sizing/selection of the system components. The first one is often based on design rules and experience with suitable architectures for the considered application. Selection and sizing of the system component is an iterative process because the choices of the individual component affect each other. Changes regarding types and sizes of components may need to be made after the first design iteration and even a change of system architecture may need to be included in the following iterations before arriving at a satisfying design.
To reduce the number of iterations the design process can be set up as a systematic and stepwise procedure based on simple steady-state considerations and empirical design rules. An example of a general procedure is described by Stecki and Garbacik (2002).
For the considered system, with the cylinder and the operating cycle given as in section 2, the remaining system may be designed through the following steps:

1. Select directional control valve.
2. Select counterbalance valve.
3. Tune control system.

Furthermore pipelines and any protective components such as shock and anti-cavitation valves also need to be sized. HPU design including selection and sizing of pump(s), sizing of reservoir, design of cooling system and selection of filtering system could represent additional steps in the procedure. However, since the HPU is used to supply several machines, this is designed through a separate procedure based on the requirements and operating cycles of all the machines it is used to supply.
After the actual design procedure the design must be evaluated, first of all to ensure that the choices of system components do not conflict with each other or with any of the design criteria.

4.1 Directional Control Valve

The DCV is selected according to the maximum flow required by the actuator:

$$Q_{max} = v_{max} \cdot A_p \tag{20}$$

To ensure enough flow for all situations, a valve with a higher capacity may be selected. However this choice is often implicitly made since rated flow of a valve is a discrete design variable and the valve with the nearest flow capacity above the required is chosen. For hydraulic systems with closed loop control, an important property of the DCV is the bandwidth. Manufacturers of servo valves usually recommend choosing a valve with a bandwidth, ω_v, which is at least three times higher than the natural frequency, ω_{sys}, of the system it is used to control, (MOOG, 2012):

$$\omega_v \geq 3 \cdot \omega_{sys} \tag{21}$$

This applies if the valve should not affect the overall bandwidth of the series connection of the valve and the hydraulic-mechanical system it is used to control.
For many applications such as material handling cranes, it is the opposite, i.e., the bandwidth of the DCV is lower than the one of the hydraulic-mechanical system. This is also reflected by the fact that pressure compensated DCVs have relatively low bandwidths, up to 5 Hz (Bak and Hansen, 2012).
Fig. 9 shows the natural frequency of the considered system as function of the cylinder piston position, s, for three different load cases.

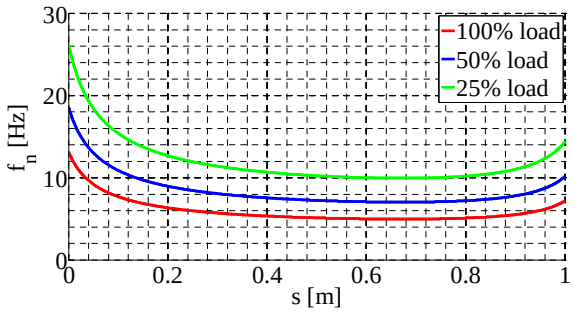

Figure 9: Natural frequency of hydraulic-mechanical system.

Choosing a DCV with a bandwidth of 5 Hz is sufficient for this application as long as the ramping times for the velocity reference are not too small.

4.2 Counterbalance Valve

The size of the CBV is chosen according to the maximum flow required or induced by the actuator or it may be chosen to match the rated flow of the DCV.
In order to avoid unintended opening of the CBV the cracking pressure is typically set to a factor of 1.3 above the maximum load induced pressure, (Sun Hydraulics, 2012):

$$p_{cr,cbv} \geq 1.3 \cdot p_{load,max} \tag{22}$$

One of the most critical design variables of a system containing CBVs is the pilot area ratio, ψ, due to its strong influence on the system stability during load lowering. It is therefore usually chosen based on experience and may need to be changed once the system has been realized and tested.
Some basic steady-state considerations for choosing ψ may be applied to ensure that cavitation does not occur on the metering side of the cylinder during load lowering.
The cylinder force during negative loads:

$$F = \frac{1}{\eta_{hmc}} \cdot (p_2 \cdot A_p - p_3 \cdot \phi \cdot A_p) \tag{23}$$

And the opening condition for the CBV:

$$p_2 + \psi \cdot p_3 = p_{cr,cbv} \tag{24}$$

Can be combined to express the upper limit of ψ:

$$\psi \leq \frac{p_{cr,cbv} - \frac{F \cdot \eta_{hmc}}{A_p}}{p_3} - \phi \tag{25}$$

p_3 is set to the preferred safety margin, e.g., $10 \ldots 20 \cdot 10^5$ Pa in order to avoid cavitation.

4.3 Control System

The feedback controller gains cannot be determined based on steady-state considerations and therefore have to be tuned after the system has been realized. The feedforward gains, on the other hand, can be estimated when using a pressure compensated DCV.
For a DCV with a symmetrical and linear flow characteristic (neglecting the deadband

of the valve) the cylinder velocity is:

$$v \approx \frac{u_{ref} \cdot Q_{max}}{A_Q} \tag{26}$$

$$A_Q = \begin{cases} A_p & 0 \leq u_{ref} \\ \phi \cdot A_p & u_{ref} < 0 \end{cases} \tag{27}$$

In Eq. (26) Q_max is the maximum flow of the valve. With a velocity reference the feedforward control signal can be computed:

$$u_{FF} = v_{ref} \cdot K_v \tag{28}$$

Combining Eq. (26) and (eq28pap3) yields the feedforward gain:

$$K_v = \frac{A_Q}{Q_{max}} \tag{29}$$

4.4 System Characteristics

Employing the sizing procedure described through Eq. (20) - (29) yields a number of design parameters for the considered system. They are listed in Table 2 together with the most important model parameters. With the velocity reference specified in section 2,

Table 2: Parameters for hydraulic system.

Directional control valve	
$\omega_v = 30$ rad/s	$\zeta = 0.8$
$C_v = 2 \cdot 10^{-6}$ m^3/s $\cdot$ Pa$^{0.5}$	overlap: 10%
$p_0 = 7 \cdot 10^5$ Pa	
Counterbalance valve	
$\psi = 3$	$C_v = 1.58 \cdot 10^{-6}$ m^3/s $\cdot$ Pa$^{0.5}$
$p_{cr,cbv} = 235 \cdot 10^5$ Pa	$k_{s,cbv} = 300 \cdot 10^5$ Pa
$p_{cr,cv} = 2 \cdot 10^5$ Pa	$k_{s,cv} = 1 \cdot 10^5$ Pa
Control system	
$K_{v,1} = 7.4$	$K_{v,2} = 4.3$

see Fig. 10, a simulation is carried out to analyze the response of the system.
With the feedforward gains given in Table 2 and the feedback controller disabled the piston position shown in Fig. 11 is obtained.

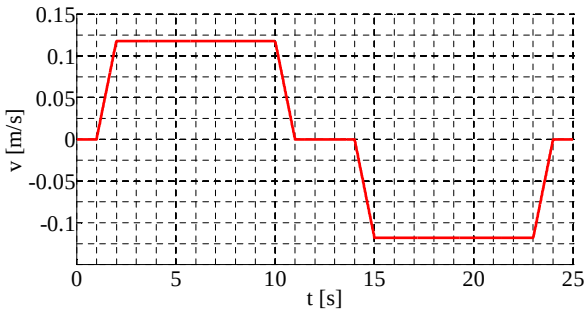

Figure 10: Velocity reference, v_{ref}.

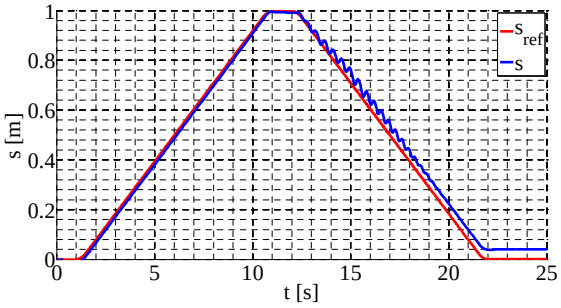

Figure 11: Position reference, s_{ref}, versus simulated position, s.

The simulated system pressures are shown in Fig. 12.

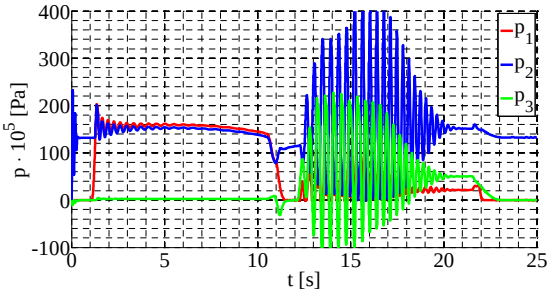

Figure 12: Simulated system pressures p_1, p_2 and p_3.

As seen from both Fig. 11 and 12 the system becomes strongly oscillatory during the lowering sequence and it is not able to follow the prescribed position reference with the feedforward controller alone. As the last step in a design procedure the feedback controller can relatively easy be tuned to remove the accumulated position error seen in Fig. 11.

5 Dynamic Considerations

The system response shown in Fig. 11 and 12 illustrates a classical problem with systems using a CBV in combination with a pressure compensated DCV. If care is not taken the system is likely to become so oscillatory that it is uncontrollable. Furthermore, the negative values of p3, though they cannot occur in reality, indicate that the oscillations are violent enough to cause cavitation in rod-side chamber of the cylinder.
The system response is directly influenced by the chosen pilot area ratio, ψ, which is usually set high for energy efficiency purposes and only lowered if the system, as in this case, becomes strongly oscillatory.
From Eq. (25) a pilot area ratio of $\psi = 3$ is obtained. In Fig. 13 the pressure response with $\psi = 1$ is shown.

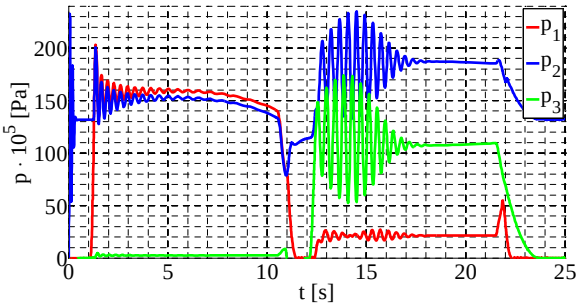

Figure 13: Simulated pressures with $\psi = 1$.

Lowering the pilot area ratio clearly reduces the oscillations. However, a significant level of oscillation remains and often it is necessary to take extra measures to further reduce the oscillations.

5.1 Reliability and Dynamic Performance

Strong oscillations may lead to excessive noise, wear and fatigue, and as shown in Fig. 12, loss of functionality. Hence, these oscillations are directly related to the reliability of the system.
The oscillatory nature of the considered system has been investigated several times (Miyakawa, 1978), (Overdiek, 1981), (Persson et al., 1989), (Handroos et al., 1993), (Chapple and Tilley, 1994), (Ramli et al., 1995), (Zähe, 1995) and (Andersen et al., 2005) and it is well established that it is caused by having two active throttling control valves in series; the pressure compensator of the DCV and the CBV. The oscillations can be reduced by lowering the pilot area ratio, bleeding of the CBV's pilot line or narrowing the return edge of the DCV. These measures can, however, not remove the oscillatory nature related to the CBV and therefore they do not improve the reliability of the system,

they only improve the dynamic performance.
Reliability may be divided into several categories, e.g., operational reliability and safety related reliability, and their importance may vary from one application to another. While both types of reliability are important for offshore applications, the first one is the main concern here. The operational reliability, i.e., how well and reliable the system can be controlled, is directly influenced by its oscillatory nature.
In order to improve the operational reliability, the concept of two throttling valves in series must be abandoned. This can be done either by removing the pressure compensator or by removing the CBV. The first measure is normally avoided in offshore applications because it increases the demands on the feedback controller and therefore introduces another loss of operational reliability. The second measure is only partially possible because the CBV has other functionalities than controlling the load lowering. It can, however, be obtained by forcing the CBV to open completely, as described by Nordhammer et al. (2012), making it work as a fixed orifice. This will, in turn, require that the throttling is handled by the return edge of the DCV.
While this eliminates the oscillations caused by the CBV and therefore improves the operational reliability, the safety related reliability is likely to be reduced due to an increased closing time of the CBV and a possibly increased risk of the CBV getting stuck open. This is critical in case of hose rupture and therefore the method may need to be combined with safety increasing features or monitoring functions. Further safety assessment, however, is not carried out here.
Reducing the pilot area ratio of the CBV or transferring the return throttling to the DCV will reduce the load range that can be handled during lowering. The loss in efficiency, on the other hand, is not a big issue since the considered system is supplied from a ring line with a constant pressure level.
Availability becomes an issue if the return throttling is to be handled by the DCV, since this requires a tailor-made main spool whereas a CBV is usually available with several different pilot area ratios.
The oscillatory behavior of the considered system can be investigated by means of simulation. The pilot area ratio and the return edge of the DCV are the design parameters that must be chosen with the objective to:

1. Minimize oscillations.

2. Maximize load range.

Simultaneously, it must be chosen if the operational reliability should be increased by forcing the CBV open and if the availability should be reduced by demanding a tailor-made main spool for the DCV.

5.2 Design Optimization

The most effective way to handle this is by means of numerical optimization using a suitable algorithm based on minimization techniques. In the following, two different design concepts are subjected to optimization and compared with the classical concept of only lowering the pilot area ratio and *throttling with the CBV*. One of them represents a semi-classical concept; *throttling with the CBV and the DCV*. The other represents a new concept; forcing the CBV to open completely and *throttling with the DCV*. Both designs, though, represent less available concepts since they require tailor-made DCV main spools. For both concepts the design variables are the pilot area ratio of the CBV and the size of the return edge of the DCV. The available range of pilot area ratios is $\psi = [1, 1.5, 2, 2.5, 3, 4, 5]$ and it is assumed that the return edge of the DCV main spool can be machined within the interval $C_{v,BT} = [0.5 \cdot 10^{-6}, 2 \cdot 10^{-6}]$ m^3/s $\cdot$ Pa$^{0.5}$.

5.2.1 Design Objectives

The first objective is to minimize the oscillations of the load controlling pressure, p_2, during the lowering sequence. To determine the oscillations level, p_2 is first low-pass filtered to determine the steady-state pressure, $p_2^{(ss)}$, around which it oscillates. The oscillations of p_2 can then be found:

$$p_2^{(osc)} = p_2 - p_2^{(ss)} \tag{30}$$

To obtain a single quantity representing the oscillation level, $p_2^{(osc)}$ is squared and integrated over the time of the lowering sequence:

$$O = \int_{t1}^{t2} \left(p_2^{(osc)} \right)^2 dt \tag{31}$$

Before starting the optimization procedure a nominal oscillation level, O_{nom}, of the initial design is found. This is used to obtain a normalized oscillation level (an error) during the optimization:

$$e_i^{(1)} = \frac{O_i}{O_{nom}} \tag{32}$$

Here Oi is the oscillation level of the i'th design suggested by the optimization routine. For the concept of *throttling with the CBV and DCV*, Eq. (32) is used for the objective function. For the concept of *throttling with the DCV*, an additional objective is used to

penalize the design if the CBV is not fully open:

$$e_i^{(2)} = 0.5 \cdot \frac{O_i}{O_{nom}} + 0.5 \cdot (1 - \overline{\xi}_{cbv_i}) \tag{33}$$

Here $\overline{\xi}_{cbv_i}$ is the mean value of the CBV opening during the lowering sequence.
In both cases two additional objectives must be met; the steady-state level of p_3 cannot exceed $180 \cdot 10^5$ Pa (to ensure the functionality of the DCV) and the steady-state level of p_2 cannot exceed $250 \cdot 10^5$ Pa (rated pressure of cylinder). If any of these two implicit constraints are violated, Eq. (32) and (33) are overruled and the error is set to $e_i = 1$. Similarly, violation of explicit constraints (limits of design variables) is penalized by setting the error $e_i = 1$.
The second objective of maximizing the load range is handled by evaluating Eq. (32) or (33) for two load cases; one with a load of 5000 kg (maximum load) and one with a lower load which is the minimum load the considered design can handle without violating any of the implicit constraints. The objective function used by the optimization algorithm can then be described as:

$$e_i = 0.5 \cdot e_i^{(maxload)} + 0.5 \cdot e_i^{(minload)} \tag{34}$$

Here, both $e_i^{(maxload)}$ and $e_i^{(minload)}$ are represented by either Eq. (32) and (33) depending on the considered design concept.

5.2.2 Optimization Procedure

The optimization problem, to minimize ei, is solved with the Complex method (Box, 1965) with the modification that violation of both implicit and explicit constraints is handled by penalization, i.e, setting $e_i = 1$ as earlier described.
The method is often used for optimization of hydraulic systems and has the advantage of being fast and easy to implement (Andersson, 2001). The structure of the optimization procedure is shown in Fig. 14.
The initial design, $\mathbf{x}_{ini} = [\psi, C_{v,BT}]$ according to Table 2, is evaluated by running a simulation to determine the system pressures, i.e., the response shown in Fig. 12. In the simulation the feedback controller is disabled and only the feedforward signal is used to control the system.
The nominal oscillation level, Onom, is determined by means of Eq. (30) and (31) and passed on for evaluation of new designs. Next, a random design population is generated within the limits of the design variables, $\mathbf{X}_{lim}$. The size of the population is twice the number of design variables, i.e., $\mathbf{X}_{pop}$ contains four designs.

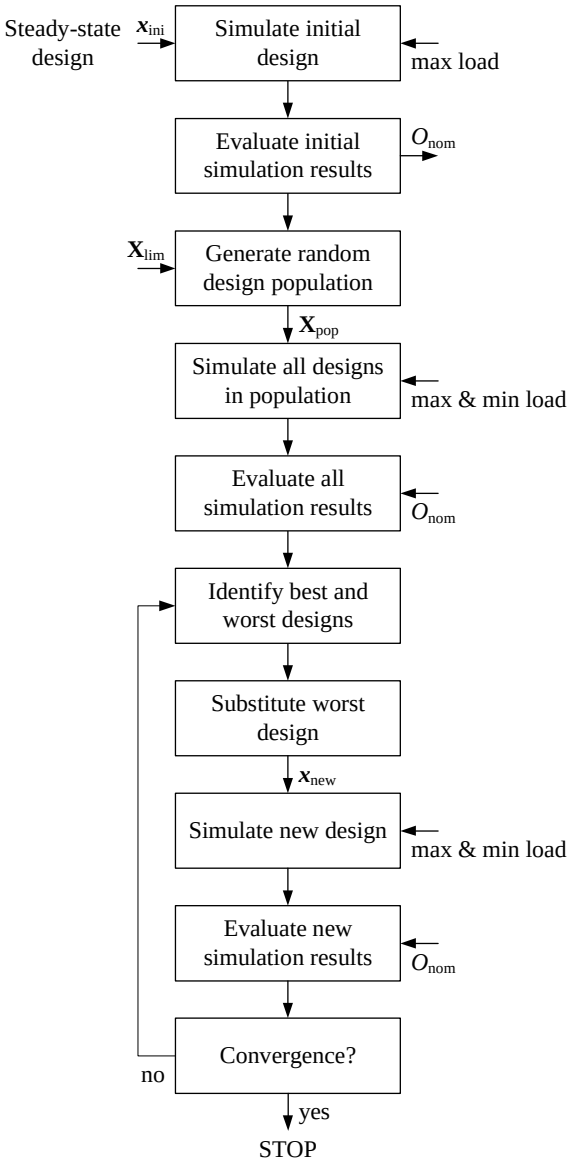

Figure 14: Structure of optimization procedure.

Two simulations are then carried out for each design; one with the maximum load to be handled and one with the minimum load the design is able to handle during lowering. The minimum load is identified by running the optimization procedure a number of times, each time reducing the minimum load until it is no longer possible to find a design that works for both maximum and minimum load.

Each design in the population is then evaluated by means of either Eq. (32) or (33) together with Eq. (34) depending on the design concept. From the four designs the best and the worst designs are identified. The best design is the one yielding the lowest objective function value and the worst the one yielding the highest. The worst design is then substituted according to the Complex method; i.e., reflecting the point representing

the worst design through the centroid of the remaining points in the design space in order to obtain a new design.
A simulation of the new design, $\mathbf{x}_{new}$, is carried out and the design is evaluated. The procedure of substituting the worst design continues until the convergence criterion is met; i.e., the objective function values of the best and the worst design are equal with some tolerance.

5.2.3 Results

First, the concept of forcing the CBV to open completely and *throttling with the DCV* is investigated. This is functional in the load range 3000 - 5000 kg (60 - 100 % load) with $\psi = 5$ and $C_{v,BT} = 0.7 \cdot 10^{-6}$ m^3/s $\cdot$ Pa$^{0.5}$ as the optimal design values. The pressures for the maximum and minimum loads are shown in Fig. 15 and 16.

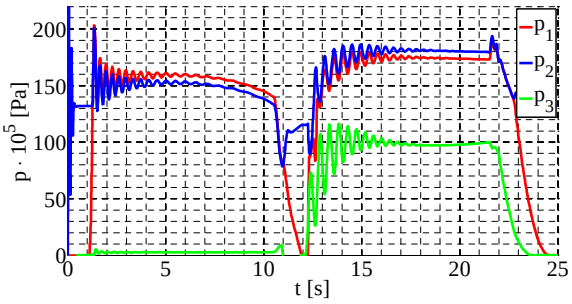

Figure 15: 100% load, $\psi = 5$, $C_{v,BT} = 0.7 \cdot 10^{-6}$ m^3/s $\cdot$ Pa$^{0.5}$.

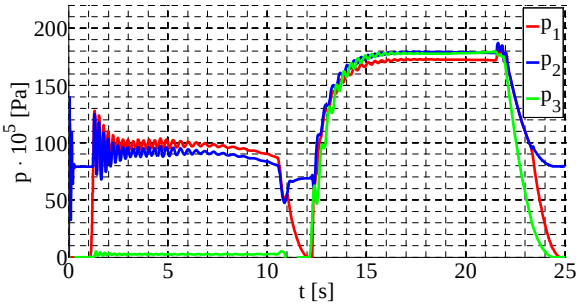

Figure 16: 60% load, $\psi = 5$, $C_{v,BT} = 0.7 \cdot 10^{-6}$ m^3/s $\cdot$ Pa$^{0.5}$.

While the oscillations are nearly removed at 60 % load, some oscillations remain at 100 % load. This is partly due to the limit $p_3^{(ss)} < 180 \cdot 10^5$ Pa which prevents further narrowing of the return edge. Also, the nature of the system together with the chosen ramping time will cause some oscillations as also seen from the lifting sequence.
Secondly, the concept of *throttling with the CBV and the DCV* is investigated. This

is functional in the load range 1500 - 5000 kg (30 - 100 % load) with $\psi = 1.5$ and $C_{v,BT} = 0.85 \cdot 10^{-6}$ m^3/s $\cdot$ Pa$^{0.5}$ as the optimal design values. The system pressures for the two load cases are shown in Fig. 17 and 18.

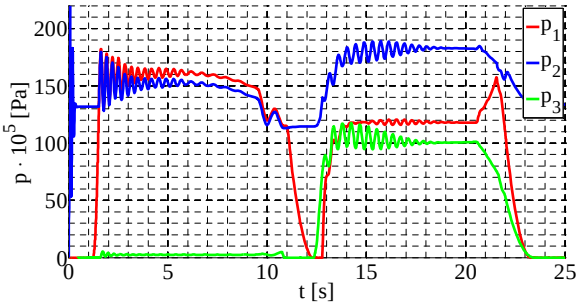

Figure 17: 100% load, $\psi = 1.5$, $C_{v,BT} = 0.85 \cdot 10^{-6}$ m^3/s $\cdot$ Pa$^{0.5}$.

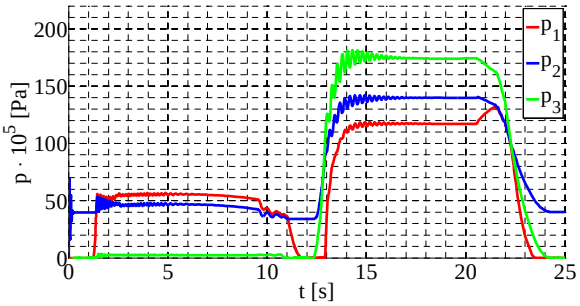

Figure 18: 30% load, $\psi = 1.5$, $C_{v,BT} = 0.85 \cdot 10^{-6}$ m^3/s $\cdot$ Pa$^{0.5}$.

In terms of dynamic performance, i.e., oscillation level, the concept of *throttling with the CBV and the DCV* generally yields slightly better results than the concept of *throttling with the DCV*. Both concepts are better than the classical concept of *throttling with the CBV*, in terms of dynamic performance.
When considering the operational reliability, however, the concept of *throttling with the DCV* is the only fully reliable design because the CBV is active in the other two concepts and, inherently, contribute to less predictable system behavior. The evaluation of the different concepts can be summarized as in Table 3.

If only small load variations are to be handled, the concept of forcing the CBV to open completely and *throttling with the DCV* represents the best design. For larger load ranges, this may not be a functional design, but *throttling with the CBV and DCV* is a better solution than only throttling with the CBV.
Requiring a tailor-made main spool for the DCV represents an additional cost of the system. For offshore applications operational reliability is the important performance

Table 3: Evaluation of return throttling concepts.

Throttling concept	Dynamic performance	Operational reliability
DCV	+	+
CBV + DCV	+	÷
CBV	÷	÷

criterion and it is therefore often accepted to acquire components with some degree of customization.

6 Conclusions

In this paper, an approach for model based design of electro-hydraulic motion control systems for offshore material handling cranes is put forward. The design procedure targets the system engineer and therefore one of the main challenges is to establish reliable system models with a suitable level of complexity. Models of the main components of the hydraulic system, which include key parameters such as bandwidth of the directional control valve (DCV) and steady-state characteristics of the counterbalance valve (CBV) is presented.
A typical steady-state design procedure is presented and used to determine the parameters of the main components of the motion control system. The presented system model is then used to demonstrate the problem of the inherently oscillatory behavior that characterizes the considered system.
In order to improve the dynamic performance and the operational reliability of the system, an optimization procedure, based on the Complex method, is applied to the simulation model in order to optimize design parameters for the DCV and the CBV.
With the objective to reduce the oscillation level during operation of the system, three different design concepts have been investigated:

1. The classical concept, *throttling with the CBV*, where the pilot area ratio of the CBV is lowered.

2. A semi-classical concept, *throttling with the CBV and the DCV*, where the pilot area ratio of the CBV is lowered and the return edge of the DCV is narrowed.

3. A new concept, *throttling with the DCV*, where the CBV is forced to open completely by increasing the pilot area ratio and narrowing the return edge of the DCV.

The main advantage of the classical concept is availability and load range. The main advantage of the new concept is operational reliability. The semi-classical concept and

the new concept both have an advantage in terms of dynamic performance.
In an offshore context where operational reliability is the most important criterion, the new concept is ideal as long as its poor load range capability is acceptable, i.e., for applications with small load variations.

Acknowledgements

The work presented in this paper is funded by the Norwegian Ministry of Education and Research and Aker Solutions.

Nomenclature

A_d	Discharge area	[m^2]
A_p	Piston area	[m^2]
A_Q	Controlled cylinder area	[m^2]
C_d	Discharge coefficient	-
C_v	Flow coefficient	[$m^3/s \cdot Pa^{0.5}$]
C_p	Pressure friction coefficient	-
D_p	Piston diameter	[m]
D_r	Rod Diameter	[m]
e	Error/ovjective function value	-
e_s	Position error	[m]
E	Young's modulus	[Pa]
f_s	Safety factor	-
F	Load force/cylinder force	[N]
$F_{friction}$	Friction force	[N]
F_h	Hydraulic force	[N]
F_S	Static friction force	[N]
h	Cylinder stroke	[m]
k_s	Normalized spring stiffness	[Pa]
K_v	Velocity feedforward gain	-
l	Cylinder length	[m]
O	Oscillation level	-
p	System pressure	[Pa]
p_0	Nominal pressure drop	[Pa]
p_{comp}	Compensated pressure	[Pa]
p_{cr}	Cracking pressure	[Pa]

p_{load}	Load induced pressure	[Pa]
p_{LS}	Load sensing pressure	[Pa]
Q	Flow	[m^3/s]
s	Piston position	[m]
t	Cycle time	[s]
t_{ramp}	Ramping time	[s]
u_{FB}	Feedback control signal	-
u_{FF}	Feedforward control signal	-
u_{spool}	Normalized spool position	-
u_{ref}	Control signal	-
v	Piston velocity	[m/s]
v_0	Transition velocity	[m/s]
V	Volume	[m^3]
β	Bulk modulus	Pa
ζ	Damping ratio	-
η_{hmc}	Hydro-mechanical efficiency	-
ξ	Relative valve opening	-
ρ	Fluid density	[kg/m^3]
ϕ	Cylinder area ratio	-
ψ	Pilot area ratio	-
ω_{sys}	System natural frequency	[rad/s]
ω_v	Valve bandwidth	[rad/s]

References

Andersen, T. O., Hansen, M. R., Pedersen, P., and Conrad, F. (2005). The influence of flow forces on the performance of over center valve systems. In *Proceedings of the Ninth Scandinavian International Conference on Fluid Power*. Linköping, Sweden.

Andersson, J. (2001). *Multiobjective optimization in engineering design. Applications to fluid power systems*. PhD thesis, Linköping University, Linköping, Sweden.

Bak, M. K. and Hansen, M. R. (2012). Modeling, performance testing and parameter identification of pressure compensated proportional directional control valves. In *Proceedings of the 7th FPNI PhD Symposium on Fluid Power*, pages 889–908. Reggio Emilia, Italy.

Box, M. J. (1965). A new method for constrained optimization and a comparison with other methods. *The Computer Journal*, 8(1):42–52.

Chapple, P. J. and Tilley, D. G. (1994). Evaluation techniques for the selection of counterbalance valves. In *Proceedings of the Expo and Technical Conference for Electrohydraulic and Electropneumatic Motion Control Technology*, pages 351–359. Anaheim, USA.

da Silva, J. C. and Back, N. (2000). Shaping the process of fluid power system design applying an expert system. *Research in Enginnering Design*, 12(21):8–17.

Handroos, H., Halme, J., and Vilenius, M. (1993). Steady-state and dynamic properties of counter balance valves. In *Proceedings of the 3rd Scandinavian International Conference on Fluid Power*, pages 215–235. Linköping, Sweden.

Hansen, M. R. and Andersen, T. O. (2001). A design procedure for actuator control system using design optimization. In *Proceedings of the 7th Scandinavian International Conference on Fluid Power*. Linköping, Sweden.

Hughes, E. J., Richards, T. G., and Tilley, D. G. (2001). Development of a design support tool for fluid power system design. *Journal of Engineering Design*, 12(2):75–92.

Krus, P., Jansson, A., and Palmberg, J.-O. (1991). Optimization for component selection in hydraulic systems. In *Proceedings of the 4th Bath International Fluid Power Workshop*, pages 219–231. Bath, UK.

Liermann, M. and Murrenhoff, H. (2005). Knowledge based tools for the design of servo-hydraulic closed loop control. *Power Transmission and Control*, pages 17–28.

Miyakawa, S. (1978). Stability of a hydraulic circuit with a counterbalance valve. *Bulletin of the JSME*, 21(162):1750–1756.

MOOG (2012). Electrohydraulic valves... a technical look. Technical report, Moog Inc. http://www.moog.com/literature/ICD/Valves-Introduction.pdf.

Nordhammer, P., Bak, M. K., and Hansen, M. R. (2012). A method for reliable motion control of pressure compensated hydraulic actuation with counterbalance valves. In *Proceedings of the 12th International Conference on Control, Automation and Systems*, pages 759–763. Jeju Island, Korea.

Ottestad, M., Nilsen, N., and Hansen, M. R. (2012). Reducing the static friction in hydraulic cylinders by maintaining relative velocity between piston and cylinder. In *Proceedings of the 12th International Conference on Control, Automation and Systems*, pages 764–769. Jeju Island, Korea.

Overdiek, G. (1981). Design and characteristics of hydraulic winch controls by counterbalance valves. In *Proceedings of the European Conference on Hydrostatic Transmission for Vehicle Applications*. Achen, Germany.

Papadopoulos, E. and Davliakos, I. (2004). A systematic methodology for optimal component selection of electrohydralic servosystems. *International Journal of Fluid Power*, 5(3):15–24.

Persson, T., Krus, P., and Palmberg, J.-O. (1989). The dynamic properties of over-center valves in mobile systems. In *Proceedings of the 2nd International Conference on Fluid Power Transmission and Control*. Hangzhou, China.

Ramli, Y., Chapple, P. J., and Tilley, D. G. (1995). Application of computer aided design (cad) in hydraulic systems using counterbalance valves. In *Proceedings of the 4th International Conference on Computer-Aided Design and Computer Graphics*. Wuhan, China.

Rasmussen, P. W., Iversen, F., Halling, B., Haugaard, J., Hounsgaard, G., Mï¿½lbak, H. G., Kristensen, F. D., Lyngbï¿½k, E., Rasmussen, N. B., Jessen, B. B., and Jannerup, O. (1996). *Hydraulik Stï¿½bi*. in danish.

Schlemmer, K. and Murrenhoff, H. (2008). Development of an expert system for electrohydraulic motion control design. In *The 20th International Conference on Hydraulics and Pneumatics*, pages 259–268. Prague, Czech Republic.

Stecki, J. S. and Garbacik, A. (2002). Fluid Power Net Publications.

Sun Hydraulics (2012). Load control and motion control cartridge valves. counterbalance and pilot-to-open check. Technical report, Sun Hydraulics. http://www.sunhydraulics.com/pdf/TT_US_Ctrbal_POCk.pdf.

Zähe, B. (1995). Stability of load holding circuits with counterbalance valves. In *Proceedings of the 8th Bath International Fluid Power Workshop*, pages 60–75. Bath, UK.

Paper IV

Analysis of Offshore Knuckle Boom Crane — Part One: Modeling and Parameter Identification

Morten Kollerup Bak and Michael Rygaard Hansen

This paper has been published as:

M. K. Bak and M. R. Hansen, “Analysis of Offshore Knuckle Boom Crane — Part One: Modeling and Parameter Identification”, *Modeling, Identification and Control*. Vol. 34 (2013), No. 4, pp. 157-174.

Analysis of Offshore Knuckle Boom Crane — Part One: Modeling and Parameter Identification

Morten Kollerup Bak and Michael Rygaard Hansen
Department of Engineering Sciences
Faculty of Engineering and Science, University of Agder
Jon Lilletunsvei 9, 4879 Grimstad, Norway

Abstract — This paper presents an extensive model of a knuckle boom crane used for pipe handling on offshore drilling rigs. The mechanical system is modeled as a multi-body system and includes the structural flexibility and damping. The motion control system model includes the main components of the crane's electro-hydraulic actuation system. For this a novel black-box model for counterbalance valves is presented, which uses two different pressure ratios to compute the flow through the valve. Experimental data and parameter identification, based on both numerical optimization and manual tuning, are used to verify the crane model.
The demonstrated modeling and parameter identification techniques target the system engineer and takes into account the limited access to component data normally encountered by engineers working with design of hydraulic systems.

Keywords — Hydraulic crane, multi-body system, flexibility, directional control valve, counterbalance valve.

1 Introduction

Today's offshore drilling equipment is characterized by high price, high level of system complexity and low production numbers. For the equipment manufacturers, it requires a great level of skill and experience to develop the equipment, since there are very limited possibilities to build prototypes for testing and verification of new designs. Increasing focus on production and development costs adds to this challenge. As a consequence, design engineers continuously have to improve their procedures for decision making regarding choice of principal solutions, components and materials in order to reach the best possible trade-off between different performance criteria such as reliability, efficiency and cost.

Computer based time domain simulation and optimization techniques have, by far, proven themselves as excellent tools for the challenged designer and have over the last couple of decades increasingly been employed by drilling equipment manufacturers. However, the use of these techniques still offers a number of challenges both in industry as well as academia.

In model based design, simulation models serve as virtual prototypes providing information, e.g., about a machine's overall efficiency, stability and accuracy, enabling engineers to test, redesign and optimize the design of the machine before it is manufactured. Model based design offers the possibility to reduce both development time and costs while also producing more reliable machines.

The main challenge in model based design lies within the ability to produce simulation models that, with a reasonable precision, are able to mimic the behavior of a real system. This challenge is especially pronounced for hydraulically actuated machines, like many offshore drilling applications, simply because suppliers of hydraulic component are not used to deliver all the data needed to develop simulation models of their products.

An application that represents a typical piece of high-end offshore equipment is the knuckle boom crane. The ability to employ a model based approach for design of such cranes is highly relevant.

Modeling, simulation, design and control of various types of cranes have been subjected to extensive research. General modeling techniques and different control concepts have been presented by Hiller (1996) and Abdel-Rahman et al. (2003) and particularly mobile (truck-mounted) cranes have attracted a considerable amount of interest from researchers (Ellman et al., 1996), (Mikkola and Handroos, 1996), (Esque et al., 1999), (Hansen et al., 2001), (Nielsen et al., 2003) and (Esque et al., 2003). The dynamics of these types of cranes is well documented and modeling techniques have been proven through experimental verification.

In (Than et al., 2002) and (Bak et al., 2011) offshore boom cranes have been investigated. Models taking the structural flexibility into account have been presented, however, with-

out any experimental verification.
Though mobile cranes are particularly flexible and behave differently than offshore cranes, the same modeling techniques can be used for both types of cranes. Modeling of mechanical systems such as boom mechanisms can be handled with different generic approaches. However, the most suitable approach is not always obvious.
Modeling approaches for hydraulic components and systems are, in general, also well-established but may cause problems when it comes to model verification. The problem is often a lack of proper model data and/or that the physics is not fully understood. Therefore, for certain hydraulic components, there may be a need to introduce new modeling approaches.
In this paper an extensive model of an offshore knuckle boom crane is developed with a view to identify a best practice for predicting the behavior of this type of crane. It is demonstrated how to overcome the modeling challenge by choosing an appropriate level of modeling detail and by using experimental work together with parameter identification techniques.
A commercially available software package, MapleSim^{TM}, is used to develop a dynamic model and MATLAB® is used for steady-state simulations and optimization based parameter identification.

2 Considered System

Knuckle boom cranes are used for a wide range of offshore and marine operations and therefore exist in different variations. The considered crane is manufactured by Aker Solutions and is used on drilling rigs to move drill pipes between the pipe deck and a transportation system leading to the drill floor of the rig.
Prior to commissioning of a crane, it undergoes a test procedure to verify the functionality and ensure that the performance corresponds to the criteria given in the design specification. This procedure facilitates an experimental study that can be used to calibrate and verify design models of the crane. In the following a description of the considered crane is given along with system variables that have been measured and recorded during a test procedure. The procedure itself is described in section 5 along with the model parameter identification.
The considered crane may be treated as a large multi-domain system consisting of three interacting systems:

1. A mechanical system.
2. An electro-hydraulic actuation system.
3. An electronic control system.

The main components of the cranes mechanical system are a rotating part mounted on a pedestal, an inner jib, an intermediate jib, an outer jib and a gripping yoke, see Fig. 1.

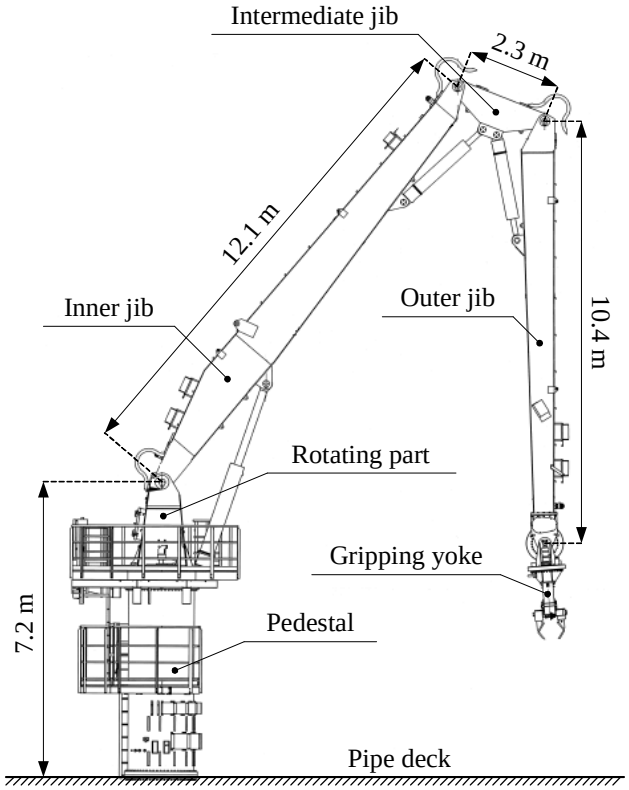

Figure 1: Main components of mechanical system.

The crane is controlled from the operators cabin (not shown) mounted on the rotating part, also called the king. A slewing bearing and transmission between the king and the pedestal allows for slewing of the crane. However, this degree of freedom (DOF) and the details of the slewing transmission are not considered here.
The gripping yoke also includes a number of hydraulically actuated DOFs which are not considered. The actuation system is supplied by a hydraulic power unit (HPU) with constant supply pressure, $p_S = 210$ bar, and return pressure, $p_R = 0$.
The considered part of the actuation system consists of three hydraulic circuits, one for each crane jib, connected to the supply and return lines of the HPU. The control system includes a human-machine interface (HMI) which facilitates the operation of the crane, a number of sensors and instruments used for feedback control and/or monitoring and a controller where the control logic is defined.
When considering the actuation and control systems together, the three circuits of the actuation system can be considered as three sub-systems of the motion control system, including both actuation and control. A simplified schematic of the motion control sub-system for the inner jib is shown in Fig. 2.

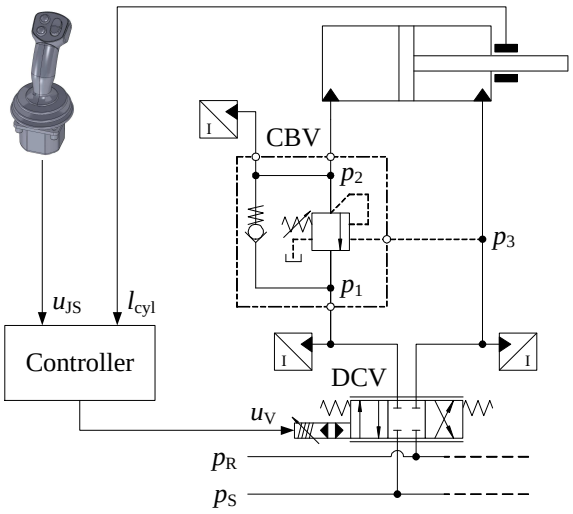

Figure 2: Simplified schematic of motion control sub-system for inner jib.

The main components of the hydraulic circuit are a cylinder with integrated position sensor, a servo-type directional control valve (DCV) and an externally vented (drained) counterbalance valve (CBV). The cylinder velocity is controlled via the DCV, which controls the flow into either of the two cylinder chambers. During retraction of the cylinder (load lowering), it is exposed to negative loads (piston velocity and load force have the same direction) and therefore the piston pressure, p_2, needs to be controlled. This is handled by the CBV, which provides a relief valve functionality on the outlet side assisted by the pressure, p_3, on the inlet side.

The DCV is controlled via a joystick (part of the HMI) from which the command signal, u_{JS}, is fed to the controller and used to generate the control signal, u_V, to the valve. The signal from the position sensor in the hydraulic cylinder is also fed to the controller, where it can be used for feedback control depending on the selected control mode. In open loop control mode joystick commands are passed through the controller and fed directly to the DCV. In closed loop control mode both joystick commands and cylinder positions are used for control of the DCV.

The motion control sub-systems for the intermediate and outer jibs are identical and contain the same control system elements as the one for the inner jib. However, as seen from Fig. 3, the elements of the actuation systems are different.

The DCV is pressure compensated and uses a load sensing (LS) circuit and a pressure reducing valve that maintains a constant pressure drop across metering edge of the main spool at any time. This makes the controlled flow independent of the load pressure and proportional to the spool position, i.e., the control signal fed to the valve.

There are two CBVs since the load force on the cylinder may act in either direction, depending on the orientation of the crane jibs. The CBVs are non-vented and include two

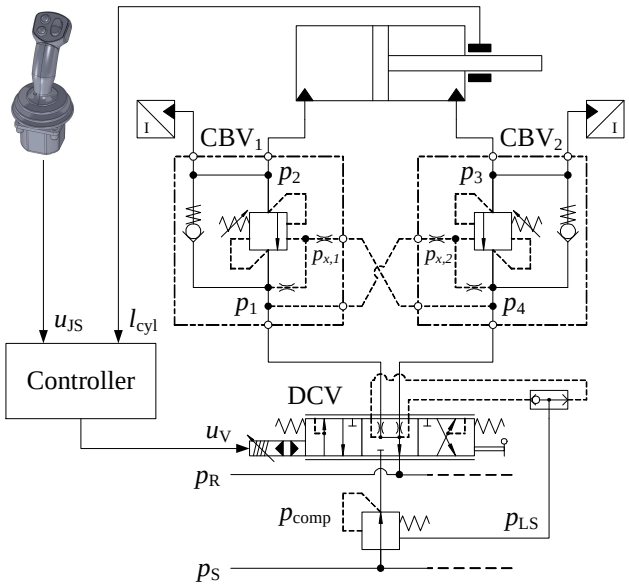

Figure 3: Simplified schematic of motion control sub-system for intermediate and outer jibs.

series connected orifices to manipulate the pilot pressures, $p_{x,1}$ and $p_{x,2}$. For practical reasons it is only possible to measure p_2 and p_3 this circuits.
In total seven pressures, three command signals and three position signals are measured and recorded during the experimental test procedure. Table 1 provides an overview of the system variables and the ones that are measured for the three considered motion control sub-systems.

Table 1: System variables for considered motion control sub-systems.

✓ = measured	Input	Output	State variables					
✗ = not measured	u_{JS}	l_{cyl}	p_1	p_2	p_3	p_4	$p_{x,1}$	$p_{x,2}$
Inner jib	✓	✓	✓	✓	✓	NA	NA	NA
Intermediate jib	✓	✓	✗	✓	✓	✗	✗	✗
Outer jib	✓	✓	✗	✓	✓	✗	✗	✗

3 Mechanical System Model

The mechanical system is modeled using the multi-body library in MapleSim^{TM}. The model includes the main components shown in Fig. 1 as well as the hydraulic cylinders for the three crane jibs.

In terms of kinematic structure, the crane can be treated as a large mechanism consisting of both rigid and flexible links connected by revolute joints. The structural flexibility of a crane similar to the one considered here has been studied by Henriksen et al. (2011) and Bak et al. (2011). It was shown that the flexibility of certain structural members can have a significant influence on the overall dynamic behavior of the crane and therefore must be accounted for in a dynamic model.
Here the *finite segment method* is used to model the flexibility. The main advantage of this method is that it is based on rigid body modeling techniques, making it easy to implement. The method was originally developed by Huston (1981) and further studied in Huston (1991), Huston and Wang (1993), Connelly and Huston (1994a) and Connelly and Huston (1994b). Hansen et al. (2001) used the method for modeling of a mobile crane and achieved encouraging results in terms of conformity between measurements and simulations.
The masses, inertias and geometry of the mechanical components have been extracted from CAD models.

3.1 Kinematic Structure

The topology of the crane is globally an open kinematic chain, formed by the crane jibs, with locally closed chains formed by the hydraulic cylinders. With the main components and the barrels and pistons of the three hydraulic cylinders, the model includes a total of 12 bodies, see Fig. 4.
Since the slewing DOF of the crane is not considered, the crane can be modeled as a planar mechanism using revolute and translational joints. However, only spatial multi-body elements are available in MapleSim^{TM}, making the selection of kinematic constraints less straight forward. To identify a suitable kinematic structure the crane is initially treated as a rigid body system.
The bottom of the pedestal is fixed at the global origin and the king is fixed to the top of the pedestal in point A. Points B, C, D and E represent revolute joints (RJ). The connection points of cylinder barrels, points F, H and J, are modeled as spherical joints (SJ) while the connection points for pistons, points G, I and K, are modeled as universal joints (UJ). The translational DOFs between the cylinder barrels and pistons are modeled as prismatic joints (PJ). This leaves four remaining DOFs (Nikravesh, 1988):

$$\begin{aligned} n_{DOF} &= 6 \cdot n_{bodies} - 6 \cdot n_{fixtures} - 5 \cdot n_{PJ} \\ &\quad - 5 \cdot n_{RJ} - 4 \cdot n_{UJ} - 3 \cdot n_{SJ} \\ &= 72 - 12 - 15 - 20 - 12 - 9 = 4 \end{aligned} \tag{1}$$

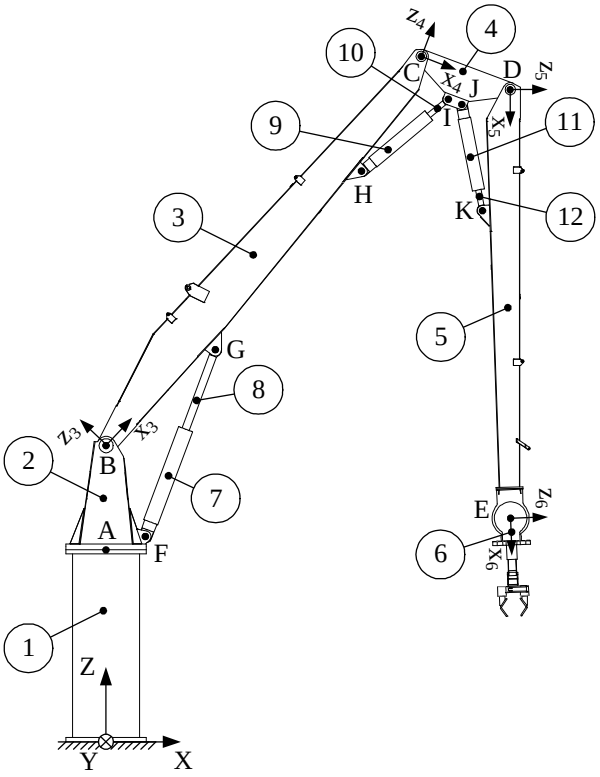

Figure 4: Topology of mechanical system model.

These are the ones of the three crane jib, which are actuated by hydraulic cylinders, and the rotational DOF of the gripping yoke (point E). The latter is actuated by a hydraulic motor, which is not considered here. The DOF is included to be able to orientate and fix the gripping in the wanted positions.

3.2 Flexibility

When applying the finite segment method to a planar mechanism, the flexible members are divided into a number of rigid segments which are connected by revolute joints and rotational springs (and dampers), see Fig. 5.

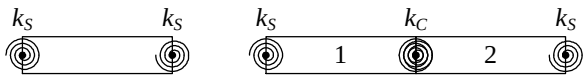

Figure 5: Concept of the finite segment method.

The left part of the figure illustrates a model of a single segment. The flexibility of the segment is represented by two rotational springs, both with the stiffness k_S. In the right part of the figure two segments are connected. The stiffness k_C of the connection between

the segments corresponds to a series connection of the springs for the two adjoining segments:

$$k_C = \frac{1}{\frac{1}{k_{S,1}} + \frac{1}{k_{S,2}}} \tag{2}$$

$k_{S,1}$ is the segment stiffness of the segment 1 and $k_{S,2}$ is the segment stiffness of the segment 2.
For bending the segment stiffness is:

$$k_S = \frac{2 \cdot E \cdot I}{L} \tag{3}$$

E is the Young's modulus, I is the area moment of inertia and L is the length of the segment.
The pedestal, the inner jib and the outer jib are assumed to dominate the overall structural flexibility of the crane since the remaining components are far more compact. Fig. 6 shows the segmentation of the three flexible members.

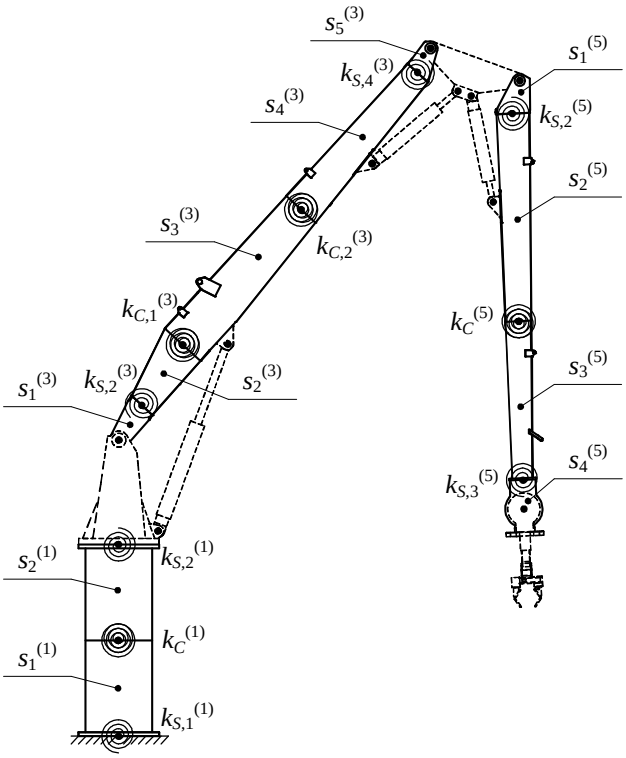

Figure 6: Segmentation of flexible model.

The pedestal, inner jib and outer jib (body numbers 1, 3 and 5) are divided into two, five and four segments, respectively. The number of segments is certainly debatable, but is kept low for computational reasons.

As seen from Fig. 6, the inner and outer jibs are beam-like structures with varying cross sections. With the chosen segmentations, the cross section areas of the individual segments vary linearly and continuously and therefore average values of the segments area moments of inertia are used to determine the segment stiffnesses, k_S. The area moments of inertia at the cross sections between the segments are extracted from CAD models and used to determine the average area moments of inertia. Henriksen et al. (2011) used this approach for a model of a single crane jib and compared both static deflections and natural frequencies of a finite segment model with results of a finite element analysis and achieved a remarkable conformity even without calibrating the model.
The segment and connection stiffnesses, determined using (2) and (3), are given in Table 2. The first and last segments of the inner and outer jibs are assumed rigid and therefore the stiffness, k_S, of the neighboring segment is used as the connection stiffness, k_C.

Table 2: Segment and connection stiffnesses.

Segment	k_S [Nm/rad]	k_C [Nm/rad]	
$s_1^{(1)}$	$5.75 \cdot 10^9$	$2.88 \cdot 10^9$	
$s_2^{(1)}$	$5.75 \cdot 10^9$		
$s_1^{(3)}$	*rigid*	$1.96 \cdot 10^9$	
$s_2^{(3)}$	$1.96 \cdot 10^9$		$6.03 \cdot 10^8$
$s_3^{(3)}$	$8.73 \cdot 10^8$	$2.77 \cdot 10^8$	
$s_4^{(3)}$	$4.05 \cdot 10^8$		$4.05 \cdot 10^8$
$s_5^{(3)}$	*rigid*		
$s_1^{(5)}$	*rigid*	$2.08 \cdot 10^8$	
$s_2^{(5)}$	$2.08 \cdot 10^8$		$8.33 \cdot 10^7$
$s_3^{(5)}$	$1.39 \cdot 10^8$	$1.39 \cdot 10^8$	
$s_4^{(5)}$	*rigid*		

The stiffnesses in the applied *lumped parameter model* are indeed uncertain (soft) parameters and (2) and (3) merely represent a means to estimate those parameters. As argued by Shabana (1997), they can also be determined by finite element analysis and parameter identification. This is, however, not the scope of this paper and instead the stiffnesses are tuned during the calibration (section 5) of the entire crane model.

3.3 Damping

The dynamic characteristics of the mechanical model depend on the damping applied to it and therefore the damping must be carefully considered. However, damping parameters are even more uncertain than those related to the flexibility. The only way to properly determine the damping parameters may be to carry out a thorough experimental study of the considered structure. As in this case, time, resources and practical circumstances seldom allow for that kind of investigations.
Therefore, whether working with design models or models for analysis and with limited possibilities for experimental investigations, there is a need for methods to determine the damping parameters with a reasonable accuracy. Mostofi (1999) presents a simple approach that can be used for lumped parameter modeling techniques such as the finite segment method. For *stiffness damping* (damping elements in parallel with the flexible elements), the damping of a structural member is:

$$\mathbf{c} = \beta_k \cdot \mathbf{k} \tag{4}$$

k contains the spring coefficients determined in section 3.2 and β_k is a stiffness multiplier determined by:

$$\beta_k = \frac{2 \cdot \zeta_S}{\omega_S} \tag{5}$$

ζ_S is the damping ratio of the structure and ω_S is the natural frequency of the structure for the considered mode of motion. Representative damping ratios for different structures are given in Adams and Askenazi (1999). For metal structures with joints, e.g., weldings and bolted connections, the damping ratio is $\zeta = 0.03 - 0.07$. Naturally, this is subject to uncertainty but, nevertheless, better than a simple guess.
To determine the damping coefficients for the models of the three flexible members, simulations without damping have been carried out to find the natural frequency of each member. In the simulations each member is fixed in one end (cantilevered) and an impulse is applied to excite oscillations from which the natural frequency can be observed. The natural frequencies and corresponding range of stiffness multipliers for the three flexible members are given in Table 3.

Table 3: Natural frequencies and stiffness multipliers.

Member	ω_S [rad/s]	β_k [s]
Pedestal (with king)	94	0.0006 - 0.0015
Inner jib	60	0.001 - 0.002
outer jib	35	0.002 - 0.004

The stiffness multipliers are tuned together with spring coefficients during the model calibration in section 5.

4 Motion Control System Model

Whereas the model of the mechanical system, in general, is based on physical (white-box) modeling, the motion control system model is mostly based on semi-physical (grey-box) modeling. The main reason for this is that manufacturers of hydraulic components do not provide enough and sufficiently detailed information to establish physical models. In addition, physical models will quickly become too complex and computational demanding for system simulation. Therefore certain model structures have to be assumed which allow for simplifications without ignoring or underestimating important physical phenomena.
The motion control system is modeled using both predefined components from the hydraulic and the signal block libraries in MapleSim^{TM} and custom made components developed via Maple^{TM}. This combination facilitates both efficient model development and modeling at a detail level that is not supported by library components.
Joystick commands and control signals are represented by normalized signal, which can vary continuously between -1 and 1, and component dynamics is modeled using transfer functions.
Hydraulic valves are generally modeled as variable orifices with linear opening characteristics:

$$Q = \xi \cdot C_V \cdot \sqrt{\Delta p} \tag{6}$$

Here ξ is the relative opening of the valve, i.e., a dimensionless number between 0 and 1. It can be a function of system pressures or controlled with an input signal depending on the considered type of valve. Q is the volume flow through the valve and Δp is the pressure drop across it.
The flow coefficient in (6) can be expressed as:

$$C_V = C_d \cdot A_d \cdot \sqrt{\frac{2}{\rho_{oil}}} \tag{7}$$

The discharge coefficient, C_d, and the discharge area, A_d, are usually not specified for a valve. Instead C_V can be obtained from characteristic flow curves given in the datasheet of the valve. From this, a nominal flow, Q_{nom}, corresponding to a nominal pressure drop,

Δp_{nom}, can be identified and used to derive the flow coefficient:

$$C_V = \frac{Q_{nom}}{\sqrt{\Delta p_{nom}}} \tag{8}$$

This corresponds to the fully opened state of the valve, so with (6) it is assumed that the discharge coefficient, C_d, is constant and only the discharge area, A_d, varies with the relative opening of the valve.
This modeling approach works well for DCVs with closed loop spool position control where dither is used to eliminate static friction and certain design details are used to reduce the disturbances from flow forces.
In some cases the approach may also work for pressure control valves like CBVs. Most often, though, attempting to establish physical or semi-physical models of such valves will encounter a number of challenges, e.g., related to friction and resulting hysteresis, non-linear discharge area characteristics, varying discharge coefficients and varying flow forces. Therefore, a better way to model those types of valves may be to use a non-physical (black-box) approach as described in section 4.2.
The following sub-sections describe models of the DCVs, the CBVs and the hydraulic cylinders.

4.1 Directional Control Valves

The main concern, when modeling a DCV, is the steady-state flow characteristics and the dynamics (bandwidth) of the valve. For system simulations, the design details of the valve are usually not important and therefore servo valves and pressure compensated DCVs can often be represented by the same model. Breaking down the model into several elements offers flexibility and facilitates changes in the model like including or excluding a pressure compensator. The general DCV model includes a representation of the valve actuation (pilot stage) and four elements for the main spool. For pressure compensated valves, the model also includes the LS circuit and the pressure compensator. The model structure for the pressure compensated DCV is shown in Fig. 7. The blue lines are signal lines transferring only a single state variable. The red lines transfer the two hydraulic state variable, pressure and flow, between the hydraulic components. These are custom made components developed in Maple$^{\text{TM}}$.
The valve is actuated with the control signal u_V, which is passed through a second order system representing the dynamics of the valve:

$$\frac{u_{spool}}{u_V} = \frac{1}{\frac{s^2}{\omega_V^2} + 2 \cdot \zeta_V \cdot \frac{s}{\omega_V} + 1} \tag{9}$$

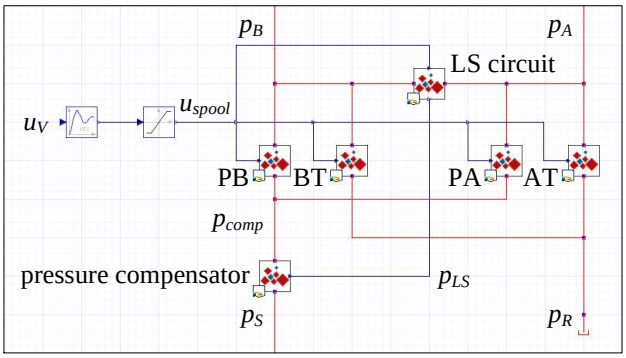

Figure 7: Structure of DCV model.

The output, u_{spool}, is a normalized signal representing the spool position, which can vary continuously between -1 and 1 with 0 being the center position of the spool. The natural frequency, ω_V, represents the bandwidth of the valve and ζ_V is the damping ratio.
For servo valves the bandwidth can usually be identified from the valves datasheet. Here the valve dynamics is usually visualized with Bode plots for several input amplitudes showing that the dynamics is non-linear. For system simulations, though, a linear model like the second order system will most often be sufficient to capture the dominant dynamics.
For pressure compensated DCVs there is usually no information available about the bandwidth and the only way to identify it may be to carry out a frequency response test of the considered valve. An approach for such a test is described in Bak and Hansen (2012) along with some test results for a Danfoss PVG32, which is identical to the DCVs used for the intermediate and outer jibs. The identified bandwidth, $\omega_V = 30$ rad/s, and damping ratio, $\zeta_V = 0.8$, are therefore also used here. This represents the overall dynamics between the control signal and the controlled flow, i.e., the dynamics of the pilot stage, the main spool, the LS circuit and the pressure compensator.
The four main spool edges are modeled as variable orifices, according to (6), for which the relative opening, ξ_{edge}, of each spool edge is a function of the normalized spool position signal as shown in Fig. 8.
The spool edge openings are piecewise linear functions that include the overlaps of the metering edges, PB and PA, and the underlaps of the return edges, AT and BT. A more detailed description of the opening functions is given in Bak and Hansen (2012).
When modeling pressure compensated DCVs, a problem often encountered is that very little or no information about the pressure compensator is available from the valves datasheet. This makes it difficult to estimate when the pressure saturation will occur and to establish a model of the compensator. However, if the nominal pressure drop across the main spool metering edge (setting of compensator spring), p_0, is known the

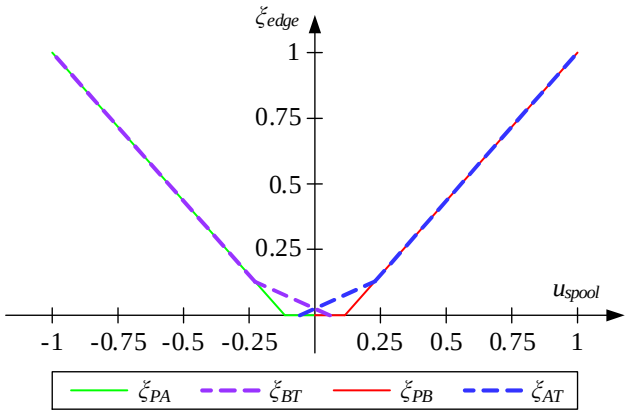

Figure 8: Opening functions for spool edges.

compensated pressure, p_{comp}, can be described as:

$$p_{comp} = \begin{cases} p_{LS} + p_0 & \text{for} \quad p_0 \leq p_S - p_{LS} \\ p_S - p_{LS} & \text{for} \quad 0 < p_S - p_{LS} < p_0 \\ p_{LS} & \text{for} \quad p_S - p_{LS} \leq 0 \end{cases} \tag{10}$$

The first case describes the normal operating condition of the compensator, maintaining the nominal pressure drop across the main spool metering edge. The second case describes the condition where the load pressure is too close to the supply pressure to maintain the nominal pressure drop. The third case describes the build-in check valve function of the compensator, which prevents negative flow if the load pressure exceeds the supply pressure.
The LS circuit directing the load pressure to the pressure compensator is modeled as a piecewise function:

$$p_{LS} = \begin{cases} p_A & \text{for} \quad u_{spool} < 0 \\ p_B & \text{for} \quad 0 < u_{spool} \\ 0 & \text{otherwise} \end{cases} \tag{11}$$

The model parameters for the servo valve (inner jib) and the pressure compensated DCVs (intermediate and outer jibs) are given in Table 4.

4.2 Counterbalance Valves

The model of the CBV consists of two components; a check valve and a pilot assisted relief valve (the actual CBV).

Table 4: DCV model parameters.

	Inner jib	Int. & outer jibs
ω_V	250 rad/s (40 Hz)	30 rad/s (5 Hz)
ζ_V	0.8	0.8
Overlap	5 %	10 %
Underlap	0	5 %
C_V	111.8 $\frac{l}{min \cdot bar^{0.5}}$	37.8 $\frac{l}{min \cdot bar^{0.5}}$
p_0	NA	7 bar

The check valve is modeled according to (6) with the relative opening given by:

$$\xi_{CV} = \frac{p_1 - p_2 - p_{cr,CV}}{k_{s,CV}} \tag{12}$$

This is only the basic part of a piecewise function that limits the relative opening to the interval $\xi_{CV} = [0,1]$. p_1 is the pressure at the port connected to the DCV and p_2 is the pressure at the port connected to the cylinder. The cracking pressure, $p_{cr,CV}$, is usually specified for a CBV and the normalized spring stiffness can be set to a low value of, e.g., $k_{s,CV} = 1$ bar.
In practice the check valve is either opened or closed. The spring stiffness is only used to handle the transition between the two states, which otherwise may cause computational difficulties.
Describing the relative opening by means of a pressure equilibrium like (12) can in some cases also be used for the CBV itself. However, for the previously mentioned reasons, it is often only valid for the condition where the CBV is just about to open (crack). For an externally vented CBV, like the one in Fig. 2, the cracking condition is described by:

$$p_2 + \psi \cdot p_x = p_{cr,CBV} \tag{13}$$

Once again, p_2 is the pressure at the port connected to the cylinder. p_x is the pilot pressure and ψ is the pilot area ratio.
For a non-vented CBV, like the one in Fig. 3 (ignoring the two internal orifices), the cracking condition is:

$$p_2 + \psi \cdot p_x = p_{cr,CBV} + (1 + \psi) \cdot p_1 \tag{14}$$

As for the check valve, p_1 is the pressure at the port connected to the DCV.
Instead of using (6) and a pressure equilibrium to model the CBV it is proposed to use a black-box approach based on the cracking condition in (13).

For the black-box model, two new variables are introduced; μ_x and μ_L. The first one is the ratio between the pilot pressure, p_x, and the load pressure, p_L:

$$\mu_x = \frac{p_x}{p_L} \tag{15}$$

The second variable is dependent on the type of CBV. For an externally vented CBV, it is the ratio between the load pressure and the cracking pressure:

$$\mu_L = \frac{p_L}{p_{cr,CBV}} \tag{16}$$

For a non-vented CBV, it is the ratio between the pressure drop across the valve and the cracking pressure:

$$\mu_L = \frac{\Delta p}{p_{cr,CBV}} \tag{17}$$

By replacing p_2 with p_L in (13) it can be combined with (15) and (16) to arrive at the following expression:

$$\mu_{L,cr} = \frac{1}{1+\psi \cdot \mu_x} \tag{18}$$

This expression, just as (13) and (14), describes the cracking condition of the CBV where there is still no flow the through the valve. It is illustrated by the solid line in Fig. 9, here for a CBV with a pilot area ratio of $\psi = 3$. The dashed lines above illustrate conditions with different levels of flow through the valve.
In the model the actual μ_x and μ_L for a given time step is computed by (15) and either (16) or (17) depending on the type of CBV. The distance, s, from the cracking line (randomly shown in Fig. 9) is then computed:

$$s = \mu_L - \mu_{L,cr} \tag{19}$$

If the distance is negative, there is no flow through the valve. Otherwise, the flow is computed as:

$$Q_{CBV} = A_{CBV} \cdot s^{n_{CBV}} \tag{20}$$

Here A_{CBV} is given by:

$$A_{CBV} = A_0 + A_1 \cdot \mu_x \tag{21}$$

Similarly, n_{CBV} is given by:

$$n_{CBV} = n_0 + n_1 \cdot \mu_x \tag{22}$$

The four parameters, A_0, A_1, n_0 and n_1 have to be experimentally determined, ideally by a thorough mapping of the flow through the CBV for different pressure combinations at

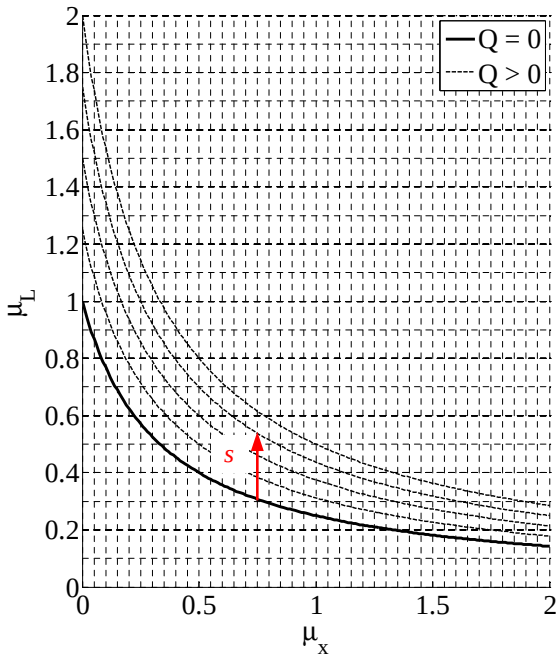

Figure 9: Example of the relation between μ_L and μ_x for the CBV model.

the individual ports. Alternatively, as described in section 5.2, they can be determined with parameter identification techniques and suitable measurements from the system where the CBV is installed.
The remaining (known) model parameters for the CBVs and the check valves for the inner jib and the intermediate and outer jibs are given in Table 5.

Table 5: CBV model parameters.

	Inner jib	Int. & outer jibs
C_V	89.4 $\frac{l}{min \cdot bar^{0.5}}$	63.2 $\frac{l}{min \cdot bar^{0.5}}$
$p_{cr,CV}$	1 bar	1 bar
$k_{s,CV}$	1 bar	1 bar
$p_{cr,CBV}$	250 bar	250 bar
ψ	3	6

4.3 Hydraulic Cylinders

The model of the hydraulic cylinder includes the capacitance of the chambers as well as the friction between the piston and the barrel. The cylinder force is:

$$F_{cyl} = \begin{cases} F_p - F_{fr} & \text{for} \quad v_{cyl} < v_0 \\ F_p - F_{fr} \cdot \frac{v_{cyl}}{v_0} & \text{for} \quad -v_0 \leq v_{cyl} \leq v_0 \\ F_p + F_{fr} & \text{for} \quad v_{cyl} < -v_0 \end{cases} \tag{23}$$

The pressure force is $F_p = p_1 \cdot A_p - p_2 \cdot \phi \cdot A_p$. Here A_p is the piston area and $\phi = (D_p^2 - D_r^2)/D_p^2$, where D_p is the piston diameter and D_r is the rod diameter. p_1 and p_2 are the pressures in the corresponding cylinder chambers. v_{cyl} is the cylinder piston velocity and v_0 is a transition velocity used to handle the change in friction force around zero velocity.
The capacitance of the two chamber volumes are accounted for by:

$$\dot{p}_1 = \frac{\beta_{oil}}{V_1} \cdot (Q_1 - v_{cyl} \cdot A_p) \tag{24}$$

$$\dot{p}_2 = \frac{\beta_{oil}}{V_2} \cdot (v_{cyl} \cdot A_a - Q_2) \tag{25}$$

β_{oil} is the effective stiffness (bulk modulus) of the hydraulic fluid. Q_1 and Q_2 are volume flows in the two cylinder chambers. The chamber volumes, V_1 and V_2, are functions of the cylinder length.
The friction in the cylinder is quite complex, especially around zero velocity. As described in Ottestad et al. (2012) it consists of both static and Coulomb friction as well as velocity dependent and pressure dependent friction, which may be described with a model of five parameters. Even though the model is not very complex, the number of parameters represents a problem because they cannot be determined without an extensive experimental study of the considered cylinder.
Consequently, an even simpler model must be used and therefore the friction force in (23) consists only of static friction and pressure dependent friction:

$$F_{fr} = F_S + C_p \cdot |F_p| \tag{26}$$

The static friction can be set to $F_S = A_p \cdot 1 \cdot 10^5$ m^2·Pa, i.e., a pressure of 1 bar on the piston-side is required to overcome the static friction. The pressure dependent friction may constitute 2...3 % of the hydraulic force, e.g., $C_p = 0.02$. The friction parameters are identified in section 5. The remaining (known) parameters for the cylinders are given

in Table 6.

Table 6: Cylinder model parameters.

	Inner jib	Int. & outer jibs
D_p	0.3 m	0.25 m
D_r	0.18 m	0.125 m
l_0	3.145 m	2.315 m
stroke	1.755 m	1.33 m
mass	1500 kg	750 kg

5 Parameter Identification

For verification of the model, experiments have been carried out where inputs, outputs and certain state variables (given in section 2) of the real system have been measured and recorded. The crane used for the experimental work is shown in Fig. 10.

Figure 10: Crane used for experiments.

In order to calibrate and verify the model, the inputs from the experiments are fed to the model and the uncertain parameters are systematically tuned (identified) until both simulated outputs and state variables correspond to those obtained in the experiments. The model can then be considered as verified as illustrated in Fig. 11.
To simplify the experiments and the following parameter identification, the individual DOFs are considered separately and one at the time. Since the procedure for identifying the parameters and verifying the model is the same for all three DOFs, only the DOF of the outer jib is considered in the following. During the experimental procedure the

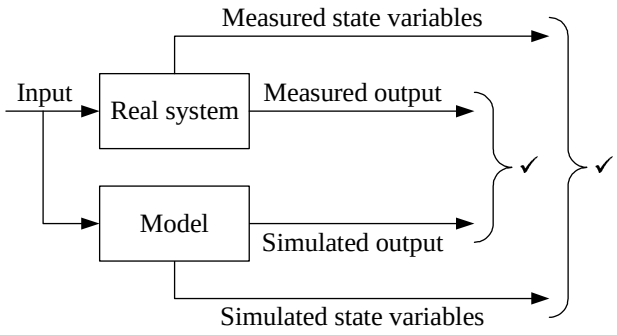

Figure 11: Principle of model verification.

crane is operated in open loop control mode, i.e., joystick signals are passed directly to the control valve of the considered DOF. The joystick signal and the resulting cylinder motion for the outer jib DOF are shown in Fig. 12.

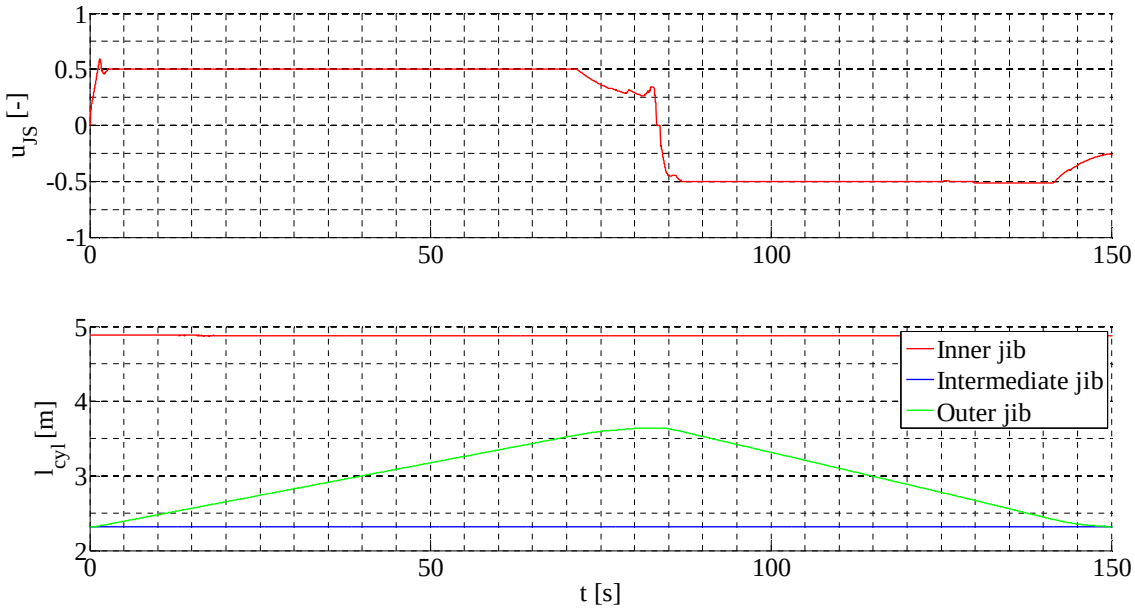

Figure 12: Experimental input and output for motion control sub-system for outer jib.

The calibration of the model is carried out in three steps; first the steady-state cylinder forces are considered, next the steady-state pressures and finally the system dynamics are considered.

Both steady-state and dynamic simulation is used for the model calibration. Steady-state simulation is carried out in MATLAB®, and dynamic simulation is carried out in Simulink® using an S-function (compiled C-code) generated from the MapleSim™ model. The main advantage of this approach is a significant increase in simulation speed. Furthermore, simulated values are quickly compared with measured values by importing

the latter from the MATLAB® workspace and plotting them together with the simulated values. The Simulink® model is shown in Fig. 13.

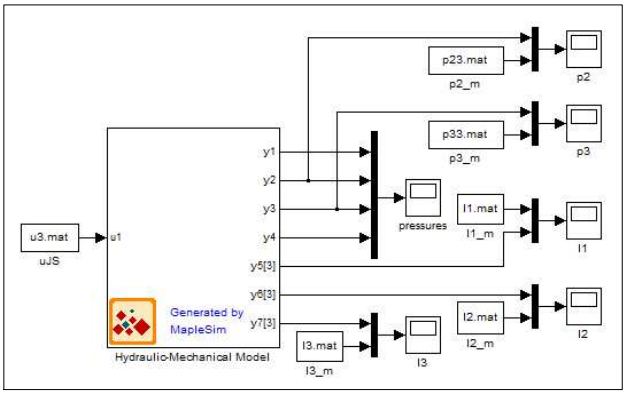

Figure 13: Simulink model of the crane.

The pressures in the circuit of the considered DOF are monitored and the measured pressures are compared with the simulated pressures. Simulated and measured lengths of all three cylinders are monitored for verification, i.e., to calibrate the motion of the considered cylinder and to ensure that the two remaining cylinders are not moving during simulation.

5.1 Steady-State Forces

A prerequisite for verification of the motion control system is to verify the mechanical model and to identify its uncertain parameters. For this purpose a rigid body steady-state model of the mechanical system, as shown in Fig. 4, is used to simulate the steady-state pressure forces in the cylinders, in order to compare these with the measured pressure forces. The simulation is carried out by using the measured cylinder motion given in Fig. 12 as input and computing the resulting steady-state force on the cylinder.
A parameter identification is carried out to identify the friction parameters for the cylinder model and to tune the mechanical model parameters, i.e., the masses and positions of the centers of gravity (COGs) originally found via CAD models. Since a CAD model seldom takes into account all the components in a mechanical assembly it is reasonable to allow for a tuning of the mechanical properties within a given set of constraints.
The parameter identification is an optimization routine, based on the `fmincon` function in MATLAB®, which minimizes the squared deviation between the measured pressure force, $\widetilde{F}_p$, and the simulated pressure force, F_p:

$$\text{minimize} \quad f = (\widetilde{F}_p - F_p)^2 \tag{27}$$

The simulated pressure force is computed as:

$$F_p = \begin{cases} F_{cyl} - F_S - C_p \cdot \left|\widetilde{F}_p\right| & \text{for} \quad v_{cyl} < 0 \\ F_{cyl} + F_S + C_p \cdot \left|\widetilde{F}_p\right| & \text{for} \quad 0 \leq v_{cyl} \end{cases} \tag{28}$$

F_{cyl} is the simulated steady-state force on the cylinder and v_{cyl} is the measured cylinder piston velocity.
The measured pressure force and simulated forces after the parameter identification are shown in Fig. 14. The parameter values before and after the identification are given in Table 7. As the pedestal and the king (bodies 1 and 2) are stationary, they are not included in the parameter identification. The positions of the COGs are according to the local coordinate systems in Fig. 4

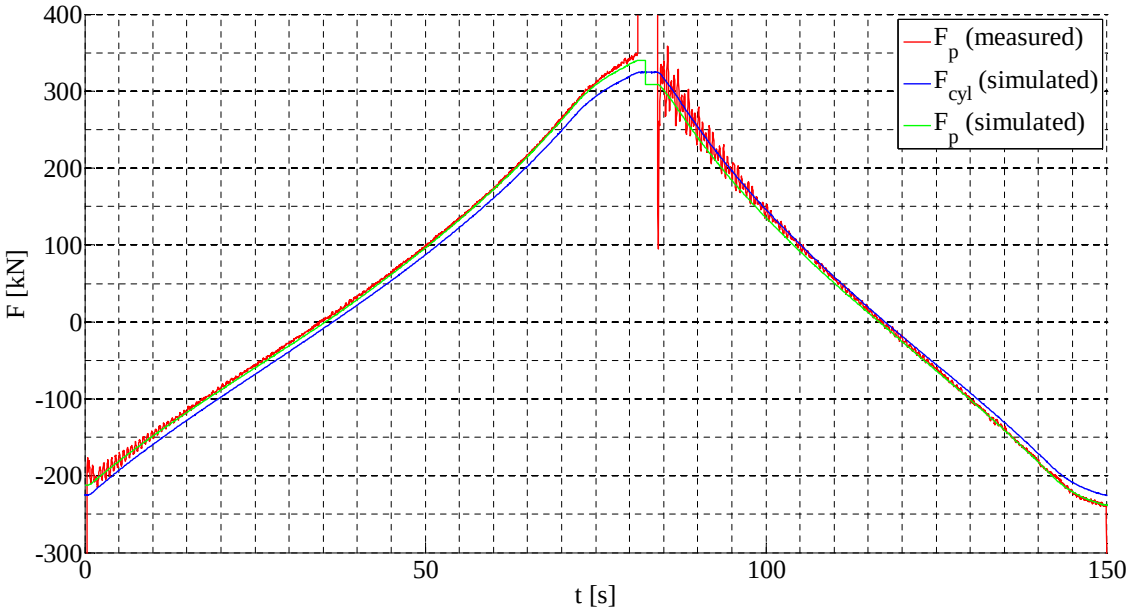

Figure 14: Measured and simulated forces for verification of steady-state characteristics.

The steady-state levels of the measured and simulated pressure forces are nearly equal and the mechanical model along with the identified parameters is therefore considered reliable.

5.2 Steady-State Pressures

The verification of the steady-state behavior of the control system model mainly depends on the calibration of the CBV model, i.e., identification of the four model parameters in

Table 7: Mechanical model parameters before and after parameter identification. Positions of COGs are according to Fig. 4.

Parameter	Before	After
m_3	5500 kg	5600 kg
m_4	1100 kg	1150 kg
m_5	2950 kg	3000 kg
m_6	2700 kg	2710 kg
x_3	5.3 m	5.4 m
z_3	0.4 m	0.35 m
x_4	1.15 m	1.1 m
z_4	-0.2 m	-0.15 m
x_5	4.9 m	4.8 m
z_5	-0.26 m	-0.21 m
x_6	1 m	1.57 m
z_0	0	0
F_S (*outer jib*)	-	6.4 kN
C_p (*outer jib*)	-	0.029

(21) and (22). For that the flows, Q_1 and Q_2, through CBV_1 and CBV_2 are computed from the measured cylinder motion shown in Fig. 12 and used in a steady-state model of the outer jib circuit, together with the two measured pressures, p_2 and p_3, in order to estimate the two remaining pressures, p_1 and p_4. The measured and estimated state variables are then used together with the CBV model to identify A_0, A_1, n_0 and n_1.

The two CBVs in the outer jib circuit are identical with a *geometric* pilot area ratio of $\psi = 6$. During operation a small amount of oil flows through the internal orifices of the active CBV, which causes a reduction of the actual pilot pressure, $p_{x,1}$ or $p_{x,2}$, compared to the external pressure, p_1 or p_4, at the pilot port. For practical reasons, the external pressure at the pilot port is often considered as the pilot pressure and therefore the orifices are said to lower the *effective* pilot area ratio.

With the given sizes of the two orifices the effective pilot area ratio is theoretically $\psi = 1.95$, which is represented by the dashed black line in Fig. 15. However, this is only valid when the flow through the orifices is turbulent and the back pressure is zero.

In practice, there is always a certain level of back pressure and the flow through the orifices may not follow the fully turbulent orifice equation at all times. Therefore the original cracking line for $\psi = 1.95$ is corrected according to:

$$\mu_{L,cr} = \frac{1}{1 + C_1 \cdot \mu_x + C_2 \cdot \mu_x^2} \tag{29}$$

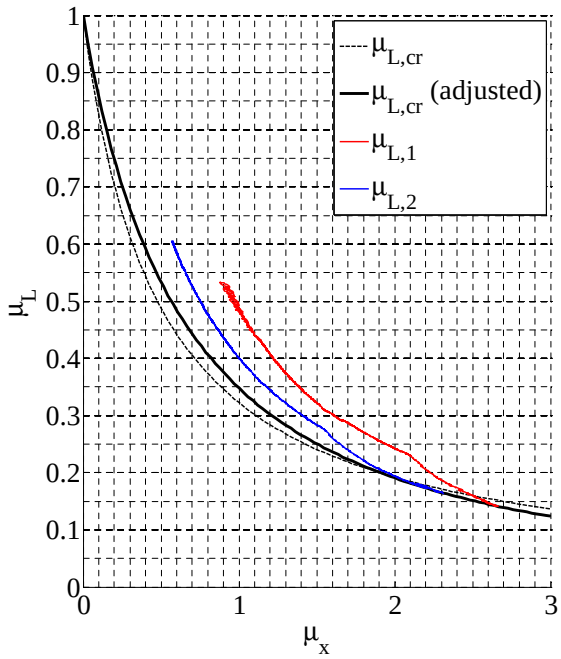

Figure 15: Relation between μ_L and μ_x for the outer jib CBVs.

The corrected cracking line, the solid black line in Fig. 15, is adjusted by tuning C_1 and C_2 until it coincides with the actual μ_L values obtained with the measured and estimated state variables.
During extension of the cylinder CBV_2 is active and μ_L is obtained by:

$$\mu_{L,2} = \frac{p_3 - p_4}{p_{cr,CBV}} \tag{30}$$

μ_x is obtained by:

$$\mu_{x,2} = \frac{p_1}{p_3} \tag{31}$$

During retracting of the cylinder CBV_1 is the active one and μ_L is obtained by:

$$\mu_{L,2} = \frac{p_2 - p_1}{p_{cr,CBV}} \tag{32}$$

μ_x is obtained by:

$$\mu_{x,2} = \frac{p_4}{p_2} \tag{33}$$

With the computed μ_x and μ_L values, (19) and (20) can be used to simulate the steady-state flow through the two CBVs and compare them with the measured flow in order to identify the four model parameters.

As for the mechanical model, the parameter identification is carried out by means of numerical optimization. Also here the optimization routine is based on the `fmincon` function in MATLAB®, which minimizes the squared deviation between the measured flow, $\widetilde{Q}_{CBV}$, and the simulated flow, Q_{CBV}:

$$\text{minimize} \quad f = (\widetilde{Q}_{CBV} - Q_{CBV})^2 \tag{34}$$

Fig. 16 show the measured and simulated flows after the parameter identification. The identified parameters are given in Table 8.

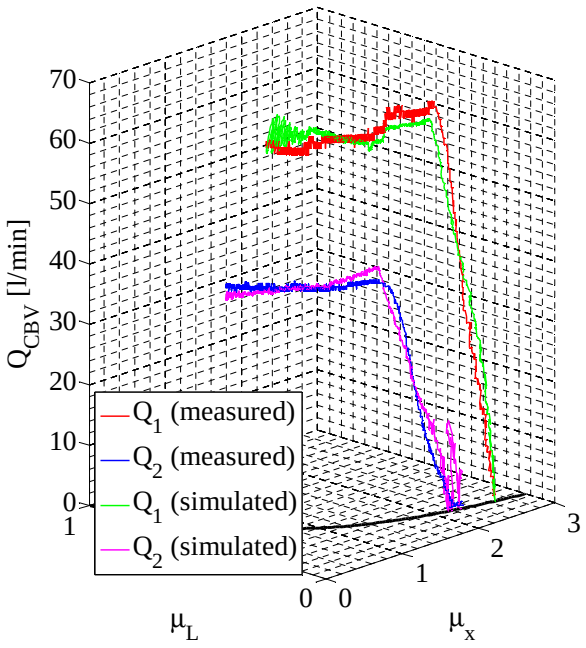

Figure 16: Measured and simulated flows through the CBVs after the parameter identification.

The steady-state simulation yields good conformity between the measured and simulated flows, which indicate that the suggested CBV model is valid and that the identified parameters are reliable. For the actual verification of the model, a dynamic simulation

Table 8: Model parameters for outer jib CBVs.

Parameter	Value	Parameter	Value
C_1	1.6267	C_2	0.2452
A_0	27.84	A_1	146.2
n_0	0.4707	n_1	0.0359

is carried out with the joystick signal in Fig. 12 as input. The flow coefficients of the DCV are adjusted manually in order to simulate the correct flow and obtain the cylinder motion shown in Fig. 17.

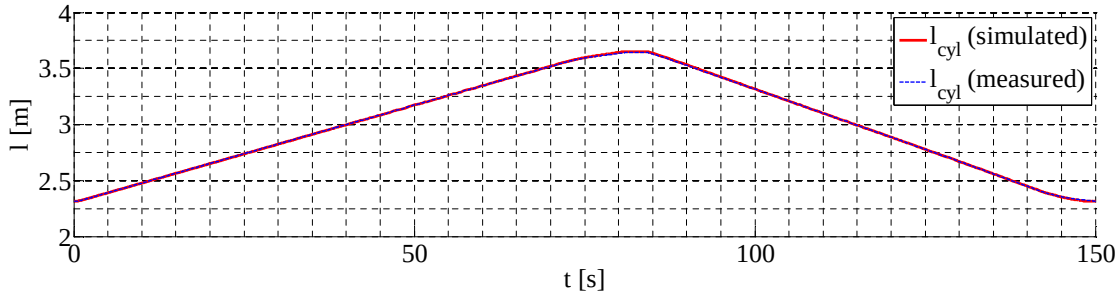

Figure 17: Measured and simulated cylinder motion.

Once the DCV model is calibrated and the simulated cylinder motion corresponds to the measured cylinder motion, the steady-state level of the simulated pressures can be compared with the measured pressures. Fig. 18 shows the simulated and measured values of p_2 and p_3.

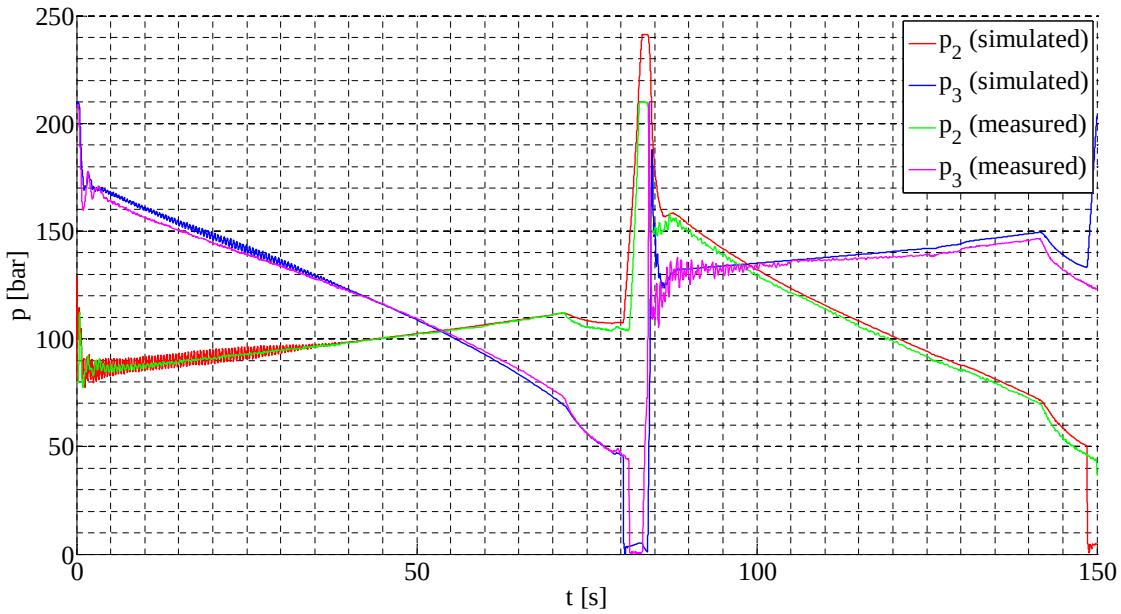

Figure 18: Measured and simulated pressures for verification of steady-state characteristics.

There is indeed a good conformity between steady-state levels of the measured and

simulated pressures, which verifies the steady-state characteristics of the CBV model and that the identified parameters are useful for simulation.

5.3 System Dynamics

The remaining uncertain parameters that dominate the system dynamics are the flexibility and damping parameters of the mechanical system and the stiffness, bulk modulus, of the hydraulic oil. The actual friction in the hydraulic cylinders, the dynamics of hydraulic valves and other hydraulic components also influence the overall dynamics to some extent, but they are considered to be less important for the considered system.
While the steady-state level of the simulated and measured pressures in Fig. 18 correspond well, there is a significant difference in dynamic response. The model is obviously stiffer than the real crane and therefore the flexibility parameters of the mechanical system are tuned by a scaling factor until the simulated dynamic response corresponds to the measured. Simultaneously, the bulk modulus is also adjusted.
The main objective for the tuning is to make the frequency of the simulated pressure oscillations correspond to the measured pressure oscillations. Naturally, the simulated amplitudes should also correspond to the measured amplitudes. However, there are more uncertain parameters related to the amplitude of the oscillations than for the frequency. Therefore some deviations are to be expected. Fig. 19 shows the simulated and measured pressures after the tuning.
During extension of the cylinder, both frequency and amplitude of the simulated pressure correspond very well with the measurements, except for the acceleration phase in the beginning of the sequence. The reason for this is most likely the un-modeled dynamics of the cylinder endstops and possibly that the CBV model is not accurate enough for accelerating flows.
During retraction of the cylinder only the frequency corresponds to some extent in the beginning of the sequence. The amplitudes do not correspond and the simulated oscillations are dampened far quicker than the measured oscillations. Also here, the likely causes are un-modeled dynamics of the cylinder endstop and inaccuracy of the CBV model. Furthermore, as described in section 4.3, the friction in the cylinder is quite complex around zero velocity and the applied cylinder model may be too simple to capture the real behavior during acceleration.
In general though, the simulated response corresponds well to the measurements. The observed deviations are within the expectations of what can be achieved with a model of the suggested detail level. The calibrated model is suitable for the type of simulations that can be utilized by system engineers working with hydraulic system design and/or control system design.
To obtain the correspondence shown in Fig. 19, all the flexibility parameters are ad-

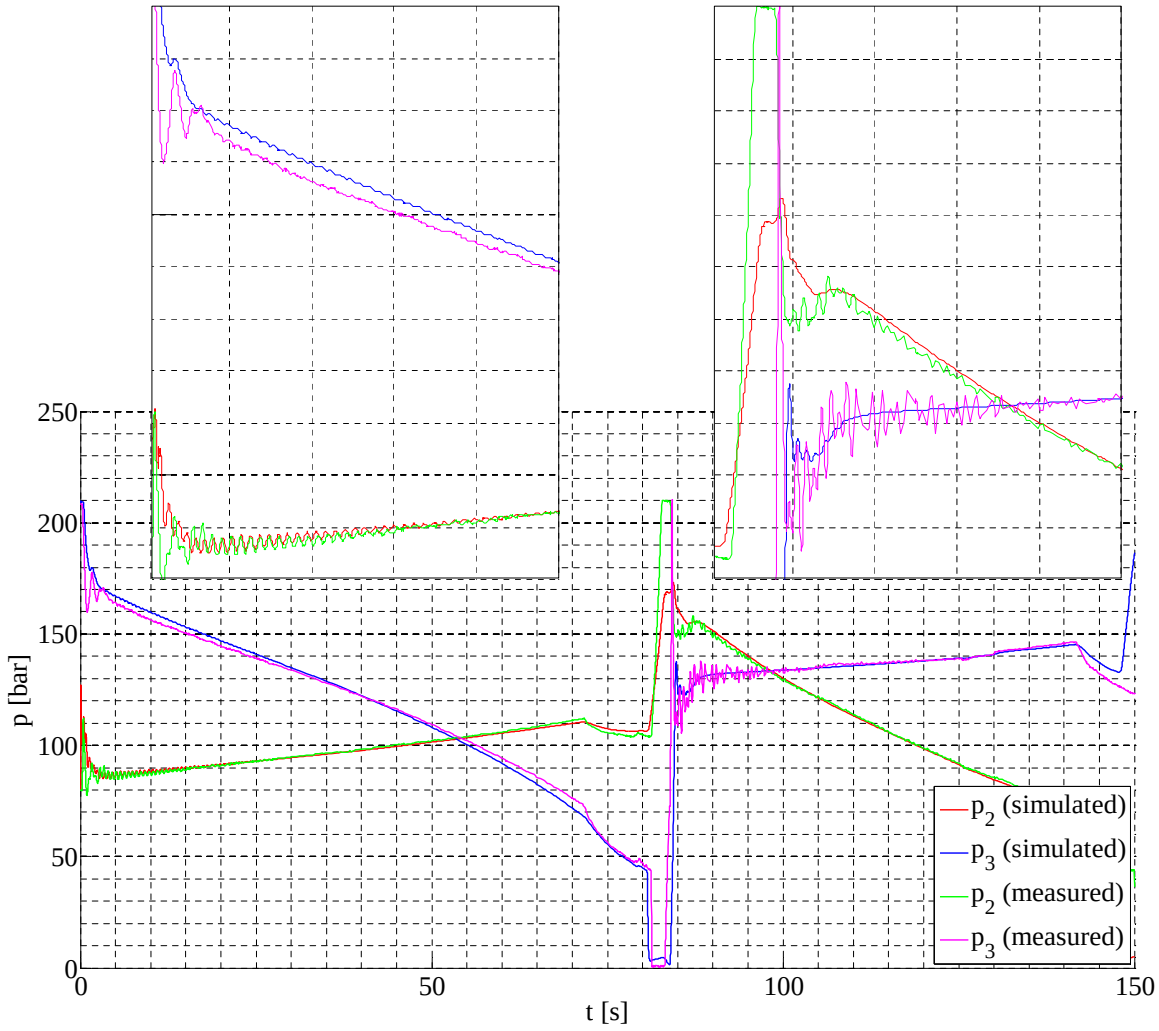

Figure 19: Measured and simulated pressures for verification of dynamic characteristics.

justed to 55% of their original value (Table 2) and the stiffness multipliers, β_k, used to determine the damping parameters for the three flexible members, are set to 0.002, 0.003 and 0.007, respectively. Bulk modulus is set to 5500 bar, which is almost half the value of the initial guess.

Immediately, it seems surprising that the estimated structural stiffness needs to be reduced nearly by a factor of two. However, only three of the crane's structural components are considered flexible and while the estimated compliance of these individual members may be correct, the flexibility of the remaining components also contributes to the overall dynamics. These components include the king, the intermediate jib and the foundation on which the pedestal is mounted. In addition, the connections between the individual structural components may also offer some flexibility.

The identified value of bulk modules is significantly lower than the theoretical value of a typical hydraulic oil, even when accounting for a certain amount of entrained air.

However, the compliance of pipes and hoses will also lower the effective bulk modulus. According to Merritt (1967) the effective bulk modulus is usually not more than 100,000 psi (approximately 6900 bar). The identified value of 5500 bar is therefore considered reliable.
Estimating the damping of a complex system like the considered crane is obviously difficult. According to (5) the stiffness multipliers should be reduced along with the stiffness of the structural members, because the natural frequencies are lowered. Since the stiffness multipliers are actually increased, it implies that the damping ratio of $\zeta = 0.03 - 0.07$ is too low. However, the un-modeled dynamics of structural components, other than the three considered, will also contribute to the total system damping. Furthermore the connections between the structural components will also offer some damping in terms of friction.
Therefore the stiffness multipliers determined in section 3.3 may be reasonable when considering the three structural members individually. For a complete model, though, the measurements show that additional damping needs to be introduced.

6 Conclusions

In this paper a model of an offshore knuckle boom crane has been presented. The model is developed in MapleSim^{TM} and includes both the crane's mechanical system and the electro-hydraulic motion control system.
The mechanical system is modeled as a two-dimensional multi-body system which includes the structural flexibility and damping. The *finite segment method* is used to model the flexibility and a procedure for estimating the structural damping is presented. Though these methods do not represent the state of the art within flexibility modeling, it is shown that they are sufficient for the given modeling purpose. Furthermore, they are advantageous in terms of modeling effort and computational requirements.
The motion control system is modeled using mostly semi-physical modeling techniques in order to reduce the computation requirements without neglecting or underestimating important physical phenomena. For modeling of the CBVs in the hydraulic system, a novel black-box approach is presented which uses two different pressure ratios to compute the flow through the valve. This approach is, however, based on having a certain amount of experimental data available.
The crane model is calibrated and verified with experimental data through three different steps:

1. Verification of the steady-state characteristics of the mechanical system model by identifying the cylinder friction parameters and tuning the masses and COG positions of the bodies in the model.

2. Verification of the steady-state characteristics of the motion control system model, mainly by identifying the unknown CBV model parameters.

3. Verification of the dynamic behavior of the crane model by tuning the flexibility and damping parameters of the mechanical system model and the stiffness, bulk modulus, of the hydraulic oil.

For the first two steps an optimization procedure is applied to efficiently identify the unknown parameters. In the last step the estimated parameters are simply adjusted by a scaling factor until the simulated response corresponds to the measured response.
The demonstrated modeling and parameter identification techniques target the system engineer by taking into account the limited access to component data normally encountered by engineers working with system design. The verified crane model is an example of a virtual prototype which can be used to evaluate and improve the design of the considered system.

Acknowledgements

The work presented in this paper is funded by the Norwegian Ministry of Education and Research and Aker Solutions.
The authors would like to thank Morten Abusdal (Aker Solutions) for his help with the experimental work.

References

Abdel-Rahman, E. M., Nayfeh, A. H., and Masoud, Z. N. (2003). Dynamics and control of cranes: A review. *Journal of Vibration and Control*, 67(7):863–908.

Adams, V. and Askenazi, A. (1999). *Building better products with finite element analysis*. OnWord Press.

Bak, M. K. and Hansen, M. R. (2012). Modeling, performance testing and parameter identification of pressure compensated proportional directional control valves. In *Proceedings of the 7th FPNI PhD Symposium on Fluid Power*, pages 889–908. Reggio Emilia, Italy.

Bak, M. K., Hansen, M. R., and Nordhammer, P. A. (2011). Virtual prototyping - model of offshore knuckle boom crane. In *Proceedings of the 24th International Congress on Condition Monitoring and Diagnostics Engineering Management*, pages 1242–1252. Stavanger, Norway.

Connelly, J. and Huston, R. L. (1994a). The dynamics of flexible multibody systems: A finite segment approach — I. Theoretical aspects. *Computers and Structures*, 50(2):255–258.

Connelly, J. and Huston, R. L. (1994b). The dynamics of flexible multibody systems: A finite segment approach — II. Example problems. *Computers and Structures*, 50(2):259–262.

Ellman, A., Käppi, T., and Vilenius, M. J. (1996). Simulation and analysis of hydraulically driven boom mechanisms. In *Proceedings of the 9th Bath International Fluid Power Workshop*, pages 413–429. Bath, UK.

Esque, S., Käppi, T., and Ellman, A. (1999). Importance of the mechanical flexibility on behaviour of a hydraulic driven log crane. In *Proceedings of the 2nd International Conference on Recent Advances in Mechatronics*, pages 359–365. Istanbul, Turkey.

Esque, S., Raneda, A., and Ellman, A. (2003). Techniques for studying a mobile hydraulic crane in virtual reality. *International Journal of Fluid Power*, 4(2):25–34.

Hansen, M. R., Andersen, T., and Conrad, F. (2001). Experimentally based analysis and synthesis of hydraulically actuated loader crane. In *Bath Workshop on Power Transmission and Motion Control*, pages 259–274. Bath, UK.

Henriksen, J., Bak, M. K., and Hansen, M. R. (2011). A method for finite element based modeling of flexible components in time domain simulation of knuckle boom crane. In *Proceedings of the 24th International Congress on Condition Monitoring and Diagnostics Engineering Management*, pages 1215–1224. Stavanger, Norway.

Hiller, M. (1996). Modelling, simulation and control design for large and heavy manipulators. *Robotics and Autonomous Systems*, 19(2):167–177.

Huston, R. L. (1981). Multi-body dynamics including the effects of flexibility and compliance. *Computers and Structures*, 14(5-6):443–451.

Huston, R. L. (1991). Computer methods in flexible multibody dynamics. *International Journal for Numerical Methods in Engineering*, 32(8):1657–1668.

Huston, R. L. and Wang, Y. (1993). Flexibility effects in multibody systems. In *Computer Aided Analysis of Rigid and Flexible Mechanical Systems: Proceedings of the NATO Advanced Study Institute*, pages 351–376. Troia, Portugal.

Merritt, H. E. (1967). *Hydraulic control systems*. Wiley.

Mikkola, A. and Handroos, H. (1996). Modeling and simulation of a flexible hydraulic-driven log crane. In *Proceedings of the 9th Bath International Fluid Power Workshop*. Bath, UK.

Mostofi, A. (1999). The incorporation of damping in lumped-parameter modelling techniques. *Proceedings of the Institution of Mechanical Engineers, Part K: Journal of Multi-body Dynamics*, 213(1):11–17.

Nielsen, B., Pedersen, H. C., Andersen, T. O., and Hansen, M. R. (2003). Modelling and simulation of mobile hydraulic crane with telescopic arm. pages 433–446.

Nikravesh, P. E. (1988). *Computer-aided analysis of mechanical systems*. Prentice Hall.

Ottestad, M., Nilsen, N., and Hansen, M. R. (2012). Reducing the static friction in hydraulic cylinders by maintaining relative velocity between piston and cylinder. In *Proceedings of the 12th International Conference on Control, Automation and Systems*, pages 764–769. Jeju Island, Korea.

Shabana, A. A. (1997). Flexible multibody dynamics: Review of past and recent developments. *Multibody System Dynamics*, 1(2):189–222.

Than, T. K., Langen, I., and Birkeland, O. (2002). Modelling and simulation of offshore crane operations on a floating production vessel. In *Proceedings of The Twelfth (2002) International Offshore and Polar Engineering Conference*. Kitakyushu, Japan.

Paper V

Analysis of Offshore Knuckle Boom Crane — Part Two: Motion Control

Morten Kollerup Bak and Michael Rygaard Hansen

This paper has been published as:

M. K. Bak and M. R. Hansen, “Analysis of Offshore Knuckle Boom Crane — Part Two: Motion Control”, *Modeling, Identification and Control*. Vol. 34 (2013), No. 4, pp. 175-181.

Analysis of Offshore Knuckle Boom Crane — Part Two: Motion Control

Morten Kollerup Bak and Michael Rygaard Hansen
Department of Engineering Sciences
Faculty of Engineering and Science, University of Agder
Jon Lilletunsvei 9, 4879 Grimstad, Norway

Abstract — In this paper design of electro-hydraulic motion control systems for offshore knuckle boom cranes is discussed. The influence of the control valve bandwidth along with the ramp time for the control signal are investigated both analytically with simplified system models and numerically with an experimentally verified crane model.
The results of both types of investigations are related to general design rules for selection of control valves and ramp times and the relevance of these design rules is discussed. Generally, they are useful but may be too conservative for offshore knuckle boom cranes. However, as demonstrated in the paper, the only proper way to determine this is to evaluate the motion control system design by means of simulation.

Keywords — Hydraulic crane, system design, directional control valve, bandwidth, ramp time.

1 Introduction

Design of offshore knuckle boom cranes is a complex and multidisciplinary task involving mechanical, hydraulic and control systems design. Naturally, this is an iterative process as the design of the crane's mechanical system and motion control system depend on each other. In practice though, detailed design of both systems is carried out separately as concurrent activities with constraints imposed by a conceptual design. This paper focuses on design of the motion control system.
Despite the fact that hydraulics, in general, is considered a mature technology, design of hydraulic motion control systems still offers a number of challenges for both component suppliers and manufacturers of hydraulically actuated machines. For the system designer, the main challenge is to meet the functional requirements for the system, a set of design constraints, while satisfying a number of performance criteria such as cost, reliability, overall efficiency and controllability, which are often conflicting and also subject to constraints. Design and optimization of hydraulic system has been subjected to quite extensive research, e.g., by Krus et al. (1991), Andersson (2001), Hansen and Andersen (2001), Krimbacher et al. (2001), Stecki and Garbacik (2002), Papadopoulos and Davliakos (2004), Pedersen (2004) and Bak and Hansen (2013b).
Besides design of the actuation system, there are generally three system elements to consider when designing electro-hydraulic motion control systems:

- Control strategy.
- Control elements (control valves).
- Reference signals (generation and shaping).

In this paper a typical control strategy for offshore knuckle boom cranes is considered and the selection of control elements and reference signals are investigated in order to identify their influence on the system performance.

2 Motion Control System Design

Offshore knuckle boom cranes generally feature a high degree of automation compared to other types of cranes. The control strategy relies on position and/or velocity feedback from the individual degrees of freedom (DOFs). For DOFs actuated by hydraulic cylinders this is usually achieved by means of a position sensor integrated in the cylinder. Fig. 1 shows the general architecture of a typical electro-hydraulic motion control subsystem for the considered type of crane.
Besides monitors, push buttons and switches the HMI contains two joysticks which the

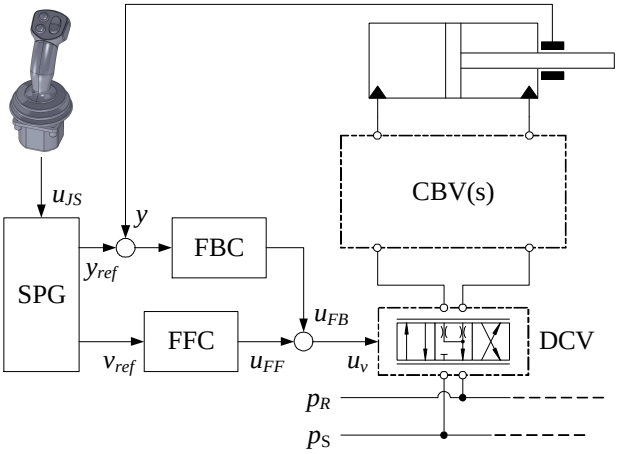

Figure 1: Simplified schematic of electro-hydraulic motion control sub-system.

operator uses to generate command signals for the control system. Joystick signals are fed to the SPG where they may be treated in different ways depending on the selected control mode. In open loop control mode the joystick signal, u_{JS}, is fed directly to the DCV as a feedforward signal. In closed loop control mode joystick signals are transformed into velocity and position references for the individual cylinder motions. The latter is used for path control of the crane's gripping yoke where several DOFs are controlled in a coordinated manner.

The FFC is a scaling of the velocity reference with the feedforward signal, u_{FF}, given by:

$$u_{FF} = v_{ref} \cdot K_{FF} \tag{1}$$

The feedforward gain, K_{FF}, is a tuning parameter, but may be computed when using a pressure compensated DCV. With a DCV with linear flow characteristics the cylinder velocity is given by:

$$v_{cyl} \approx \frac{u_v \cdot Q_{max}}{A_Q} \tag{2}$$

Q_{max} is the maximum flow of the DCV and A_Q is either the piston area or the rod-side area of the cylinder, depending on the sign of the valve control signal, u_v, i.e., the sign of the velocity reference, v_{ref}:

$$A_Q = \begin{cases} A_p & \text{for} \quad 0 \leq u_v \\ A_p \cdot \phi & \text{for} \quad u_v < 0 \end{cases} \tag{3}$$

The cylinder area ratio is $\phi = (D_p^2 - D_r^2)/D_p^2$, where D_p is the piston diameter and D_r is the rod diameter.

Combining (1) and (2) yields the feedforward gain:

$$K_{FF} = \frac{A_Q}{Q_{max}} \tag{4}$$

Theoretically, the cylinder could be controlled by the feedforward controller alone. However due to internal leakages in the hydraulic system, deadband of the DCV and nonlinear characteristics of the main spool this is not possible in practice.
The FBC is a PI controller which compensates for disturbances and accumulated position errors. The control system usually also contains an element which compensates for deadband of the DCV. This deadband compensator, however, is not considered here.
The system architecture shown in Fig. 1 is a popular structure because of its simple and, consequently, robust design. Furthermore, the controllers are easy to tune because of the load independent flow control.

3 Dynamic Considerations

A critical point in the design process is the selection of the DCV and, more specifically, to determine which dynamic properties are required from the valve. According to Merritt (1967) the bandwidth of the DCV should be greater than any of the natural frequencies of the hydraulic-mechanical system it is used to control. Manufacturers of servo valves usually recommend choosing a valve with a bandwidth, ω_v, which is at least three times higher than the natural frequency, ω_{hm}, of the hydraulic-mechanical system (MOOG, 2012):

$$\omega_v \geq 3 \cdot \omega_{hm} \tag{5}$$

This applies if the valve bandwidth should not affect the overall bandwidth of the total system consisting of the valve and the hydraulic-mechanical system it is used to control. Furthermore, it applies for servo applications where fast response and high precision is required and where non-compensated DCVs are used.
In order to investigate the relevance and usefulness of the design rule stated by (5) a simplified model of a hydraulic servo system is considered. The system structure is illustrated by the block diagram in Fig 2 which corresponds to a single DOF of the considered crane.
The G_c block represents the controller and contains both the FFC and the FBC. The G_v block represents the DCV including the closed loop spool position control and the dynamics of the valve. For simplified analysis this block is normally modeled as a second order system:

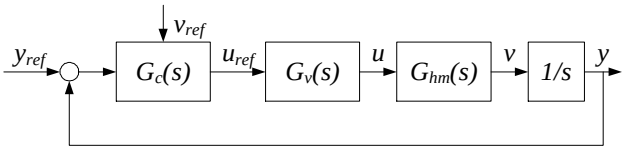

Figure 2: Block diagram representation of hydraulic servo system controlling a single DOF.

$$G_v(s) = \frac{1}{\frac{s^2}{\omega_v^2} + \frac{2 \cdot \zeta_v \cdot s}{\omega_v} + 1} \tag{6}$$

The G_{hm} block is the hydraulic-mechanical system to be controlled, in this case also represented by a second order system:

$$G_{hm}(s) = \frac{K_{hm}}{\frac{s^2}{\omega_{hm}^2} + \frac{2 \cdot \zeta_{hm} \cdot s}{\omega_{hm}} + 1} \tag{7}$$

The performance of any hydraulic servo system depends on the bandwidth of these two series connected systems, i.e., the product of the two transfer functions in (6) and (7). If the design rule in (5) is followed the overall dynamics of the valve and the hydraulic-mechanical system will approximately be that of the hydraulic-mechanical system. If the valve has a smaller bandwidth then the overall bandwidth of the system is markedly reduced. In Fig. 3 the Bode plot of G_{hm} is shown together with the product $G_v \cdot G_{hm}$ for $\omega_v = 3 \cdot \omega_{hm}$ and $\omega_v = \omega_{hm}$. The remaining system parameters are $K_{hm} = 1$, $\omega_{hm} = 10$ rad/s, $\zeta_{hm} = 0.2$ and $\zeta_v = 0.8$.
Clearly, choosing $\omega_v = \omega_{hm}$ yields a system with distinctly poorer dynamic performance whereas choosing $\omega_v = 3 \cdot \omega_{hm}$ justifies the simplification:

$$G_{vhm}(s) = \frac{K_{hm}}{\frac{s^2}{\omega_{vhm}^2} + \frac{2 \cdot \zeta_{hm} \cdot s}{\omega_{vhm}} + 1} \approx G_v \cdot G_{hm} \tag{8}$$

where

$$\omega_{vhm} = 0.9 \cdot \omega_{hm} \tag{9}$$

Equation (8) and (9) are valid for frequencies up to and around ω_{hm}. Frequencies beyond this value are rarely of interest for hydraulic servo systems. Therefore, when applying (5), the valve dynamics can simply be disregarded and the effective bandwidth (natural frequency) of the total system, ω_{vhm}, may be used as a design reference, which is 90 % of ω_{hm}.
Besides the bandwidth of the DCV also the motion reference for the control system must

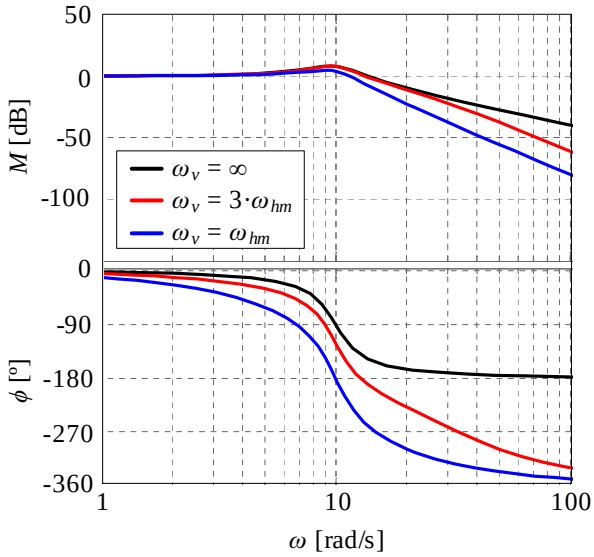

Figure 3: Bode plot of different combinations of valve dynamics and hydraulic-mechanical system dynamics.

be considered. Also here the natural frequency of the hydraulic-mechanical system must be taken into account as it gives an indication of the limit that the system imposes on the desired motion.

Consider the mass-spring-damper system shown in Fig. 4 with a mass, m, a stiffness, k, and a damping, b. This may be represented by an underdamped second order system with a natural frequency, ω_n, and a damping ratio, ζ. The mass is traveling at a speed, $\dot{y} = v_0$, and the motion of the mass should be ramped down via the reference input, x. In principle, this corresponds to halting a hydraulically controlled payload by ramping down the input flow.

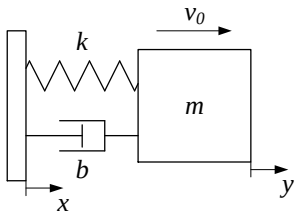

Figure 4: Second order system with a mass travelling at a speed $\dot{y} = v_0$.

Initially, $\dot{x} = \dot{y} = v_0$ and then the reference velocity is ramped down according to:

$$\dot{x} = v_0 \cdot \left[1 - \frac{t}{t_r}\right], \quad t \leq t_r \tag{10}$$

Here t is the time and t_r is the ramp time during which the mass is decelerated. The analytical solution to the motion of the mass during the ramp down is:

$$\begin{aligned} y &= C_0 + C_1 \cdot t + C_2 \cdot t^2 \\ &\quad - C_0 \cdot e^{-\alpha \cdot t} \cdot \left[\cos(\beta \cdot t) + \frac{\alpha}{\beta} \cdot \sin(\beta \cdot t) \right] \end{aligned} \tag{11}$$

where

$$C_0 = \frac{v_0}{\omega_n^2 \cdot t_r} \qquad C_1 = v_0 \qquad C_2 = -\frac{v_0}{2 \cdot t_r} \tag{12}$$

and

$$\alpha = \zeta \cdot \omega_n \qquad \beta = \omega_n \cdot \sqrt{1 - \zeta^2} \tag{13}$$

The reference velocity in (10) becomes zero at $t = t_r$. At that instant the position error, referred to as the overshoot, is:

$$\begin{aligned} e &= |x_{t=t_r} - y_{t=t_r}| \\ &= \tfrac{v_0}{\omega_n^2 \cdot t_r} \cdot \left\{ 1 - e^{-\alpha \cdot t_r} \cdot \left[\cos(\beta \cdot t_r) + \tfrac{\alpha}{\beta} \cdot \sin(\beta \cdot t_r) \right] \right\} \end{aligned} \tag{14}$$

The relative overshoot is the absolute position error relative to the nominal travel:

$$\begin{aligned} e_{rel} &= \frac{e}{x_{t=t_r}} \\ &= \tfrac{2}{\omega_n^2 \cdot t_r^2} \cdot \left\{ 1 - e^{-\alpha \cdot t_r} \cdot \left[\cos(\beta \cdot t_r) + \tfrac{\alpha}{\beta} \cdot \sin(\beta \cdot t_r) \right] \right\} \end{aligned} \tag{15}$$

In Fig. 5 the relative overshoot is plotted as a function of the ramp time for two different damping ratios. The natural frequency has no influence on the curves.

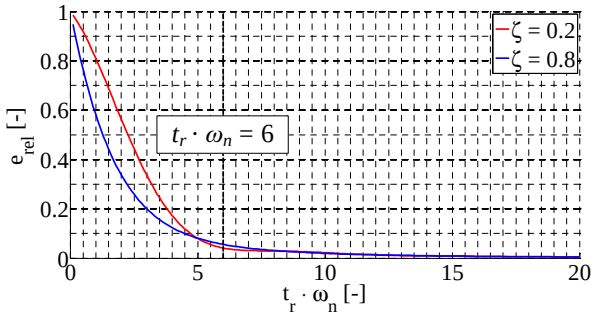

Figure 5: Relative overshoot as function of ramp time for two different damping ratios.

Most hydraulic-mechanical systems have dynamic characteristics that are not significantly more complicated than for the system in Fig. 4. Therefore the result shown in Fig. 5 may be utilized for hydraulic servo systems. It is clear that for a typical hydraulic-mechanical system, ramp times should be considered whenever motion is prescribed. Also, it is clear that a useful ramp time depends on the acceptable overshoot. Hence, if high overshoot is acceptable then small ramp times may be prescribed and vice versa.

As a rule of thumb, the ramp time of a prescribed motion should obey the inequality:

$$t_r \geq \frac{6}{\omega_n} \tag{16}$$

It is important to keep in mind that the natural frequency of a real system may be substantially smaller than the one computed for a model of the system. The discrepancy is mainly because the modeled stiffness typically is higher than the actual stiffness. This can be taken into account in many ways, for example by using a smaller stiffness in the computation or by means of experimental work that can reveal the actual natural frequency of the system to be controlled.

4 Practical Application

With the experimentally verified simulation model described in Bak and Hansen (2013a) it is possible to generate a realistic picture of the natural frequency of the crane. Theoretically, there may be several mode shapes and natural frequencies for the crane. In practice, though, it will only be possible to excite the lowest of these frequencies. This frequency will be common for all the considered DOFs, i.e., the ones for three crane jibs, but will vary with positions of the jibs, i.e., the lengths of the hydraulic cylinders. By orienting the crane jibs in different positions in the simulation model and applying an impulse the natural frequency for the given positions can be observed from the following pressure oscillations in the cylinders. As seen from Fig. 6 the crane is a redundant mechanism, since there are more DOFs than needed to position the gripping yoke within the work space of the crane. This redundancy is not exploited for control purposes but only to improve foldability. Therefore, the cylinders 2 and 3 are simply operated equally in practical operations.

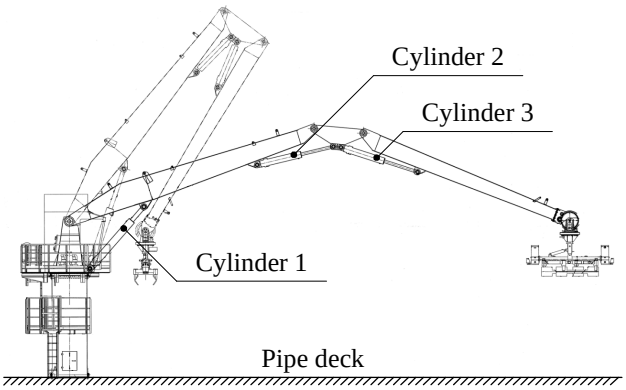

Figure 6: Knuckle boom crane with redundant DOF.

The variation of the natural frequency can be mapped in a three-dimensional representation as shown in Fig. 7 as function of only two independent cylinder lengths.

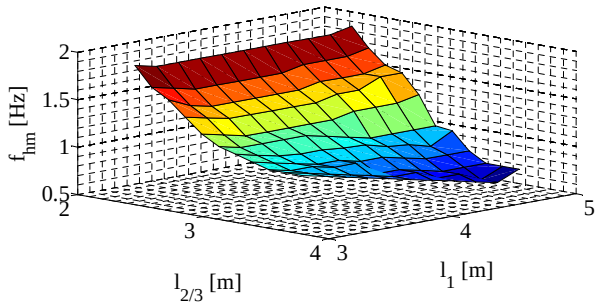

Figure 7: Variation of natural frequency of the crane.

The figure provides a clear picture of how the natural frequency varies with the length of the cylinders. The orientation of the inner jib has no major influence, except when cylinders 2 and 3 are nearly fully extended. The natural frequency varies between $f_{hm} \approx 0.65...1.9$ Hz corresponding to $\omega_{hm} \approx 4...12$ rad/s.
In order to investigate how well the simplified analysis in section 3 applies to a real system like the considered crane, simulations with parameter variations are carried out with the experimentally verified crane model. To limit the extent of the analysis a simple sequence of extending the outer jib cylinder is considered. While cylinders 1 and 2 are held at rest cylinder 3 is extended with trapezoidal velocity reference, see Fig. 8, using the FFC only. The FBC is disabled to ease comparison and the deadband of DCV is set to zero in order to simulate the function of a deadband compensator.

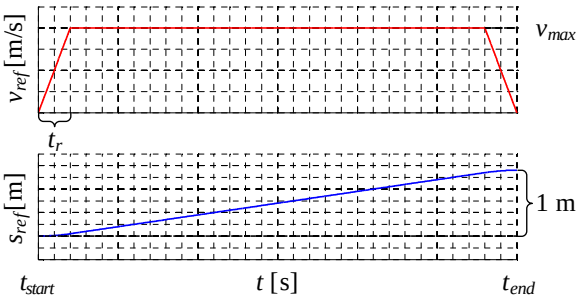

Figure 8: Velocity and position references.

The reference cylinder travel is 1 m, starting and ending 0.15 m from the end stops. In this range the natural frequency varies between $f_{hm} \approx 1.65...0.65$ Hz corresponding to $\omega_{hm} \approx 10...4$ rad/s. Since the highest natural frequency is present at the beginning of the sequence only the performance during the ramp up is considered and $\omega_{hm} = 10$ rad/s is used as the reference frequency. According to (5) the DCV bandwidth should then be

at least $\omega_v = 30$ rad/s, which is at the performance limit of most pressure compensated DCVs. Bak and Hansen (2012) tested a Danfoss PVG32 and identified a bandwidth of $f_v = 5$ Hz or slightly more than 30 rad/s.
Simulations are carried out with variations of both ramp time, t_r, and DCV bandwidth, ω_v, where relative position error at the end of the ramping period and maximum position error during the sequence are observed. In Fig. 9 the relative position error is shown as function of $t_r \cdot \omega_{hm}$ for different DCV bandwidths.

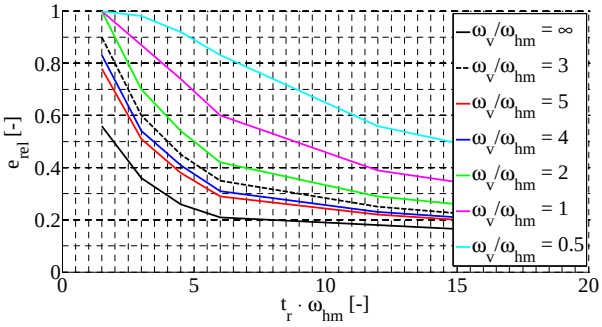

Figure 9: Relative error at the end of the ramp.

The effect is the similar to the one seen in Fig. 5. The relative error increases significantly for $t_r \cdot \omega_{hm} < 6$ at least for $\omega_v > \omega_{hm}$. Furthermore, it is seen that e_{rel} is doubled by choosing $\omega_v = 2 \cdot \omega_{hm}$ and tripled for $\omega_v = \omega_{hm}$ compared to the ideal situation of $\omega_v = \infty$. Only minor improvements are achieved for $\omega_v > 3 \cdot \omega_{hm}$. The results seem to support the design rules in (5) and (16).
In Fig. 10 the maximum position error is shown as function of $t_r \cdot \omega_{hm}$ for different DCV bandwidths.

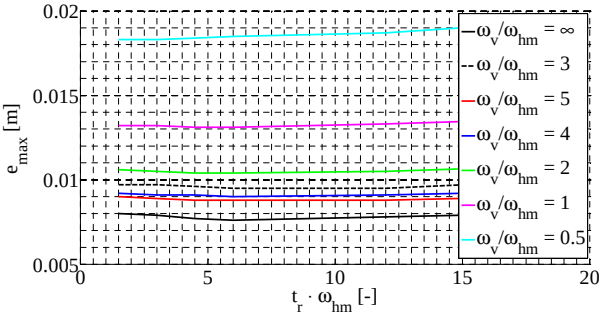

Figure 10: Maximum error during the sequence.

The maximum position error is almost independent of the ramp time and only depends

on the DCV bandwidth. This indicates that if the relative error is irrelevant, then the ramp time does not need to be taken into account. However too short ramp times may cause instability while too long ramp times increase the maximum reference velocity and consequently the required flow.
The results once again support the design rules in (5) and (16) since there is no significant improvement for $\omega_v > 3 \cdot \omega_{hm}$, but a significant increase in error for $\omega_v = \omega_{hm}$ compared to $\omega_v = 3 \cdot \omega_{hm}$.
The absolute errors are small compared to the reference travel of the cylinder and well within the acceptable range for typical offshore knuckle boom crane operations. The simulation results confirm the validity of (5) and (16) and usefulness as general design rules. In general, the choice of DCV and ramp times will always depend on the acceptable levels of relative and absolute errors. A prerequisite to evaluate this is to have a simulation model, like the one described in Bak and Hansen (2013a), with which a frequency map, like the one in Fig. 7, can be generated and relevant control sequences can be simulated.

5 Conclusions

In this paper design of electro-hydraulic motion control systems for offshore knuckle boom cranes has been discussed and a typical system architecture has been presented. A critical point in the design process is the selection of the directional control valve (DCV) and more specifically to determine which dynamic properties are required from the valve. A commonly used design rule is to select a valve with a bandwidth, ω_v, which is at least three times higher than the natural frequency, ω_{hm}, of the hydraulic-mechanical system it is used to control.
The influence of the DCV bandwidth along with the ramp time for the control signal have been investigated both analytically with simplified system models and numerically with the experimentally verified crane model described in Bak and Hansen (2013a).
The results of both types of investigations confirm the relevance and usefulness of design rules for required DCV bandwidth and suitable ramp times. However the selection of these design parameters always depend on the acceptable error level for the application to be controlled and for offshore knuckle boom crane the investigated design rules may be too conservative.
However, the only way to properly evaluate the performance of the motion control system design, without building a prototype, is to have simulation model of the application like the one described in Bak and Hansen (2013a).

Acknowledgements

The work presented in this paper is funded by the Norwegian Ministry of Education and Research and Aker Solutions.

References

Andersson, J. (2001). *Multiobjective optimization in engineering design. Applications to fluid power systems*. PhD thesis, Linköping University, Linköping, Sweden.

Bak, M. K. and Hansen, M. R. (2012). Modeling, performance testing and parameter identification of pressure compensated proportional directional control valves. In *Proceedings of the 7th FPNI PhD Symposium on Fluid Power*, pages 889–908. Reggio Emilia, Italy.

Bak, M. K. and Hansen, M. R. (2013a). Analysis of offshore knuckle boom crane — part one: modeling and parameter identification. *Modeling, Identification and Control*, 34(4).

Bak, M. K. and Hansen, M. R. (2013b). Model based design optimization of operational reliability in offshore boom cranes. *International Journal of Fluid Power*, 14(3):53–66.

Hansen, M. R. and Andersen, T. O. (2001). A design procedure for actuator control system using design optimization. In *Proceedings of the 7th Scandinavian International Conference on Fluid Power*. Linköping, Sweden.

Krimbacher, N., Garstenauer, M., and Scheidl, R. (2001). Optimization of hydraulic systems by means of numerical simulation. In *Proceedings of the 2nd International Workshop on Computer Software for Design*, pages 76–83. Ostrava-Malenovice, Czech Republic.

Krus, P., Jansson, A., and Palmberg, J.-O. (1991). Optimization for component selection in hydraulic systems. In *Proceedings of the 4th Bath International Fluid Power Workshop*, pages 219–231. Bath, UK.

Merritt, H. E. (1967). *Hydraulic control systems*. Wiley.

MOOG (2012). Electrohydraulic valves... a technical look. Technical report, Moog Inc. http://www.moog.com/literature/ICD/Valves-Introduction.pdf.

Papadopoulos, E. and Davliakos, I. (2004). A systematic methodology for optimal component selection of electrohydralic servosystems. *International Journal of Fluid Power*, 5(3):15–24.

Pedersen, H. C. (2004). Power management in mobile hydraulic applications - an approach for designing hydraulic power supply systems. In *Proceedings of the 3rd FPNI PhD Symposium on Fluid Power*, pages 125–139. Terrassa, Spain.

Stecki, J. S. and Garbacik, A. (2002). Fluid Power Net Publications.